UNIVERSITY OF CALIFORNIA SAN DIEGO

Establishing a Single-cell and High-throughput Phenotypical Platform to Identify Novel Arrhythmia-Causing Genes

A dissertation submitted in partial satisfaction of the

requirements for the degree Doctor of Philosophy

in

Bioengineering

by

Michael Shenghan Yu

Committee in charge:

Professor Andrew D. McCulloch, Chair
Professor Alexandre R. Colas
Professor Adam J. Engler
Professor Sylvia M. Evans
Professor Stephanie I. Fraley
Professor Mark K. Mercola
Professor Shyni Varghese

2018

The Dissertation of Michael Shenghan Yu is approved, and is acceptable in quality and form for publication on microfilm and electronically:

_____

_____

_____

_____

_____

_____

_____

Chair

University of California San Diego

2018

EPIGRAPH

Feeling my way through the darkness,

Guided by a beating heart.

I can't tell where the journey will end

But I know where to start.

— *Avicii, Wake Me Up*

TABLE OF CONTENTS

LIST OF ABBREVIATIONS

Abbreviation	**Explanation**
4-AP	4-aminopyridine
ACM	Atrial-like cardiomyocyte
AF	Atrial fibrillation
AI	Arrhythmia index
$APD_{10,25,50,75,90}$	Action potential duration at 10%, 25%, 50%, 75%, 90% of repolarization
bHLH	Basic-helix-loop-helix
BMP	Bone morphogenic protein
CICR	Calcium-induce calcium release
CM	Cardiomyocyte
CMP	Cardiac mesoderm progenitor
CRE	Cis-regulatory element
CRISPR-Cas	Clustered Regularly Interspaced Short Palindromic Repeats - CRISPR-associated genes
CRISPRa	CRISPR activation
$CTD_{50,75}$	Calcium transient duration at 50%, 75% of relaxation
DAD	Delayed afterdepolarizations
DCM	Dilated cardiomyopathy
EAD	Early afterdepolarizations
ERF	Effective refractory period
FGF	Fibroblast growth factor
FHF	First heart field
Fib	Human neonatal foreskin fibroblast
GO-terms	Gene ontology terms
GWAS	Genome-wide association study
HCM	Hypertrophic cardiomyopathy
HDR	Homology-directed repair
hESC	Human embryonic stem cell
HF	Heart failure
HLH	Helix-loop-helix
hPSC	Human pluripotent stem cell
hPSC-CM	Human pluripotent stem cell-derived cardiomyocytes
I_{CaL}	L-type Ca^{2+} current
I_K	Outward K^+ flux
I_{K1}	Inward delayed rectifier K^+ current
I_{KAch}	Acetylcholine-sensitive K^+ current
I_{Kr}	Rapid delayed rectifier K^+ current
I_{Ks}	Slow delayed rectifier K^+ current
I_{Kur}	Ultra-rapid delayed rectifier K^+ current

I_{Na}	Inward Na^+ current
Isop	Isoproterenol
I_{to}	Lesser transient outward current
mESC	Mouse embryonic stem cell
mV	Millivolts
NCX	Na^+/Ca^{2+} exchanger
NHEJ	Non-homologous end joining
PCA	Principal component analysis
PeT	Photo-induced electron transfer
Prop	Propranolol
qPCR	Quantitative polymerase chain reaction
RA	Retinoic acid
ROI	Region of interest
SCD	Sudden cardiac death
sgRNA	Single-strand guide RNA
SHF	Second heart field
SNP	Single-nucleotide polymorphisms
SR	Sarcoplasmic reticulum
ssODN	Single-strand oligodeoxynucleotide
T_{Decay}	Active tension relaxation
T_{Depol}	Depolarize time
T_{Rise}	Active tension generation
VCM	Ventricular-like cardiomyocyte
VF	Ventricular fibrillation
V_{Rest}	Resting membrane potential
VT	Ventricular tachycardia
WGA	Wheat germ agglutinin

LIST OF FIGURES

LIST OF TABLES

LIST OF SUPPLEMENTAL FILES

Supplement 2.1 CM incubated with voltage-sensing probe and recorded at 20x, 100 Hz frame rate.

ACKNOWLEDGEMENTS

This would not happen without the guidance from both my mentors, from my committee member, help from colleagues, and support from my friends and family.

I would like to express my most profound gratitude to both of my mentors, Dr. Mark Mercola and Dr. Alexandre Colas, for their consistent support of my research for the past five and a half years. I would like to thank Dr. Andrew McCulloch for his guidance as the co-chair of my committee. I would also like to thank Dr. Engler, Dr. Evans, Dr. Fraley, and Dr. Varghese for their participation in my committee and providing valuable suggestions for my study. I also want to thank my colleagues at Sanford Burnham Prebys Medical Discovery Institute, who were always helpful in my research.

Finally, I would like to thank my parents and my elder brother for their patience and best wishes. My girlfriend for her incredible support and company along this journey. Also, all my friends here in San Diego and Taiwan who get me through every adversity and maintain the life in balance. This dissertation is dedicated to the endless love of them.

Chapter 2, in part, contains material partly from "Id genes are essential for early heart formation" by Thomas Cunningham*, Michael S. Yu*, Wesley Mckeithan*, Sean Spiering, Florent Carrette, Chun-Teng Huang, Paul J. Bushway, Matthew Tierney, Sonia Albini, Mauro Giacca, Miguel Mano, Pier Lorenzo Puri, Alessandra Sacco, Pilar Ruiz-Lozano, Jean-Francois Riou, Muriel Umbhauer, Greg Duester, Mark Mercola, and Alexandre R. Colas (*co-first authors), which has been published in *Genes and Development, 2017*. The dissertation author was the co-first investigator and author of this paper.

Chapter 3, in part, contains material partly from "Generation of First Heart Field-

Like Cardiac Progenitors and Ventricular-like Cardiomyocytes from Human Pluripotent Stem Cells" by Michael S. Yu*, Sean Spiering*, and Alexandre R. Colas (*co-first authors), which has been submitted to *Journal of Visualized Experiments* and is currently in press. The dissertation author was the co-first investigator and author of this paper.

VITA

2010 Bachelor of Science, National Tsinghua University, Taiwan.

2018 Doctor of Philosophy, University of California San Diego, La Jolla.

ABSTRACT OF THE DISSERTATION

Establishing a Single-cell and High-throughput Phenotypical Platform

to Identify Novel Arrhythmia-Causing Genes

by

Michael Shenghan Yu

Doctor of Philosophy in Bioengineering

University of California San Diego, 2018

Professor Andrew D. Mcculloch, Chair

Atrial fibrillation (AF) is the most prevalence form of arrhythmia, affecting around 3% of the general population. The mechanism and disease-causing factor of AF are remaining unclear. Thus, the establishment of a high-throughput phenotypical screening platform could advance the understanding of AF and identify novel cardiac rhythm regulators that could inform future anti-arrhythmic development.

AF is an atrial-specific arrhythmia. Thus, to specify the screening target space, human pluripotent stem cell-derived atrial like cardiomyocytes (ACM) is required. To effectively generate large scales of ACM, the regulatory network and differentiation protocol of cardiac mesoderm progenitor (CMP) has to be established. We performed genome-wide microarray and identified Id1 is required and sufficient to direct the differentiation of CMP from pluripotent cells both in mouse and human. Moreover, *in vivo* data have shown the essential role of Id gene family during mammalian early heart tube formation. Retinoic acid (RA) was applied as the atrial-specific cue for the differentiation of ACM from CMP. The resulting ACMs were molecularly validated. The qPCR, immunofluorescence, and RNA-seq results demonstrated atrial-specific genes were highly expressed in the ACM compared to non-RA-treated ventricular-like cardiomyocyte (VCM). Functional validation including action potential, calcium transient, and contractility also confirmed the atrial-like physiology behavior of ACM.

To efficiently screen through the genome to identify potential arrhythmia-causing genes, a fully automated single-cell and high-throughput phenotypical platform was established. The platform record and analyze action potential traces from each cell within the field of view with image processing software and algorithm. Physiological metrics were then retrieved. Action potential duration at 75% of repolarization (APD_{75}) and arrhythmia index (AI) were calculated as metrics to determine the degree of arrhythmia-like activity induced by the treatment. To further validate the platform, siRNA against 20 previously shown AF-associated genes identified through rare variants and genome-wide association study (GWAS) were transfected to ACM. The down-regulation of some of the genes in the list induced the prolongation or shortening of action potential duration (APD), but not

sufficient to trigger the arrhythmia-like activity. AF-associated perturbagens such as β-adrenergic agonists/antagonist, and tissue fibrosis, mimicking by co-culturing fibroblasts with ACM also induced electrical remodeling but not arrhythmia-like activity. However, by applying perturbagens along with siRNA against AF-associated genes that had the most severe phenotype triggered dramatic arrhythmia-like behavior. Moreover, distinct combinations of siRNA against AF-associated gene with perturbagens induced different arrhythmia-like-phenotypes.

The overall result indicated the complexity of the disease mechanisms as well as the unmet need to identify novel cardiac rhythm regulators and potential AF-causing genes. The ACM differentiation protocol and the high-throughput phenotypical screening platform could further advance the understanding of AF and catalyze the discovery of antiarrhythmics.

Chapter 1

Introduction

Atrial fibrillation is the most common cardiac arrhythmia affecting more than 33 million individuals world wild that can cause detrimental complications such as stroke, heart failure, and death. Current treatments of AF are surgical ablation and the prescription of antiarrhythmics. Surgical ablation is an invasive and sophisticated technique and might require several ablations to eliminate the ectopic firing loci. On the other hand, anti-atrial fibrillation drugs have relatively low efficacy and a considerable high off-target effect that could increase the risks, especially pro-arrhythmia, highlighting the needs to develop novel anti-arrhythmic treatments. The elucidation of underlying molecular determinants and the identification of novel AF-causing genes are the primary goals.

With the advance of sequencing technology and CRISPR-Cas gene-editing technique, genetic researches on familial AF and GWAS disclosed several AF-related genes. Despite the effort, the molecular basis of the majority of AF patients is still poorly understood. Two common techniques to model cardiomyocyte physiology are the whole-cell patch-clamp electrophysiology and optical recording-based system. The patch-clamp

method is able to record major currents of cardiomyocyte during the excitation-contraction coupling through carefully monitored current amplitude. However, one of the constraints of the patch-clamp method is the limited throughput that is insufficient for large-scale screens. The optical recording-based system utilizes fluorescent dyes such as voltage-sensing dyes or calcium-sensing dyes to visualize cardiomyocyte physiology responses. Image analysis and physiological parameter calculation are then conducted using recorded whole-well images. Although the automated workflow provides tremendous throughput, the limitation of the system is the resolution of physiology metrics due to the whole-well averaged fluorescent signal analysis. Thus, establishing a platform that combines the automated high-throughput physiology system with the single-cell level resolution to rapidly generate physiological measurements of CM could substantially advance the understanding of molecular basis of AF and the discovery of new anti-AF drugs.

This thesis summarizes the effort that has been made for establishing a physiology screening platform to elucidate novel AF-causing candidates. The contributions comprise three main significances: (1) The generation of Id1-derived CMP and ACM. (2) The establishment of the single-cell and high-throughput CM functional analysis platform. (3) The modeling of arrhythmia-like activity in ACM with misregulation of known AF-causing genes and AF-related perturbagens. The main text of this thesis is organized along the following thematic lines.

Chapter 2 describes an original Id1-induced CMP differentiation protocol. Id1, identified through genome-wide microarray, is required and sufficient to promote mesoderm formation. The resulting Id1-induced CMP is highly cardiogenic. Moreover, the *in vivo* data demonstrated the Id family is essential for mammalian early heart tube

formation.

Chapter 3 addresses CM subtype-specific differentiation and the validation of the resulting ACM and VCM. VCM were derived from spontaneous differentiation, and ACM were generated by the administration of atrial-specific differentiation cue, retinoic acid. The identity of resulting CM subtypes was comprehensively validated in both molecular signature and functional assessment aspects.

Chapter 4 exhibits an automated single-cell and high-throughput functional screening platform. Based on optical recording system, the platform utilized custom built image processing software and trace analysis algorithm to generate the single-cell resolution of CM physiology.

Chapter 5 validates the platform with a list of previously known AF-associated genes. siRNAs against these genes were transfected into ACM and physiology parameters were retrieved through the platform. The result showed that the down-regulation of several of these genes induced electrical remodeling but not sufficient to induced arrhythmia-like activity. Only with the presence of common AF-associated perturbagens, knocking down the genes triggers arrhythmia-like activity. Moreover, different combinations of siRNA and perturbagens induced distinct arrhythmia phenotypes.

Chapter 6 summarizes the contributions of this dissertation and discusses three possible future research directions.

Chapter 2

Identification of Id Family as Multipotent Mesoderm Progenitor Regulator

2.1 Background

The ability to produce unlimited amounts of cardiomyocytes in the laboratory is the pre-requisite of being able to study and conduct large-scale screenings on cardiac diseases. In the late 2000s, when researchers begin to harness the power of human pluripotent stem cells (hPSCs), there was no efficient cardiomyocyte differentiation protocol. Serum-based protocols often provide unstable and poor cardiomyocyte yields. Therefore, there is an unmet need to establish a differentiation protocol that could robustly and efficiently generate massive amounts of cardiac progenitors and subsequent cardiomyocytes for cardiac disease studies.

Heart formation begins during the early gastrulation when the specification of the three distinct germ layers, ectoderm, endoderm, and mesoderm, undergo migration and

forming cardiac primordium consist of CMPs. The progenitors then move ventrally and compose the linear heart tube that undergoes cardiac looping and further assembles into a fully functional heart. The spatiotemporal activation and inhibition of various signaling pathways orchestrate the allocation of the germ layers and the formation and patterning of the organs. Studies of developmental biology over the past two decades have established the mechanisms of how mesoderm was induced through the activation of extracellular signals, such as Activin/Nodal and bone morphogenic proteins (BMPs) signaling pathways. However, the understanding of the down-stream intracellular mediators controlling this process has never been adequately explained. Understanding the regulatory network of mesoderm formation could further advance the design of mesoderm and cardiac differentiation protocol, and gain insights into the development and regenerative aspects of the heart.

2.2 Results

2.2.1 Identification of Regulators of Cardiac Mesoderm Progenitor Formation

Previous studies have illustrated the mechanism of cardiac specification is initiated through the activation of transcription factors Eomes, Mesp1, and Mesp2, which then further activate series of cardiac-specific transcription factors (Gata4, Nkx2-5, Hand2, and Myocd) and repress pluripotency genes (Oct4, Nanog, and Sox2) as well as endoderm effectors (Foxa2, Sox17) [1, 2]. Furthermore, attenuating Activin/Nodal signaling via the blockade of activin receptor Acvr1b directs the differentiation mesendoderm towards mesoderm progenitor [3]. Thus, we hypothesize that the down-stream regulators in

response to the inhibition of activin signaling play a critical role during the differentiation of CMP [Figure 2.1A].

Mouse embryonic stem cells (mESCs) reaches the mesendoderm stage (Gsc^+, $Fox2^+$, and T^+) at day 3 after the initiation of differentiation with Activin/Nodal signaling. Mesendoderm progenitors then further differentiate into either endoderm progenitors ($Foxa2^+$) or CMPs (Kdr^+, $Meps1^+$, $Cdh11^+$, $Snai1^+$). The attenuation of Acvr1b directs mesendoderm progenitors towards CMPs very efficiently [Figure 2.1B–C]. To elucidate the downstream effectors of cardiogenic mesoderm formation, we performed mRNA microarray to evaluate the differential expressions of the mRNA during the process [Figure

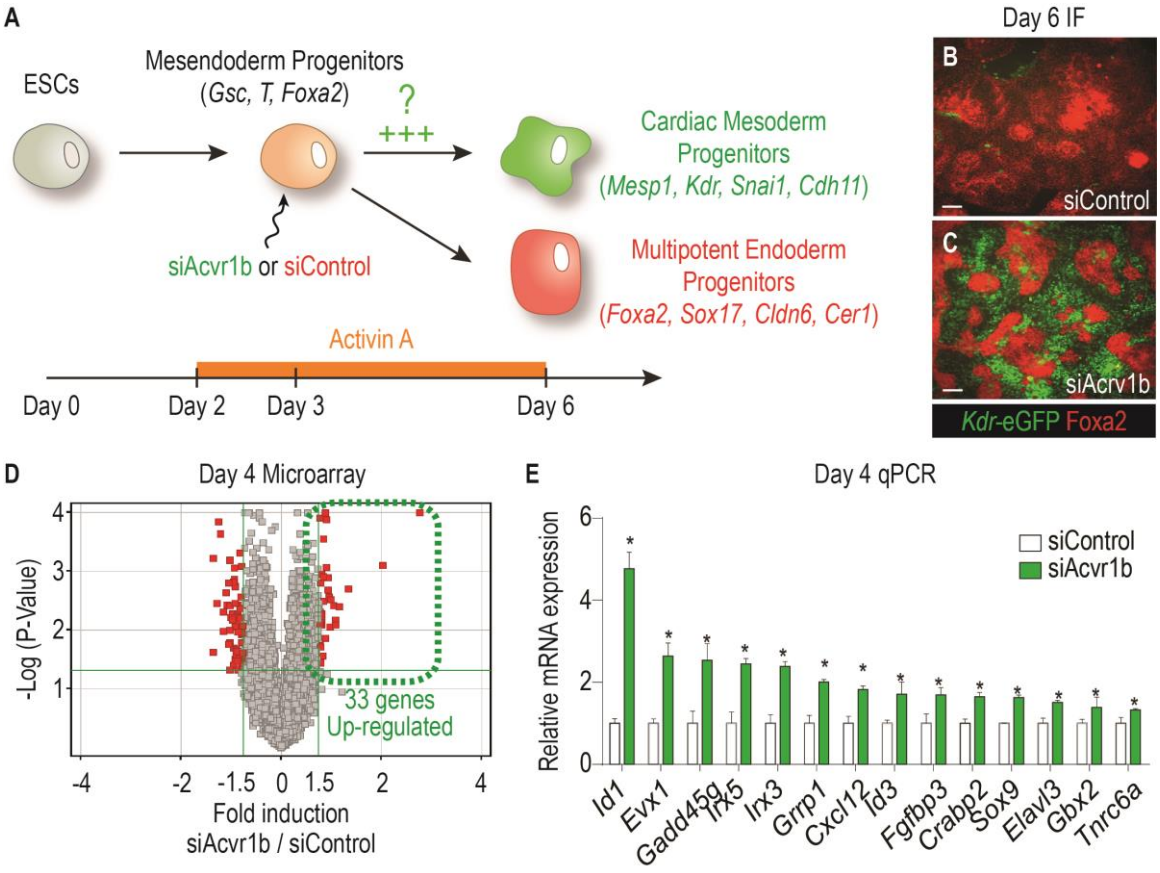

Figure 2.1 Identification of mesoderm effectors. (A) Schematic diagram of CMP differentiation protocol. (B–C) IF of resulting day 6 cells. (D) Microarray to identify genes up-regulated in response to siAcvr1b. (E) 14 qPCR validated mesoderm effector gene candidates.

2.1D]. We identified 33 genes were up-regulated in response to siRNA against Acvr1b relative to the scrambled sequence of siRNA, and of which 14 were further confirmed by quantitative PCR (qPCR) [Figure 2.1E]. In the list of 14 candidate genes, eight of them are involved in the regulation of gene transcription, including transcription factors (Evx1, Gbx2, Irx3, Irx5, and Sox9), helix-loop-helix (HLH) protein that forms heterodimers with basic HLH family of transcription factors (Id1 and Id3), and DNA repair mediator (Gadd45g). Three of the candidates involved regulation of signaling pathway (Fgfbp3, Crabp2, and Cxcl12), two are related with RNA binding and regulation (Elavl3 and Tnrc6a), and one with possible centrosome-associated function (Grrp1).

2.2.2 Id1 is Required and Sufficient to Direct the Formation of Cardiac Mesoderm Progenitor in mESC and hESC

To further assessed the role of the 14 candidate genes during mesoderm differentiation, we transfected mESCs on day 3 with siAcvr1b along with siRNA against all 14 candidate genes individually. Of all the candidate genes, only siRNAs against Grrp1, Evx1, and Id1 substantially decrease the number of Kdr^+ mesoderm cells in the expense of the increasing population of $Fox2^+$ endoderm cells along with the down-regulation of mesoderm markers including Mesp1, Snai1, and Cdh11[Figure 2.2A–E]. These results indicate that Grrp1, Evx1, and Id1 is required during the process of mesoderm formation. We then examined the sufficiency of these remaining three candidate genes during the differentiation by the overexpressing system with lentivirus. We first generated mESC

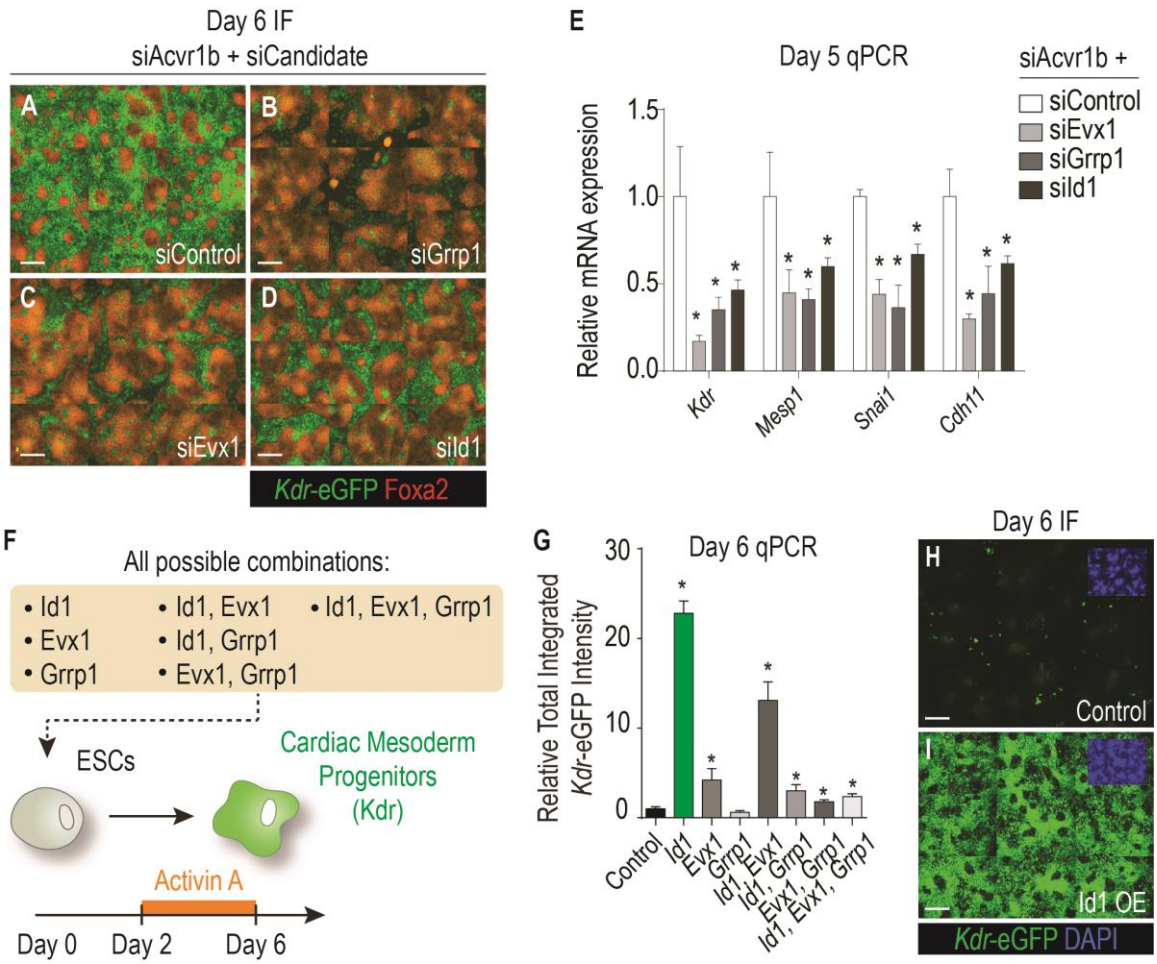

Figure 2.2 Id1 is required and sufficient to promote CMP formation. (A-D) 3 genes are required during mesoderm differentiation. (E) Down-regulation of the 3 genes reduce mesoderm marker expression. (F) All possible combination of overexpression of 3 genes were examined. (G–I) qPCR and IF result indicates the overexpression of Id1 is sufficient to promote mesoderm formation.

lines overexpressing all seven possible combinations of Grrp1, Evx1, and Id1 [Figure 2.2F]. These mESC lines were than differentiate into mesendoderm and further evaluate the mesoderm formation efficiency without the blockade of Acvr1b. Surprisingly, Id1 along without attenuating Acvr1b signaling was sufficient to significantly induce more than 22-fold of Kdr^{+} mesoderm cell formation over parental control mESC [Figure 2.2G–I].

We then investigate whether the role of Id1 during mesoderm progenitor differentiation is evolutionarily conserved in human embryonic stem cells (hESCs). Consistent with the result in mESC, flow cytometry data indicates Id1 drastically increase the population of Kdr^+ mesoderm cells during the mesoderm-endoderm specification in hESC system [Figure 2.3A–D]. Moreover, the temporal mRNA expression results of Id1-induced Kdr^+/KDR^+ mesoderm progenitor (iMPs) showed Id1 overexpression not only promotes known mesoderm regulators Mesp1/MESP1 and Kdr/KDR, as well as the early upregulation of Exv1/EVX1 and Grrp1/GRRP1 [Figure 2.3E–L]. Collectively, these data

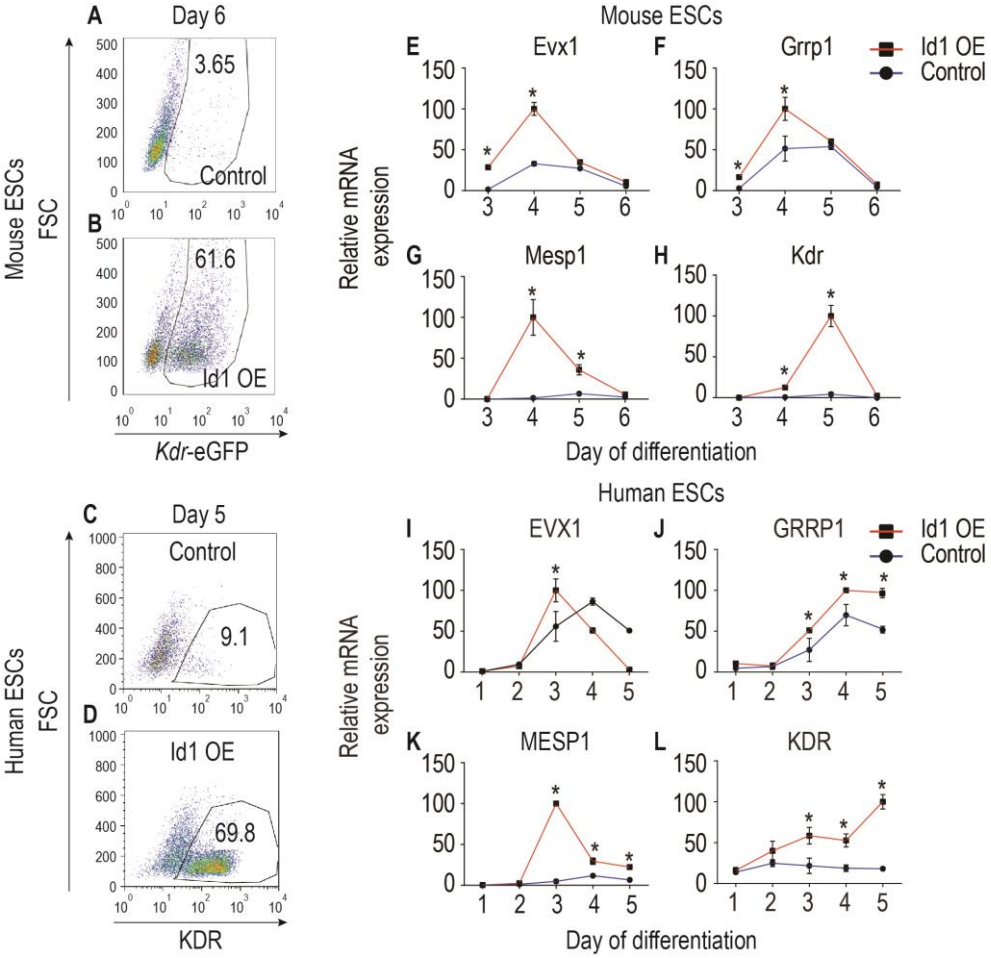

Figure 2.3 Id1 overexpression induced mesoderm mechanism is conserved in human. (A–D) Overexpression of Id1 increase Kdr^+ cell percentage. (E–H) Mouse mesoderm marker expression pattern. (I–L) Human mesoderm marker expression pattern.

show that Id1 act as an evolutionarily conserved initiator of mesoderm differentiation program and plays a central role within the regulatory network in both mESC and hESC.

To examine the multipotency and the cardiogenic character of the iMPs, cells were first produced until day 6 of differentiation for mouse and day 5 for human. At this point, iMPs could be cryopreserved or used fresh. On day 15 of spontaneous differentiation under basal media without cytokines, we performed qPCR on markers of various mesoderm lineage ordinarily present in the heart, including cardiomyocyte (Myh6, Tnnt2, and Actc1), vascular endothelial cells (Pecam1 and Cadh5), smooth muscle cells (Myh11), and

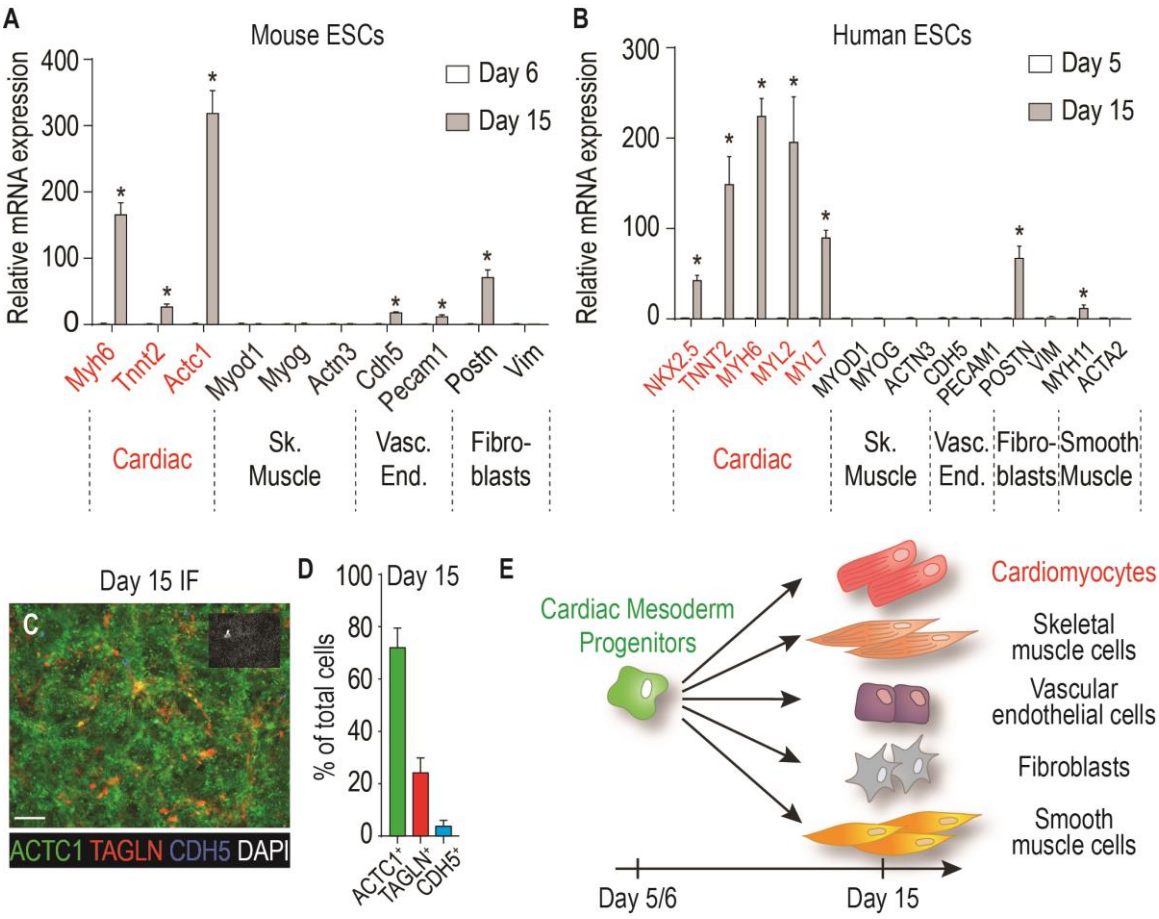

Figure 2.4 The multipotency of CMP. (A) qPCR result of mESC-derived CMP on markers of mesoderm lineages. (B) qPCR result of hESC-derived CMP on markers of mesoderm lineages. (C–D) IF and quantification result of day 15 hESC-derived CMP. (E) Schematic diagram of the multipotency of CMP.

fibroblasts (Postn and Tagln) as well as immunofluorescence staining [Figure 2.4A–B]. Both mouse and human iMPs were able to give rise to multiple lineages, and most importantly, the vast majority of the cells derived from iMPs were ACTC1^{+} cardiomyocytes [Figure 2.4C–E].

In addition to identifying the cardiogenic aspect of these iMPs, we further investigate the function of the iMP-derived cardiomyocytes which includes the rhythmical contraction behavior, electrical excitability, calcium-induce calcium release (CICR) mechanism, and response to hormonal stimuli. High-speed microscopic kinetic imaging revealed the rhythmical contraction activities of day 15 iMP-derived cardiomyocytes [Supplement 2.1]. By labeling cells with voltage-sensing probes or fluorescent calcium indicator, we observe periodic action potential activities and CICR cycles [Figure 2.5A–D]. Additionally, these cardiomyocytes showed increase beat rate in response to β-adrenergic agonist Isoproterenol [Figure 2.5E–F]. In summary, we have identified a novel pathway to generate multipotent CMPs that spontaneously differentiate into functional cardiomyocyte efficiently.

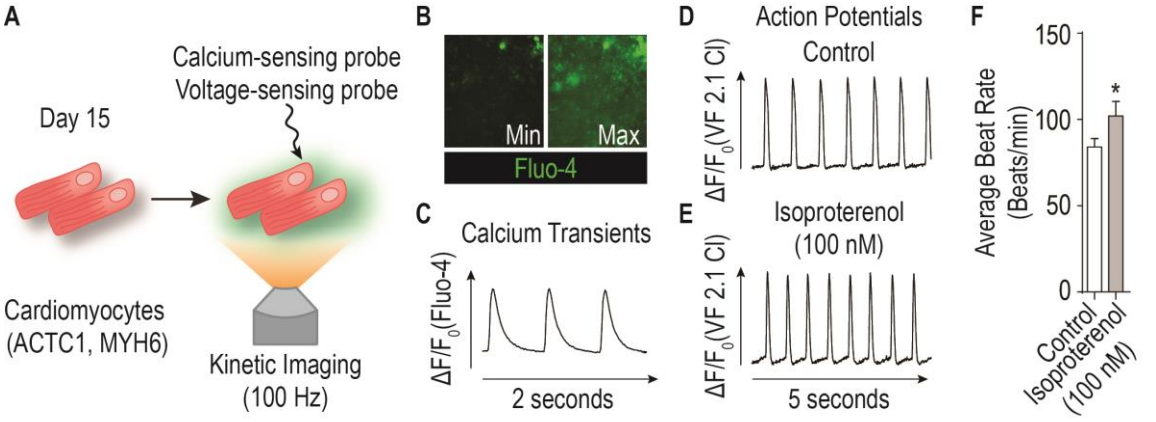

Figure 2.5 Functional assessment of resulting CM. (A) Schematic diagram of functional assessment protocols. (B–C) Calcium-sensing probe recording and calcium transient trace. (D) Action potential trace in the baseline condition. (E) Action potential trace of CM abruptly treated with isoproterenol (100 nM) (F) Quantification result on the average beat rate of baseline and isoproterenol-treated CM.

2.2.3 Id1 Promotes Cardiac Mesoderm Differentiation by Binding and Inhibiting Tcf3 and Foxa2

As a family member of HLH protein, Id1 regulate gene expressions through forming heterodimers with basic-helix-loop-helix (bHLH) transcription factors rather than directly binds with the DNA [4]. The canonical binding targets are class I bHLH transcription factors, also known as E proteins, Tcf3, Tcf4, and Tcf12 [4-6]. To elucidate the regulatory network during mesoderm differentiation, we examined whether the down-regulation of E proteins with siRNA individually or in combinations were able to phenocopy the result of Id1 overexpression promoting Kdr^{+} mesoderm progenitor formation in mESCs during the mesoderm specification process. All combinations promote mesoderm formation and interestingly, the combinations that contain siTcf3 have a better yield of CMP compares to other combinations without siTcf3 [Figure 2.6A–C]. The inhibition of Tcf3 through heterodimerization with Id1 plays a crucial role in mesoderm specification. Although studies implicated Tcf3 as a direct binding target of Id1, the down-regulation of Tcf3 could only partially phenocopy the result of inducing mesoderm formation through siAcvr1b or Id1 overexpression.

To further identify additional roles of how Id1 mediates mesoderm induction, we hypothesized Id1 might promote mesoderm formation through down-regulating the repressors of cardiogenic mesoderm formation. Thus, genes identified in microarray that were down-regulated in response to siAcvr1b at day 4 mesoderm differentiation could be potential cardiogenic mesoderm repressors regulated by Id1. We identified 53 gene candidates, and 17 were validated through qPCR [Figure 2.6D]. We then verified whether down-regulating any of these 17 genes through siRNA would be sufficient to induce MCP

formation. Out of these 17 genes, only the knock-down of Foxa2 was sufficient to promote Kdr^{+} mesoderm progenitor formation without the attenuation of Acvr1b signal [Figure 2.6E–F]. Although no reports have shown that Id1 has direct interaction with forkhead

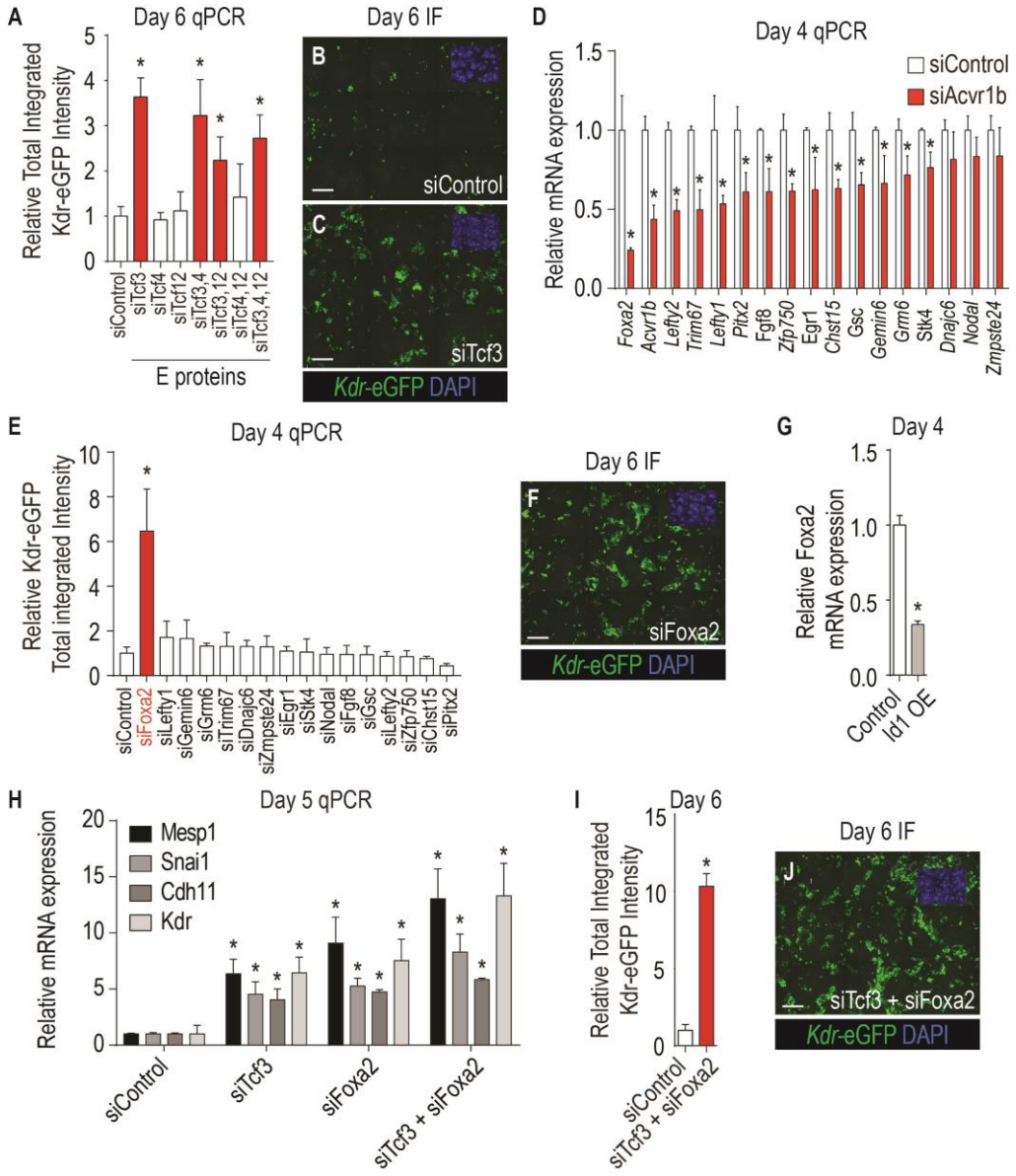

Figure 2.6 Id1 promote mesoderm formation mainly by inhibiting endoderm genes Tcf3 and Foxa2. (A) Down-regulation of canonical binding partner Tcf3 promotes mesoderm formation. (B–C) IF result of down-regulation Tcf3 promotes mesoderm formation. (D–F) Identification of Foxa2 as an inhibitor of mesoderm differentiation. (G) qPCR result shows Id1 inhibits Foxa2 expression level. (H–I) Downregulation of Tcf3 and Foxa2 increase mesoderm marker expression. (J) IF result shows the downregulation of Tcf3 and Foxa2 partially recapitulate Id1 overexpression phenotype.

transcription factors, in the constitutively Id1-overexpressing mESC, the expression level of Foxa2 was strongly decreased on day 4 of differentiation, indicating that Id1 may indirectly inhibit the expression of Foxa2. [Figure 2.6G].

As predicted, Kdr^{+} mesoderm progenitor induced by Tcf3 and FoxA2 knock-down expressed a prominent level of mesoderm markers (Mesp1, Snai1, Cdh11), and co-transfection of siRNA against Tcf3 and FoxA2 further enhances the differentiation of cardiogenic mesoderm [Figure 2.6H–J]. Taken together, these results clarify the regulatory network of Id1 promoting MCP formation partially through forming heterodimers with canonical binding target Tcf3 and repressing the antagonist of mesoderm formation Foxa2.

2.2.4 Id genes are essential for early heart development *in vivo* in mammalian

To further identify the role of Id gene family *in vivo* during heart development, first, we used Xenopus embryo as our validation platform. Since Xid2 is the closest ortholog to mouse Id1 (with amino acid sequence 79% identical and 93% positive), we performed equatorial and hemilateral injection of Xid2 mRNA directly to the embryo [Figure 2.7A–B]. Xid2 injection caused a dramatic expansion of mesoderm tissue, stained with Xbra and Xmespb in gastrula stage embryos [Figure 2.7C–F]. Next, to examine the underlying mesoderm has cardiogenic differentiation ability, Xnkx2-5 expression was assessed at the tailbud stage (stage 25). Remarkably, the overexpression of Xid2 massively induced the expression area of Xnkx2-5, and conversely, the area marked by skeletal muscle marker Xmlc remained unchanged [Figure 2.7G–I]. Collectively, these data show that the mechanism of Xid2 in Xenopus embryos, ortholog to mouse Id1 in the mESC, has an evolutionarily conserved function of promoting the formation of cardiogenic mesoderm.

The gain-of-function experiment shows that Id proteins are sufficient to direct the formation of cardiogenic mesoderm *in vitro* (mESC and hESC) and *in vivo* (Xenopus embryo). We then further explore the requirement of Id protein during mesoderm differentiation. Total four members, Id1, 2, 4 and 4, are there in the family, and previous studies have performed triple-knockout (Id1, 2, and 3) in mouse and observed complex cardiac defects but did not completely ablate the heart [7]. We hypothesized that there are functional redundancy or compensatory activity between the Id family members. To further test the hypothesis, we performed whole Id family quadruple-knockout using CRISPR-Cas9 genome editing strategy in mouse embryos. To enhance the knockout efficiency, we designed single-stranded RNA guide against both the start codon (ATG) and the beginning

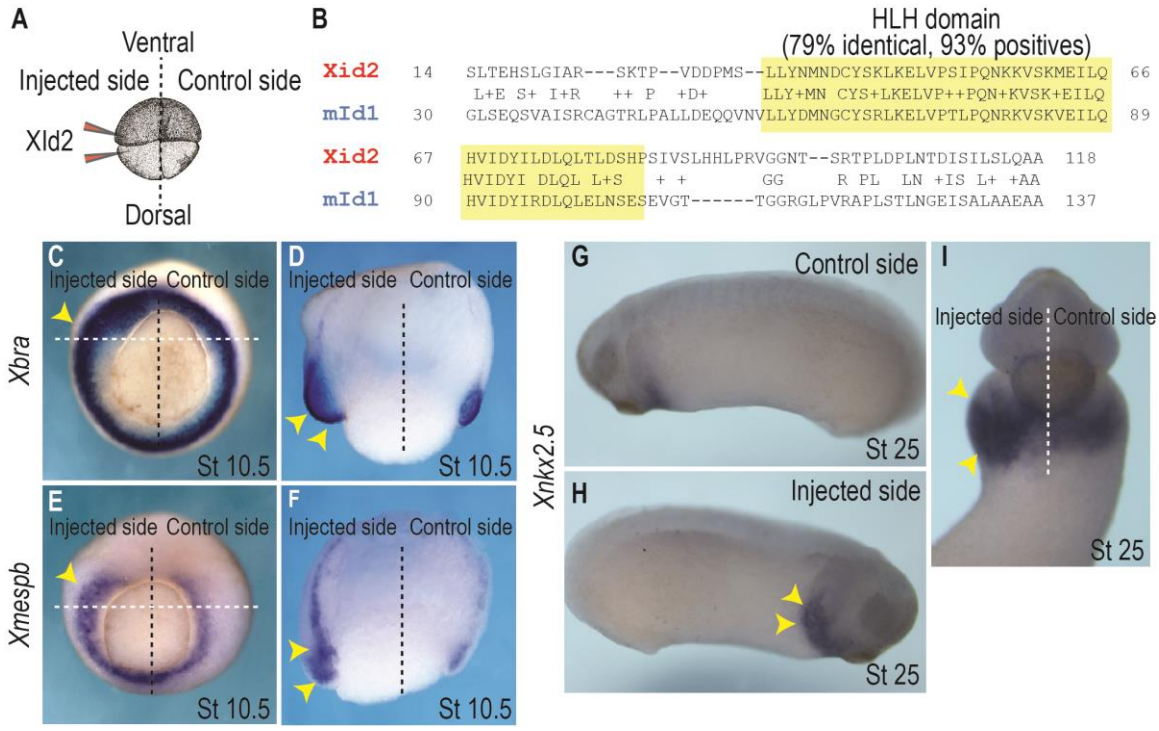

Figure 2.7 In vivo validation of Id genes gain of function. (A) Schematic diagram of injecting Xid2 into xenopus embryo. (B) Xid2 and Id1 sequence alignment. (C–F) Injection of Xid2 on only one side of the embryo enlarges mesoderm tissue. (G–I) Enlarged mesoderm tissue further differentiated into cardiac progenitors in later stage.

of HLH binding domain [Figure 2.8A]. Guide RNAs and Cas9 were injected into mouse zygotes and reimplanted back to a female surrogate mouse. Embryos were then harvested at various stages. In situ hybridization of the early cardiac precursors (Smarcd3 and Tbx5), and cardiac marker (Nkx2-5) were evaluated throughout the wild-type and Id1-4 mutants. Remarkably, the most anterior region of the cardiac crescent was missing in the Id1-4

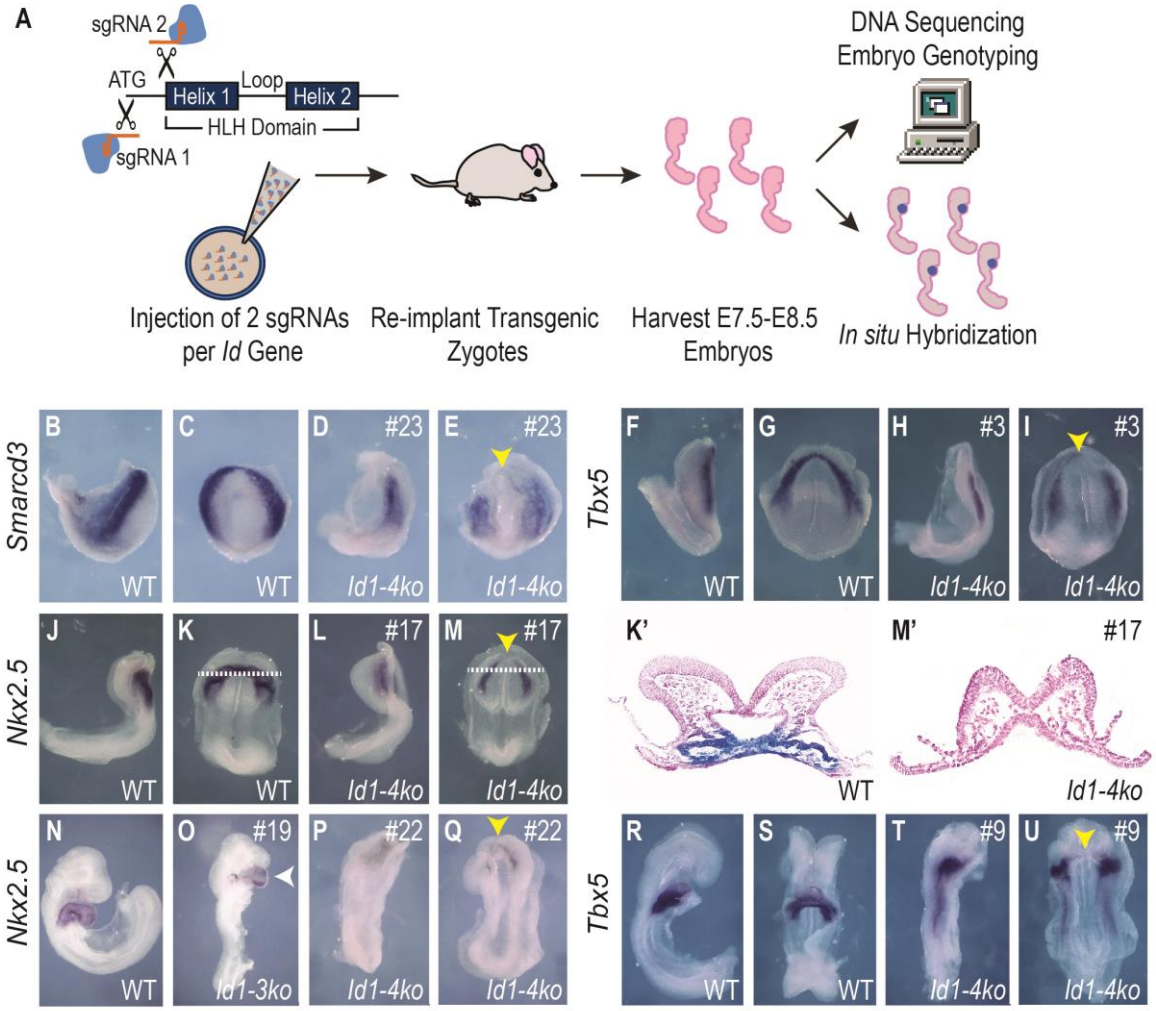

Figure 2.8 Id genes are essential during mammalian early heart formation. (A) Schematic diagram of generating Id genes mutant with CRISPR-Cas9 gene-editing tool. (B-U) In situ hybridization results from the most severe Id1–4 mutants—compared with wild type (individual mutants are marked by #) and plus one less-affected mutant (O); analysis of Smarcd3 at E7.75 (B-E), Tbx5 at E8.0 (F–I), Nkx2.5 at E8.25 (J–M; plus transverse sections through the heart tube-forming region [K′,M′]), Nkx2.5 at E8.5 (N–Q), and Tbx5 at E8.5 (R–U). (Yellow arrowheads) Missing heart tube (or missing heart tube-forming region at cardiac crescent stages) in Id1–4 mutants; (white arrowhead) malformed heart tube; (black arrows) the plane of transverse sectioning through the heart tube-forming region; (white dash lines) posterior–lateral cardiac regions.

mutant embryo stained with Smarcd3 and Tbx5 at E7.75 and E8.0 respectively. The two lateral domains in the posterior of the heart tube formation region remained in the mutant embryo suggested that mesoderm was only partially ablated and the remaining CMPs were able to migrate to the proper region [Figure 2.8B–M]. Histological sections demonstrated the absence of anatomical heart tube formation and failure of the foregut closure [Figure 2.8K'–M']. Moreover, at a slightly later time point, E8.25 and E8.5, due to the absence of the anterior region of the cardiac crescent, the embryo failed to form heart tube that normally looped at the time [Figure 2.8N–U]. In summary, the heart tubes were ablated in the whole-family Id1-4 knockout embryos indicate the requirement of Id family during *in vivo* cardiogenic mesoderm formation.

2.3 Discussion

2.3.1 Id Genes Orchestrated the Cardiogenic Mesoderm Differentiation *in vitro, in vivo,* and across Different Species

Activin/Nodal signaling thresholds dictate the cell fate decision of whether mesendoderm differentiates toward mesoderm or endoderm. High levels of activin have been shown favoring endoderm formation across different biological systems including mESC, hESC, zebrafish, Xenopus, and mice [8-11]. Through the blockade of Acvr1b signaling, we identified Id proteins in the downstream acts as a potent mesoderm agonist by up-regulating Evx1 and Grrp1, which are shown required during the mesoderm differentiation process, as well as repressing the antagonists of mesoderm formation, Foxa2 and Tcf3 [Figure 2.9]. The pro-mesoderm function of Id proteins can override the signaling

pathways of high concentration of Activin that leads to the endoderm program, indicating the molecular mechanism of Id proteins act in the down-stream of Activin signaling pathway. Consistent to our finding, studies have shown BMP signaling directly activates

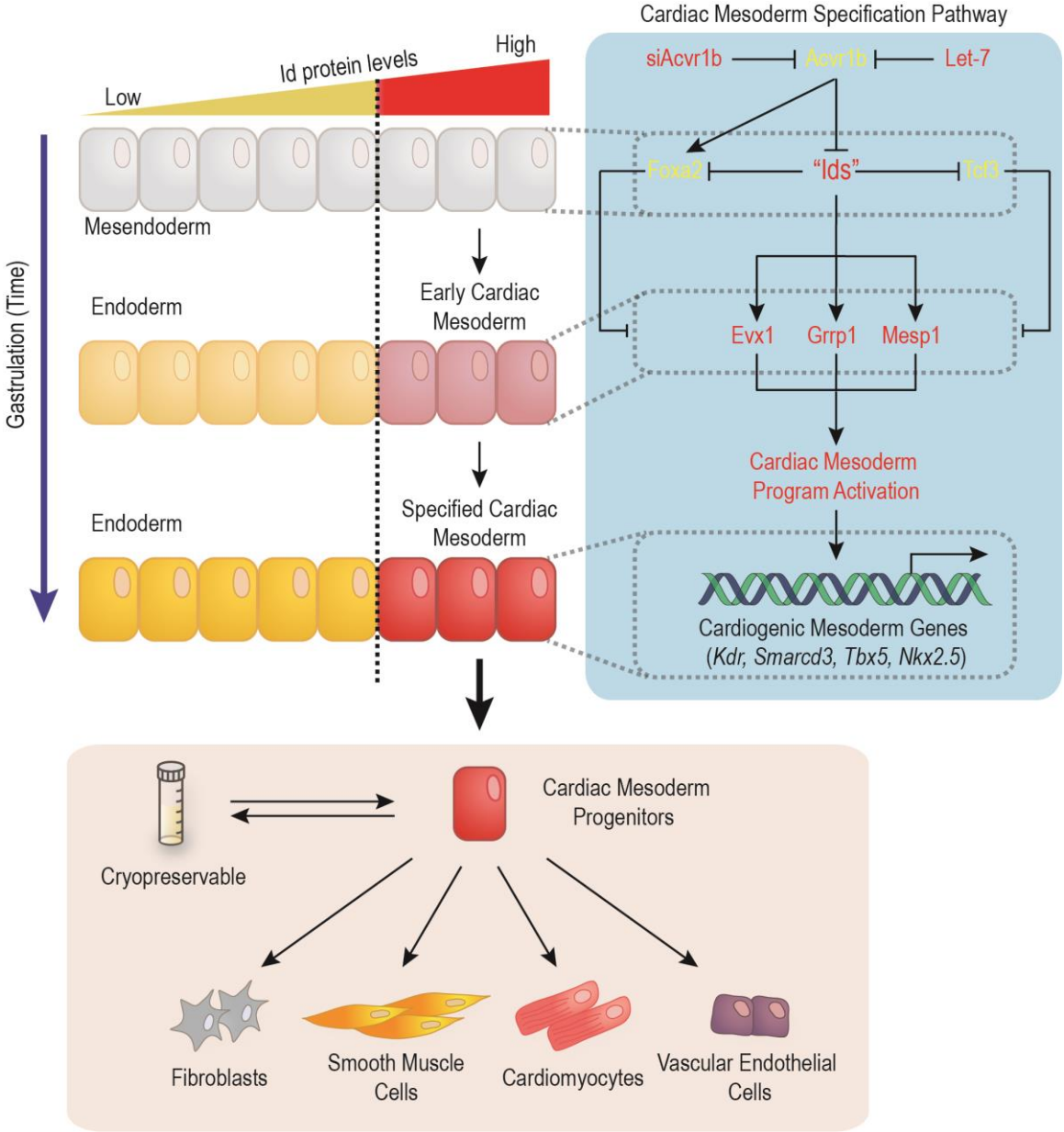

Figure 2.9 Id genes orchestrate cardiogenic mesoderm differentiation in vertebrates. Id genes control the activation of the cardiogenic mesoderm differentiation program in mesendoderm progenitors by inhibiting the activity of repressors (Tcf3 and Foxa2) while promoting the expression of activators of cardiogenic mesoderm differentiation (Evx1, Grrp1, and Mesp1). The Id-controlled network induces cardiogenic mesoderm (Mesp1 and Kdr) differentiation from pluripotent cells. Id1-induced CMPs generated from pluripotent stem cells are cryopreservable and spontaneously form contracting cardiomyocytes as well as vascular endothelial cells,,smooth muscle, and fibroblasts.

the transcription of Id protein [12-15] and BMP signaling pathways have been known for inducing mesoderm progenitor by negatively regulates endoderm induction in mouse and Xenopus [16, 17]. Additionally, the blockade of BMP singling completely abolished mesoderm formation [11]. In conclusion, Id proteins act as a dominant molecular cue of mesoderm induction and play a central role in the evolutionary conserved regulatory network of the formation of CMP [Figure 2.9].

2.3.2 Id genes are required for cardiac progenitor that forms heart tube during cardiac development

Mesp1 is the earliest known marker of cardiac progenitor [18, 19], and the overexpression of Mesp1 promotes the specification of cardiac progenitors [20]. In our study, Mesp1 temporal expression data shows that the overexpressing Id1 in both mESCs and hESCs promotes the level of Mesp1/MESP1. Additionally, the direct injection of Xid2 mRNA in Xenopus embryo confirms the enlargement of Xmespb^{+} tissue area, which both suggest Id proteins expressed precedes and up-regulates Mesp1 [Figure 2.7E–F]. However, the cardiac progenitor population (Nkx2-5^{+} and Tbx5^{+}) is not entirely ablated in CRISPR-Cas9 induced Id1-4 knockout mouse embryos. The small fraction of lateral domains on both sides of the mesoderm posterior to the heart tube-forming region suggesting that these cardiac progenitors may have different origins than Id proteins-induced cardia progenitors [Figure 2.8H–I, L–M, P–Q, T–U].

Mammalian heart arises from a series complex morphogenetic process via cardiac progenitor originated distinctly, the first and second heart fields (FHF and SHF). The FHF give rise to the left ventricle and part of the atria and the SHF to the right ventricle, outflow

tract and part of the atria [21]. Colonel and molecular lineage tracing analysis of Mesp1-expressing cells within the cardiac tissue demonstrated that Mesp1 marks distinct classes of cardiac progenitors with limited lineage differentiation ability during gastrulation. Early (E6.5) and more anterior $Mesp1^{+}$ mesoderm progenitors first give rise to the FHF, whereas late (E7.5) and more posterior $Mesp1^{+}$ mesoderm progenitors to SHF [22]. Together, these observations suggest that cardiomyocytes arise from the early Mesp1 activation, due to the induction of Id proteins, contribute to the FHF derivatives. Additionally, RNA expression data show that Id1-induced cardiomyocytes express high levels of FHF markers (HCN4 and TBX5) and down-regulated SHF markers (ISL1 and SIX2) during cardiac differentiation. Thus, these findings suggest that there are at least two different distinct populations of CMPs, Id-dependent and Id-independent, which very likely to give rise to FHF and SHF respectively.

2.3.3 Id1-induced Cardiac Mesoderm Progenitors as a novel, robust, and efficient way of generating Cardiomyocytes

In this study, we show the importance of the role of Id protein during cardiogenic mesoderm differentiation as well as the evolutionarily conserved mechanisms across different species and systems, including mESCs, hESCs, hPSCs (data not shown), Xenopus, and mouse. The cardiac-centric, single-factored Id proteins signaling transduction allowed us to have simple, robust, and tight controls over cardiac differentiation. Also, the ability to cryopreserve MCPs and uncouple cardiogenic progenitor generation from subsequent cardiomyocyte differentiation production allows us to bank, validate, and access to different batches easily. Furthermore, the resulting

cardiomyocytes were functionally validated which displayed rhythmic action potential and calcium handling, as well as being able to respond to hormonal stimuli. The average cardiomyocyte differentiation efficiency (percentage of $ACTC1^+$ cells over $DAPI^+$ cells) is around 85%. Also, the simple protocol could easily be scaled up into the 15-cm petri dish format that generates a large number of cardiomyocytes ($>10^8$ per batch). Taken these features together, Id1-induced CMP is a promising new protocol for varies applications, including deciphering gene networks regulating heart development and studying fundamental mechanisms controlling cardiomyocyte physiology. The resulting cardiomyocytes have the potential for transplanting and abilities to regenerate in patients after heart injuries and myocardial infarction. Lastly, generating hESC or hPSC-derived cardiomyocytes efficiently provides the field materials for patient-specific cardiac disease modeling and high-throughput screenings to identify disease mechanisms and drug discovery.

2.4 Conclusion

This study presents Id genes are crucial regulators during mesoderm differentiation. Through the microarray screening, we have identified Id1 is required and sufficient to promote mesoderm cardiac mesoderm formation. Moreover, the result shown Id1 induces mesoderm by up-regulating downstream mesoderm genes, including Kdr and Mesp1, as well as inhibiting the functions of endoderm genes, such as FoxA2. The resulting Id1-induced CMP could differentiate into CM efficiently. Furthermore, the in vivo gain of function result indicates the enlarged cardiac mesoderm progenitor region could later give

rise to cardiac tissue. The CRISPR-Cas mediated loss of function demonstrated the essential role of Id genes during mammalian early heart formation.

Acknowledgements

This chapter contains material partly from “Id genes are essential for early heart formation” by Thomas Cunningham*, Michael S. Yu*, Wesley Mckeithan*, Sean Spiering, Florent Carrette, Chun-Teng Huang, Paul J. Bushway, Matthew Tierney, Sonia Albini, Mauro Giacca, Miguel Mano, Pier Lorenzo Puri, Alessandra Sacco, Pilar Ruiz-Lozano, Jean-Francois Riou, Muriel Umbhauer, Greg Duester, Mark Mercola, and Alexandre R. Colas (*co-first authors), which has been published in *Genes and Development, 2017*. The dissertation author was the co-first investigator and author of this paper.

Chapter 3

The Establishment of Id1-induced hPSC-derived Ventricular-like and Atrial-like Cardiomyocytes

3.1 Background

The generation of a significant amount of functional human pluripotent stem cell-derived cardiomyocytes (hPSC-CM) of defined heart field origin is a prerequisite for studying cardiac diseases in large-scale screenings, disease modeling, and cell-based regenerative therapies. The mammalian heart is originated from the first and second heart field (FHF and SHF) that further developed into a four-chambered organ. Atriums served as reservoirs for receiving and delivering blood from the systemic and pulmonary veins, and ventricles expel blood back to the lungs and body. Given the fact of diverse physiological properties and distinct development origins, studies have shown major differences between atrial and ventricular cardiomyocyte in multiple aspects including cell morphology, gene and protein expression landscape, and electrophysiology [23, 24].

Additionally, the intrinsic differences between the subtypes also contribute to distinct chamber-specific cardiomyopathies. For instance, hypoplastic left heart syndrome or arrhythmogenic right ventricular dysplasia occurs only in the ventricles, whereas atrial fibrillation takes place in the atriums [25-27]. Current chamber-specific disease studies and preclinical screening assays are mainly performed using non-cardiac recombinant cell lines expressing non-native cardiac genes, mixed population culture of cardiomyocyte subtypes, or non-primate animal models. However, these models may not accurately reflect as a physiologically relevant biological system. To overcome the limitations, a highly efficient subtype-specific hPSC-CM differentiation technique is required for the study and development of novel therapies and disease modeling in a subtype-specific manner.

3.2 Results

3.2.1 Retinoic Acid Promotes Atrial Specification During Cardiomyocyte Differentiation

Several studies have described efficient cardiomyocyte differentiation protocols [28-34]. However, none have discussed the heart field origin of the resulting cardiomyocytes. Retrospective lineage analysis and genetic tracing have shown two distinct populations of cardiac progenitors contribute the FHF and SHF during heart development in varies vertebrate systems, where FHF progenitors would than give rise to the left ventricle and part of atriums [35-38]. Furthermore, several studies have reported RA signaling drives mesodermal progenitors toward an atrial fate in mouse, rat, hESC, and hPSC system, indicating the mechanism of RA inducing atrial cardiomyocyte is essential

and conserved across vertebrates [39-42]. Thus, we postulated Id1-induced hPSC-CM, originated from the first heart field, have the potential to differentiate into VCM in spontaneous differentiation condition, and ACM by activating RA signaling pathway.

To test the hypothesis, first, we ask whether promoting RA signals to Id1-induced CMP would affect cardiogenic potential [Figure 3.1A]. We provided different concentrations of RA cues on day 5 Id1-induced CMP and performed ACTC1 immunofluorescent staining on day 15 [Figure 3.1B]. The result shows that the RA

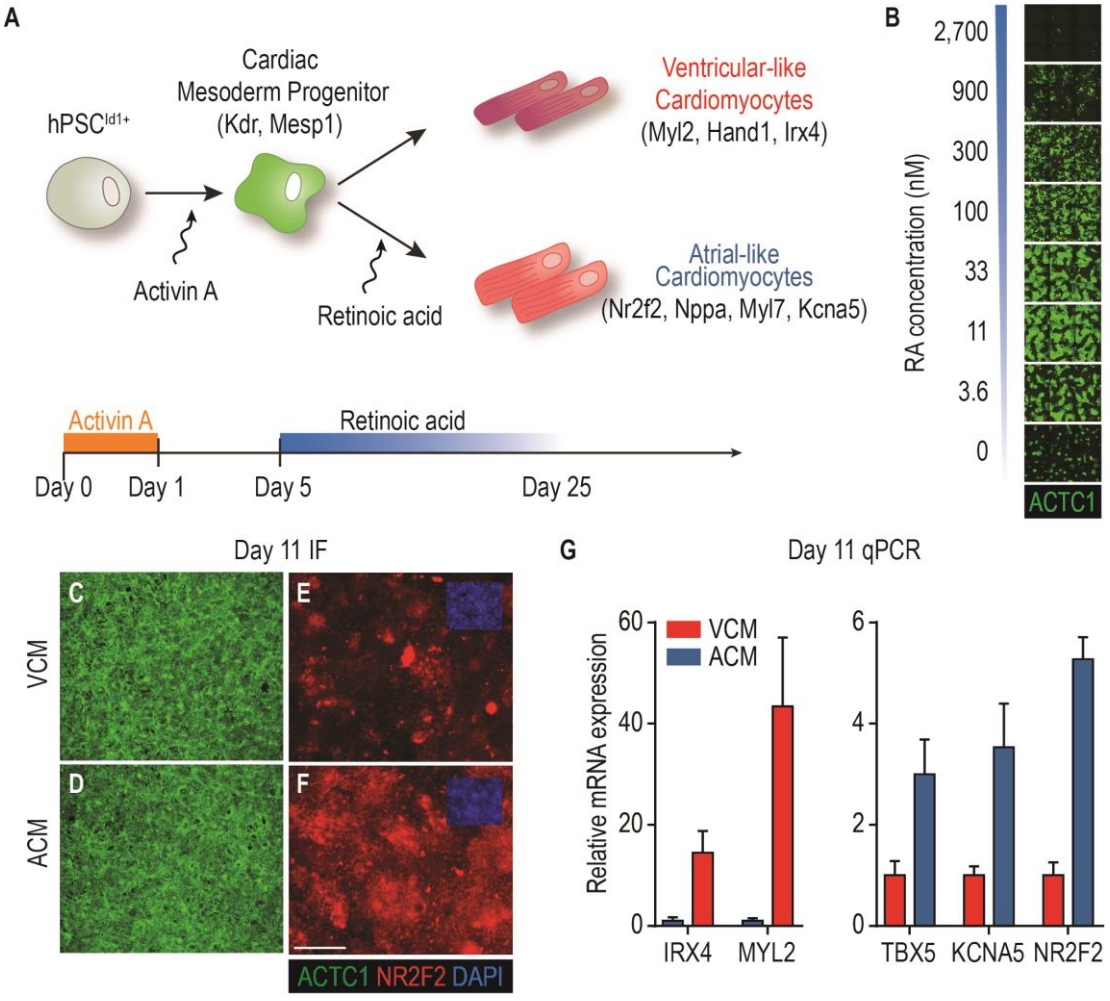

Figure 3.1 CM subtype (ventricular and atrial-like CM) differentiation. (A) Schematic diagram of CM subtype differentiation protocol. (B) RA dose-dependent cardiac differentiation efficiency indicates optimal dose range of RA during ACM differentiation. (C–D) Cardiac differentiation efficiency is not effected by the addition of RA. (E–F) Atrial-specific transcription factor NR2F2 was highly expressed in the RA-induced ACM. (G) qPCR showed subtype-specific marker genes were highly expressed in CM subtypes.

concentration between 30 nM to 300 nM, the cardiac differentiation efficiency was not substantially affected. Also, the optimal RA concentration that has minimal impact on differentiation is cell-number dependent, for example, 384-well plate format with 2 x 10^4 cells, media volume 100 µl per well and RA concentration 160 nM. Thus, RA molecules-per-cell could be calculated as 8 x 10^{16} mole per cell, and the concentration varies according to different differentiation format. Collectively, we established optimal RA concentrations for various plating formats without reducing the efficiency of cardiomyocyte differentiation compared to the spontaneous basal media differentiation.

Next, to validate the molecular differences between spontaneous differentiated CMs and RA-treated CMs, we selected NR2F2 as the marker for ACM. Based on previous reports, orphan nuclear receptor transcription factor NR2F2 (COUP-TFII) regulates atrial identity in mouse and leads to severe atrial abnormalities in loss-of-function mouse mutant [43, 44]. NR2F2 expression level was substantially up-regulated in the RA-treated condition comparing with the spontaneous differentiation on day 15 CMs [Figure 3.1C–F]. Additionally, we performed qPCR on ventricular (IRX4 and MYL2) and atrial marker genes (TBX5, KCNA5, and NR2F2). The ventricular markers were significantly expressed in CMs with spontaneous differentiation, and in contrast, atrial markers were markedly up-regulated in RA-treated condition [Figure 3.1G]. In summary, based on the immunofluorescent and qPCR results, Id1-induced CMPs spontaneously differentiate into VCM, and with exogenous addition of RA during cardiomyocyte differentiation, CMPs are effectively directed toward ACM.

3.2.2 Unbiased Transcriptome-wide Analysis Identify Distinct Cell Populations Representing Ventricular-like and Atrial-like Cardiomyocyte

To further elucidate the differentially active molecular programs between CM subtypes, we performed the whole transcriptome RNA sequencing (RNA-seq) on ACM and VCM at two different time points, day 13 and day 25 of differentiation [Figure 3.2A].

Fibroblast growth factor (FGF) signaling pathway has been found to directly regulate transcription factors that mediate the formation of ventricles [45]. FGF family members FGF8 and 10 are highly up-regulated in the VCM. The receptor FGFR, as well as the downstream target of FGF signaling including ETS1, ETV5, HES1, and FOXC1, were differentially expressed in the VCM. Also, NOTCH signaling plays an essential role in balancing the proliferation and differentiation during heart development. More specifically, NOTCH signaling pathway regulates cell fate decision and is crucial for ventricular chamber development [46]. NOTCH2 and its downstream targets BMP10, NRG1 and HES1 were highly expressed in the VCM. HOPX, transcription factor that binds and regulates HDAC2, which has been known to strictly controlling left ventricle function, is also up-regulated. Additionally, SOX6 as an inhibitor of NPPA, a well-studied atrial marker, was also differentially and explicitly expressed in the VCM.

In contrast, in the early time point (Day 13), targets of RA signaling, including RORA, HOXB3/4, and NFY-B were found increased in ACM. Master regulator of the atrial specification, NR2F2, also known as COUP-TF II, was differentially expressed in ACM [43]. Also, TBX5, TBX20, and GATA6, crucial atrial-specific transcription factors during development, were highly expressed in ACM. In the later time point (Day 25), NPPA and NPPB were also highly expressed in the ACM, which have been shown

regulating multiple aspects of atrial function [47]. Several transcription factors related to the expression of NPPA were all differentially expressed in ACM, including the up-stream targets, GATA6 and ATF2, and the down-stream targets JUNB, EGR1, EGR2, and EGR3. Transcription factor PITX2, known for the co-regulation of multiple atrial-specific genes with TBX5, was up-regulated in ACM. Atrial-specific metabolic enzyme TECRL was highly expressed in ACM. Lastly, HIF3A and SMAD9, related to atrium development and function, were overexpressed in ACM. In summary, we identified several transcription factors related to FGF and NOTCH signaling, ventricular morphology and functions were up-regulated in VCM. Conversely, transcription factors in the RA signaling pathway, NPPA regulatory network, as well as atrial-specific metabolic enzyme TECRL, were differentially expressed in ACM.

CM subtypes also display functional differences in action potential morphology and contractility. These differences could also reflect on differentially expressed ion channels and contractile proteins between the subtypes. KCNA5, responsible for atrial-specific ultrarapid delayed rectifier potassium inward current I_{Kur}, and KCNJ3, member of G protein-coupled inwardly-rectifying potassium channel I_{KACh}, were both up-regulated in ACM. Myl2, a structural protein that is responsible for ventricular sarcomere formation, was up-regulated in the VCM. However, we did not observe remarkably expression differences in Myl7, which is an atrial-specific isoform of myosin light chain. GJA5, a protein component of gap junctions that expressed exclusively in atrial myocytes and is crucial for electrical impulse conductions, was significantly expressed in the ACM. Next, we performed principal component analysis (PCA) upon populations and asked whether the analysis could distinguish distinct CM subtypes arise from our differentiation protocol

unbiasedly. Informative PCA components clustered cells into four groups [Figure 3.2B]. Clusters were clearly segregated by temporal differences (PC1) and CM subtypes (PC2). Moreover, gene ontology result also reveals several gene cluster differences between VCM and ACM. They could be categorized into three major groups: (1) Ion channels and action potential; (2) Cardiac conduction; and (3) Muscle development and contraction. With all the gene ontology terms (GO-terms) fold enrichment > 9, there are total 4 related to ion channels and action potential, "Membrane depolarization during SA node cell action

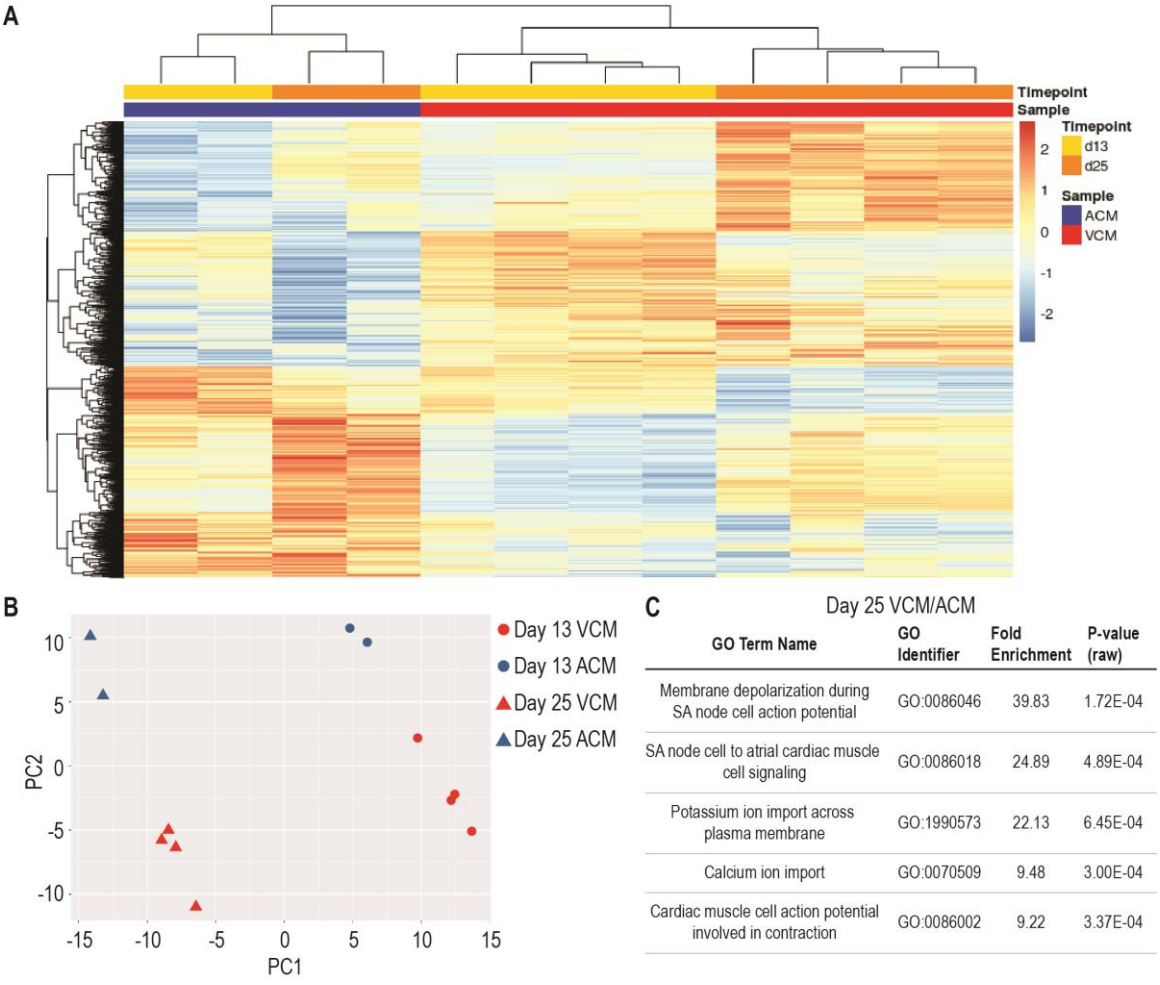

C

Day 25 VCM/ACM

GO Term Name	GO Identifier	Fold Enrichment	P-value (raw)
Membrane depolarization during SA node cell action potential	GO:0086046	39.83	1.72E-04
SA node cell to atrial cardiac muscle cell signaling	GO:0086018	24.89	4.89E-04
Potassium ion import across plasma membrane	GO:1990573	22.13	6.45E-04
Calcium ion import	GO:0070509	9.48	3.00E-04
Cardiac muscle cell action potential involved in contraction	GO:0086002	9.22	3.37E-04

Figure 3.2 Molecular validation of CM subtypes in two different timepoint (VCM at day 13, VCM at day 25, ACM at day 13, ACM at day25). (A) RNA-sequencing result of all four conditions showed distinct gene expression culsters. (B) Four major clusters were observed in principle component analysis. (C) Five GO-term related with cardiac functions with fold enrichment > 9 were listed, indicates differentially expressed genes in CM subtypes results in functional difference between CM subtypes.

potential" (GO:0086046), "Cardiac muscle cell action potential" (GO:0086001), "Potassium ion import across plasma membrane" (GO:1990573), and "Calcium ion import" (GO:0070509). Next, there are 3 GO-terms involved in cardiac conduction, "Cell-cell signaling involved in cardiac conduction" (GO:0086019), "Regulation of heart rate by cardiac conduction" (GO:0086091), and "Cell communication involved in cardiac conduction" (GO:0086065). Lastly, 4 GO-terms that could be categorized in muscle development and contraction, which include "Cell migration involved in heart development" (GO:0060973), Cardiac muscle cell action potential involved in contraction" (GO:0086002), and "Cardiac muscle cell contraction" (GO:0086003). These GO-terms coincide with the functional validation data of action potential, calcium transient, and contraction showed in the following section.

3.2.3 Action Potential Assessment on Ventricular-like and Atrial-like Cardiomyocyte

Heart, responsible for propelling blood throughout the body and lungs, has precise and sophisticated mechanisms to initiate and maintain the contraction in rhythm throughout our entire lifespan. The pumping action requires highly coordinated efforts from the generation of action potentials to the CICR process that further triggers the contraction and relaxation of the muscle fibers[Figure 3.3A] [48]. Miss-regulations of the process could quickly lead to varies heart diseases, such as arrhythmia and cardiac arrest [49-51]. Cardiomyocytes in the atria and ventricles are functionally distinct in their electrophysiological and contractile properties [24, 52, 53]. Thus, a thorough

characterization of the cardiac physiology of VCM and ACM is essential for further applications.

The cardiac action potential can be categorized into five distinct phases; the membrane depolarization of rapid activation of inward Na^+ current (phase 0), followed by transient repolarization (phase 1), and a plateau phase due to the counterbalance between inward Ca^{2+} current and outward K^+ current (phase 2). Afterward, membrane potential quickly repolarized (phase 3) then restore back to the resting state (phase 4) and ready for another cycle [Figure 3.3B].

Whole-cell patch-clamp is a common technique used to measure the action potential and the activation/inactivation of the ion channels. Cardiomyocytes in the electrophysiological perfused chamber were patched by glass pipettes. The recording was

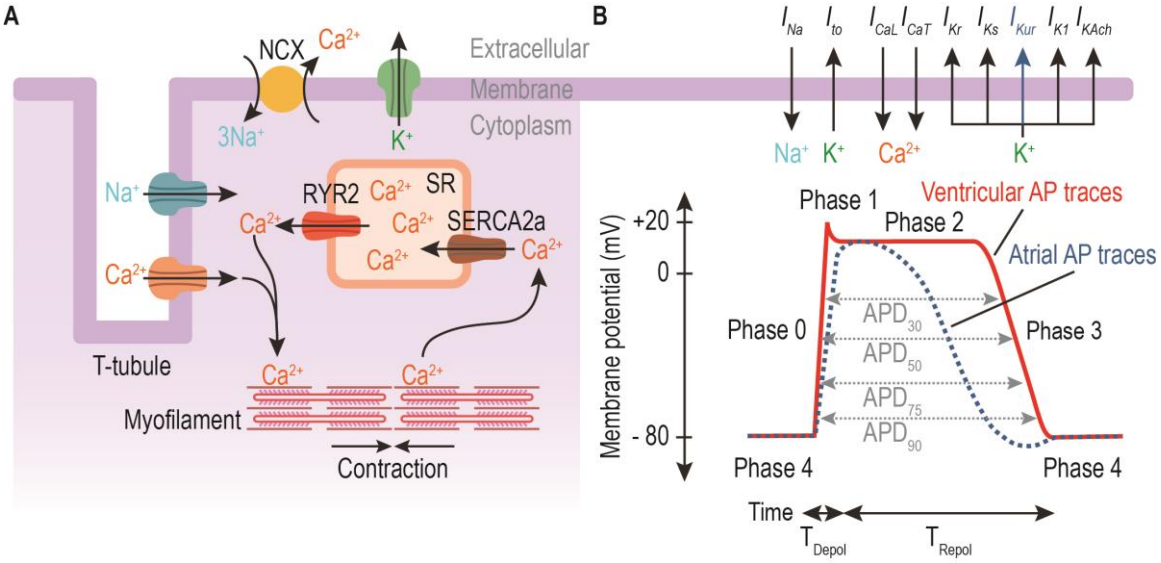

Figure 3.3 CM functional assement through action potential, calcium transient, and contractility. (A) Simplified CM function cartoon. Action potential: membrane potential is initiated by the activation/inactivation of various ion channels (Na^+, Ca^{2+}, and K^+). Calcium transient: elavated intracellular Ca^{2+} concentration then induces CICR cycle. Contractility: intracelluar Ca^{2+} bind and facilitate the contraction of myofilment. (B) Action potential traces is the synergistic result of a sequce of activation/inactivation of ion channels. The composition of ion channels are differentially expressed on the membrane of CM subtypes which leads to distinct action potential morphology. Various action potential durations (APDs), the depolariztion and replariztion time (T_{Depol} and T_{Repol}) are measured as parameters to discribe the shape of the action potential traces.

then performed in Tyrode's solution, and the current response was acquired using an amplifier. The result displayed that VCM had a faster and steeper upstroke during the phase 1 depolarization. The average APD_{75}) ranges between 200 to 300 milliseconds (ms), and the resting membrane potential (V_{Rest}) was around -60 to -80 millivolts (mV) [Figure 3.4A]. The ACM had shorter APD_{75} values, around 60 to 120 ms, and similar V_{Rest} to VCM [Figure 3.4B]. The action potential of VCM exhibits prolonged plateau phase 2, which is a typical hallmark of ventricular cardiomyocyte action potential traces, and in contrasts, the action potential traces of ACM showed a triangular-like morphology, which is the most pronounced difference between atrial and ventricular action potential waveforms.

To gain insight into the cardiomyocyte sub-type electrophysiology in a more unbiased and efficient way, we performed the action potential analysis on the automated high-throughput fluorescent-based kinetic image acquisition platform with McKeithan et

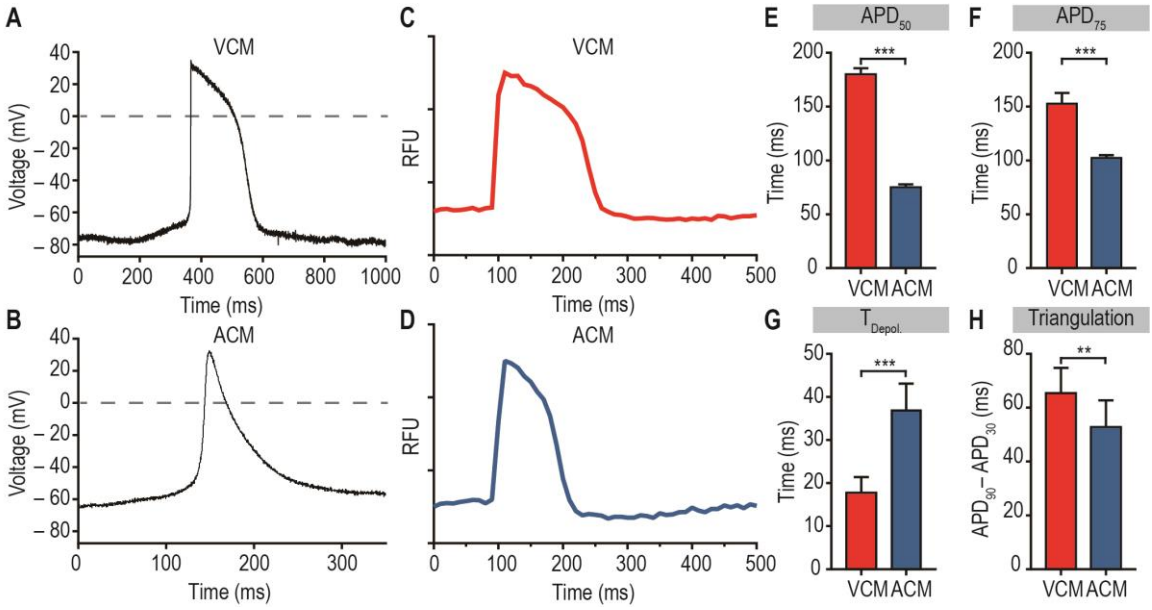

Figure 3.4 Action potential analysis indicates functional differences between VCM and ACM. (A–B) Patch-clamp electrophysiology demostrate action potential morphylogy difference between CM subtypes, where VCM has longer and plateu-like shape in phase 2, and ACM has a more triangular-like shape morphology. (C–D) Flourascent-based voltage-sensing probe analysis showed similar action potential morphoogy with patch-clamp elctrophyiology. (E–H) Quantification result of APD_{50}, APD_{75}, depolarization time (recorded under 225 Hz), and traiangulation.

al [54]. Briefly, this co-developed platform acquires time-series images with high-speed/high-resolution automated microscopy. Incubating cardiomyocytes with a fast response membrane potential sensitive probe (FlowVolt) which intercalates into the plasma membrane and senses changes in transmembrane potential by photo-induced electron transfer (PeT) mechanism enabled us to record membrane potential fluctuation through florescent signals [55]. Remarkably, action potential waveforms had matching features compared with traces retrieved from the whole-cell patch-clamp and published *in vivo* data, with prolonged phase 2 in VCM and triangular-shape in ACM [Figure 3.4C–F] [56]. We next examined the depolarize time (T_{Depol}) differences between the two sub-types. Utilizing the high frame-rate microscopy that is capable of recording up to 225 Hz, we could distinguish the temporal difference during the rapid depolarization of phase 1. Consistent with the result in whole-cell patch-clamp experiment and published data, VCM had faster Td_{epol} for less than 20 ms, and the time ACM took to reach full depolarize state is doubled [Figure 3.4G] [57]. Triangulation parameter (APD_{30} - APD_{90}) provide an additional aspect to quantify the plateau and repolarization phases of the action potential. As expected, due to the prolonging of phase 2 in VCM, it had greater triangulation, whereas, in ACM, the faster repolarization leads to lower triangulation [Figure 3.4H]. Collectively, consistent results in whole-cell patch-clamp and fluorescent-based kinetic image acquisition platform elucidate the action potential morphology differences between VCM and ACM, which in turn are the manifestations of the underlying different ionic currents in distinct cardiomyocyte subtypes.

3.2.4 Calcium Transient and Contractility Assessment on Ventricular-like and Atrial-like Cardiomyocyte

Calcium handling is the critical intermediary of the excitation-contraction coupling, the process of electrical stimulus triggering the contraction and relaxation of the muscle fiber. During the course of an action potential, the membrane was depolarized thereby inducing the activation of L-type calcium channels that activate the inward L-type Ca^{2+} current (I_{CaL}), which contributes to the plateau part of the phase 2 action potential. Cytoplasmic calcium ion concentration then accumulates and subsequently triggers the opening of the Ryanodine receptor type 2 (Ryr2) and induced massive Ca_{2+} release from the sarcoplasmic reticulum (SR) [48, 58]. The influx signal of inward Ca^{2+} is known as the "calcium sparks," and the process of Ryr2 activation induced by prominent levels of cytoplasmic Ca^{2+} concentration is named CICR. Significantly raised cytoplasmic Ca^{2+} level facilitates the binding of Ca^{2+} to the cardiac troponin, exposing myosin binding sites and switching on the contractile machinery. During the muscle relaxation phase, Ca^{2+} is mainly recycled through Sarcoplasmic reticulum Ca^{2+} ATPase (SERCA2a) back to the SR, partially got extruded out of the cell by Sarcolemmal Na^{+}/Ca^{2+} exchanger (NCX) [Figure 3.3A].

To better characterize and assess the calcium handling differences between VCM and ACM, we incubated cardiomyocytes with the fluorescent Ca^{2+} indicator (Flow4-NW) which emits strong fluorescence upon binding with cytoplasmic Ca^{2+}. We imaged cells under the kinetic image acquisition platform and calculated physiological parameters from the fluorescent-change-over-time calcium transient traces. As expected, the calcium transient duration from the induction to relaxation lasted much longer compared to the

action potential duration [Figure 3.5A–B]. Quantitatively, calcium transient duration at 50% and 75% of relaxation (CTD_{50} and CTD_{75}) of VCM is greater than ACM [Figure 3.5C-D]. Altogether, calcium transient morphology and CTDs showed distinct features of VCM and ACM, which also coincide with previously reported data [59].

In addition to calcium handling, contractile force production is the central participant of the excitation-contraction coupling machinery. To characterize the contractility differences between cardiomyocyte subtypes, we labeled the cellular membrane with wheat germ agglutinin (WGA), and record the contracting cardiomyocyte with the high-speed microscopy. By measuring the membrane movement with pixel-to-pixel comparison algorithm, we are able to retrieve the contraction speed and rate of the cell. The rate of active tension generation (T_{Rise}) and relaxation (T_{Decay}) were faster in ACM than VCM, which are consistent with previous findings [Figure 3.5E–H] [53]. In summary,

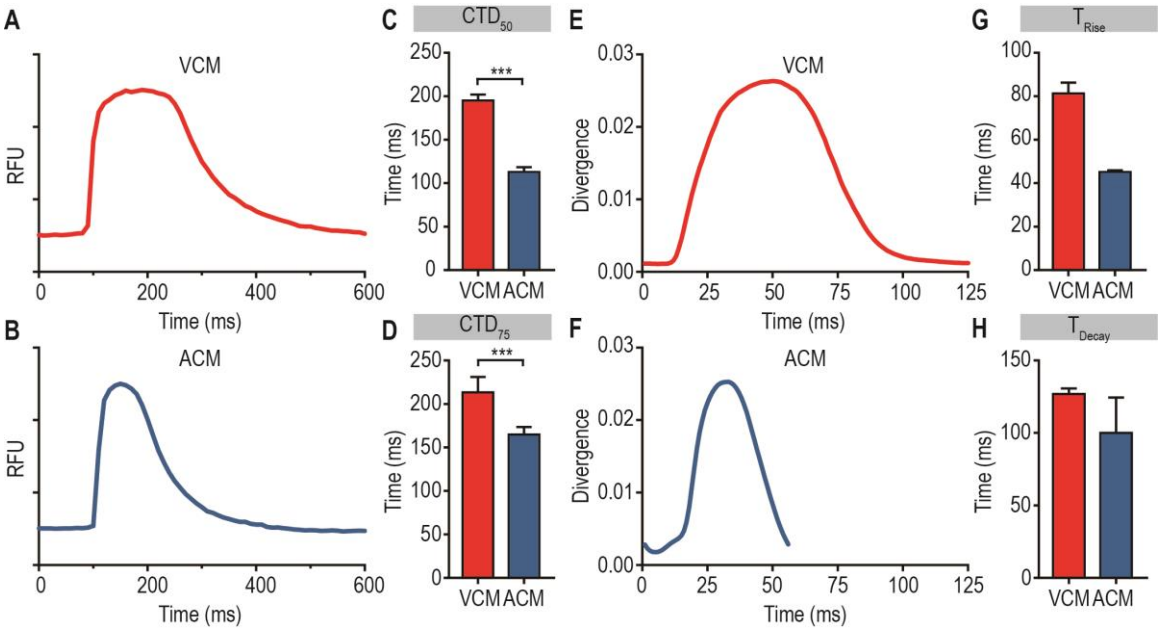

Figure 3.5 Distinct functional differences between CM subtypes on calcium transient and contractility. (A-B) Calcium transient analysis through calcium-sensing probe showed VCM has longer calcium transient duration compares to ACM. (C–D) Quantitative measeurment of CTD_{50} and CTD_{75}. (E–F) Pixel tracking algorithm reveals difference in contractility (contracting speed) between VCM and ACM. (G–H) Quntification result of contractility on curve rising and decay time (T_{Rise} and T_{Decay}).

we have functionally validated the subtypes on calcium handling and contractility. We concluded that VCM has elongated calcium transient morphology and slower contraction speed both in T_{Rise} and T_{Decay} comparing to ACM.

3.3 Discussion

3.3.1 Retinoic Acid Signaling is Crucial for Atrial-specification

During vertebrate development, body plan is determined by signaling gradients in complex spatiotemporal manner. RA has a central role during early embryogenesis and later stages of heart morphogenesis [60-62]. RA is synthesized through the oxidization of retinol (dietary vitamin A) to Retinaldehyde by Retinol dehydrogenase 10 (RDH10), then oxidizes to RA by Retinaldehyde dehydrogenase (RALDH2), and further inactivated into polar metabolites by cytochromes. As a lipophilic signaling molecule, RA binds to nuclear RA receptors (RARs) and forms RAR-retinoid X receptor (RXR) heterodimer complex that binds to DNA located by RA response elements (RAREs) and regulates the transcription of target genes. Forming complexes with co-activators and co-repressors allows RA to mediate the activation or repression of target genes [61, 63]. During embryo development, RA gradient is carefully governed by the generation and degradation machinery. The combination of opposite gradients such as fibroblast growth factor-8 (FGF8) and enzymatic inactivation of RA, enables the patterning and organogenesis of heart, liver, eye, forebrain, limb, and body axis [64-67].

The mammalian heart is formed by the migration, pattering, diversification, and acquisition of functions of cardiac progenitor cells. RA signaling has long been known to

play a critical part in heart morphogenesis, both excess retinoids and RAR or RXR knockout mouse models caused myocardial defects [68]. More specifically, vitamin A-deficient quail embryos had close caudal and failed to form sinoatrial tissue. Mouse embryos treated with RA synthesis inhibitor or RALDH2 knockout mutations also showed sinoatrial morphological defects [39, 69, 70]. Furthermore, the overexpression or down-regulation of TBX5, one of the downstream targets of RA signaling pathway, produced myocardial defects, indicating the essential role of RA regulating heart patterning and cardiomyocyte subtype-specification [71].

Consistent with our result, recent studies reported RA as an atrial-selective cue in the *in vitro* hPSC system [42, 72]. During differentiation, the addition of RA in early cardiac progenitor stage (Day 4-8), direct the differentiation towards ACM, conversely, spontaneous differentiation or applying RA inhibitor, BMS493, instruct the progenitor to become VCM. In summary, we successfully demonstrated cardiomyocyte subtype-specific differentiation from Id1-induced CMPs using RA as an atrial-selective cue.

3.3.2 Id1-induced Cardiomyocytes have Distinct Gene Expression Landscape between Subtypes

The opposing gradients of RA and FGF8 have been shown widely applied through the embryo body axis establishment and patterning of the heart [73, 74]. During heart chamber specification, the identity of cardiomyocyte progenitors remains relatively plastic. The role of FGF signaling in early-differentiation is to initiate ventricle development, and in later differentiation, to stabilize ventricular identify [45]. NOTCH, another crucial signaling pathway that involved in the specification of the ventricular CM subtype, is

shown active in the ventricular RNA-seq data [75]. NOTCH signaling is required in chamber patterning, ventricular myocardial differentiation. The activation of downstream NOTCH target also requires the NOTCH-dependent activity of BMP10 and NRG1 to promote the differentiation of ventricular myocardium, which could be seen up-regulated in the RNA-seq VCM data [46]. Lastly, the mutations in several NOTCH signaling elements underlie congenital heart diseases in the mouse model, indicating the importance of the signaling pathway during chamber specification [76, 77]. Collectively, the activation of FGF and NOTCH signaling suggest the ventricular-like identity in Id1-induced VCM.

FGF signaling in the atrium is mediated and repressed via the upstream RA response complex RAREs. The RA-FGF antagonism, activation of RA and repression of FGF signaling pathway, further enhance TBX5 and TBX20 expression during atrial specification *in vivo* [71]. Haploinsufficiency mouse model of Tbx5 showed structural defects in the atrium and abnormally prolonged P-waves during atrial depolarization [78]. Additionally, NPPA, an atrial-selective marker that has been extensively used for the studying of the subtype-specific differentiation and transcriptional regulatory pathways in cardiac gene regulation, is involved in multiple atrial-specific transcriptional pathways. NPPA, as a downstream responsive element of the NKX family, GATA family, and TBOX family, revealed its essential and selective role of the molecular mechanisms regulating regionalized cardiac expression and atrial subtype-specification [47, 79]. Atrial-abundant ultra-rapid delayed rectifier K^+ current (I_{Kur}) and acetylcholine-sensitive K^+ current (I_{KAch}), encoded by KCNA5 and KCNJ3, are the primary determinates of electrophysiological difference between CM subtypes. Ventricular CMs have a prolonged plateau-like phase 2

morphology, and atrial CM has shorter and triangular-like traces due to the selectively expressed K^+ channels I_{Kur} and I_{KAch} in humans [57]. The selective expression of KCNA5 and KCNJ3 in ACM from the RNA-seq result reflects the electrophysiological differences between Id1-induced VCM and ACM. In summary, various genes involved in atrial-specification during the heart development and chamber patterning, as well as in atrial physiology are up-regulated in the Id1-induced ACM, confirm the atrial-like molecular identity of the resulting ACMs.

3.3.3 Subtype-Specific Cardiomyocyte Differentiation Provides a Physiologically Relevant System for Cardiac Disease Modeling and Drug Discovery

Cardiomyocytes in the atria and ventricles are not only molecularly, but also functionally distinct. Functionally, they differ significantly in electrophysiology, calcium handling, and contractile properties. To generate stronger contraction force due to the increased calcium influx via L-type calcium channels in phase 2, VCM has faster depolarization speed and stronger inward sodium current (I_{Na}), as well as lesser transient outward current (I_{to}). The most noticeable difference in morphology of action potential between the subtypes is the duration of the depolarized plateau (phase 2). The membrane potential was carefully balanced by inward I_{CaL} through L-type calcium channels and outward potassium flux (I_K) through various potassium channels. To produce higher contraction force, stronger calcium influx and more extended calcium channel activation are required in VCM. Conversely, outward potassium currents, including slow (I_{Ks}), rapid (I_{Kr}), and inward delayed rectifier (I_{K1}) are stronger in ACM, along with atrial-abundant I_{Kur}, resulting in faster repolarization and shorter action potential duration [Figure 3.3B]

[24, 80]. Coherent with the result, Id1-induced VCM has more extended depolarized plateau and ACM has shorter and more triangular action potential waveform.

Due to strong activation of I_{CaL} and higher Ca^{2+} content in SR in VCM, the CICR cycle lasts longer, in contrast to ACM [81]. Moreover, SERCA2a, which involved in recycling cytoplasmic Ca^{2+} back into SR, is abundantly expressed in the atrial cardiomyocyte, which lowers systolic Ca^{2+} transient and therefore leads to rapid relaxation of the atrial myocytes [82]. Myofilaments require the binding of Ca^{2+} to reveal the myosin binding sites and initiate the contraction. Thus, elevated Ca^{2+} level in VCM produced stronger and long-lasting contraction forces. On the contrary, mechanistically, served as blood reservoirs for the passive and active filling of the ventricle, atria have both faster tension generation and relaxation than ventricle [53]. These findings correlate with our subtype-specific functional data of calcium transient and contractility rate in VCM and ACM. The results confirm the physiological relevance of Id1-induced cardiomyocyte subtypes and the potential of modeling cardiac disease in a subtype-specific manner.

3.4 Conclusion

To target the atrial-specific target space of AF, RA was administered to generate ACM from CMP. The resulting ACMs were than validated molecularly through qPCR, IF, and RNA-seq. The data suggest atrial-specific genes were highly expressed in the ACM, whereas the ventricular-specific genes were up-regulated in the VCM. Furthermore, the differentiated CM subtypes were also functionally validated in action potential, calcium

transient, and contractility. All 3 functional aspects resemble the physiology features observed in adult human cardiomyocyte subtypes. In summary, the resulting ACM present atrial-specific features both molecularly and functionally.

Acknowledgements

This chapter contains material partly from “Generation of First Heart Field-Like Cardiac Progenitors and Ventricular-like Cardiomyocytes from Human Pluripotent Stem Cells” by Michael S. Yu*, Sean Spiering*, and Alexandre R. Colas (*co-first authors), which has been submitted to *Journal of Visualized Experiments* and is currently in press. The dissertation author was the co-first investigator and author of this paper.

Chapter 4

Single-cell High-throughput Functional Screening Platform for Arrhythmia Modeling

4.1 Background

Being able to generate unlimited amounts of Id1-induced hPSC-derived ACM and VCM made connecting gene variants to disease phenotypes, modeling cardiac disease in-a-dish, and conducting large-scale screens for discovering novel therapeutic targets possible. However, a major hurdle of implementing the cells for further application is the lack of throughput due to conventional methods, that are costly, time-consuming, and technically challenging. To better advance the efficiency and increase the robustness for monitoring action potential and conduct *in vitro* phenotypical screenings, we established a subtype-specific cardiomyocytes high-throughput platform with single-cell resolution functional readouts. This platform integrates automated liquid handler, high-speed

microscopy with the optical recording of fluorescent dyes, which enable the monitoring of membrane potential, calcium transient, or contractility [Figure 4.1A–C]. Furthermore, the analysis algorithm enables the segregation of single-cell level cellular autonomous activity from the whole-well, providing an in-depth physiological matrix for individual cardiomyocytes [Figure 4.1D–F]. The technique can be readily adapted to common high content automated imager to study cardiomyocyte physiology in vitro for arrhythmia modeling and phenotypical screening applications.

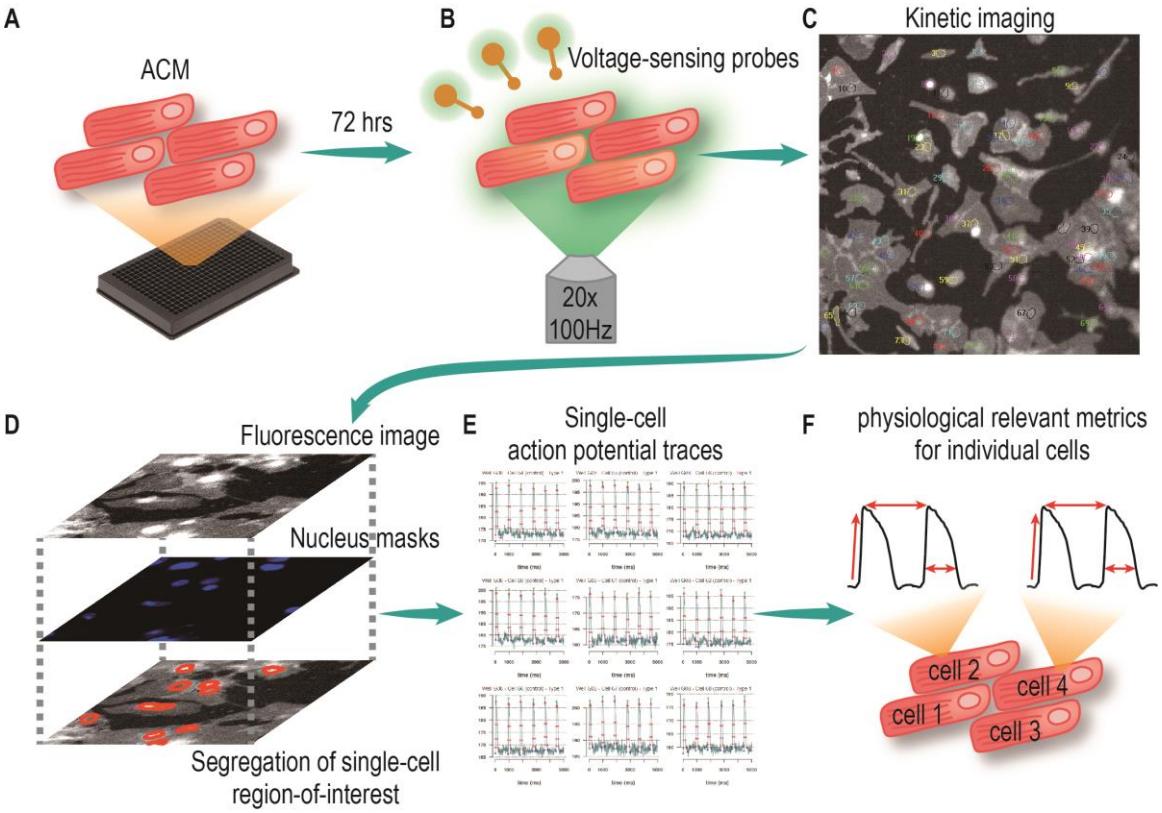

Figure 4.1 Schematic diagram of high-throughput single-cell functional screening platform workflow. (A) ACMs were replated into 384-well plate and recoverd for 72 hours. (B–C) Voltage-sensing probe were added and incubated for 45 minutes, and cells were than imaged by high-speed microscopy with 20x, 100 Hz, 5 second recording. (D) Movies were analyzed by software and generate reagion of interests (ROI) via nucleus masks. (E) Flourescent intensity of each ROI was measured and action potential traces for each cell were generated. (F) Single-cell physiology metrics were then retrieve by trace analysis algorithm.

4.2 Results

4.2.1 High-throughput Single-cell Functional Assessment Platform

Current cardiomyocyte-related physiology studies were commonly performed on the whole-cell patch-clamp technique that provides information on ion channel activities and the transmembrane potential status. However, the primary constraint of patch-clamp electrophysiology lies in the limited throughput (around 12 cells per day). The technique is more suited in the later phases of candidate validation, whereas the primary candidate identification should be conducted in systems with unbiased screening strategies and higher throughput.

To establish the high-throughput single-cell functional assessment platform, liquid handler (Microlab Star, Hamilton) with environmental control is integrated for CM culturing and dye incubation in 384-well micro-pipette plate format [Figure 4.1A]. Fluorescent-based automated microscopy acquires high resolution (up to 40x) and frame rate (up to 225 Hz) videos [Figure 4.1B]. To evaluate CM physiology and model arrhythmia in-a-dish, we focused on cell-autonomous activities and local cell cluster behavior. Plating density was carefully modified to deliberately avoided the mono-layer culturing condition. Sparsely plated 4,000 cardiomyocytes per well of 384-well plate, provide the state that the electrical syncytium appears locally between proximate clusters, but not in a whole-well level, as it was in the mono-layer culturing condition [Figure 4.1C]. Next, to achieve single-cell action potential resolution, analysis software generates the region of interests (ROIs) via DAPI nucleus staining before acquiring movies. The image analysis software processed the fluorescent-change-overtime in individual ROIs that

represents each cell within the field of view to obtain specific action potential traces for each cell recorded [Figure 4.1D]. Action potential traces were then analyzed by the algorithm described in the following section to retrieve single-cell physiology data. In summary, consolidating CM subtypes with automated microscopy and analysis algorithms, the single-cell resolution functional assessment platform is a novel technology for high-throughput phenotypical screenings and arrhythmia modeling in-a-dish.

4.2.2 Algorithm of Retrieving Physiological Relevant Metrics for Arrhythmia Modeling

To retrieve physiological metrics from extensive data of single-cell action potential kinetic imaging, stream-lined data analysis, and batch processing are required. The data handling could be divided into two main parts: the retrieval and conversion of fluorescence-intensity-changes-overtime to action potential traces; and the interpretation and categorization of physiological metrics from the traces [Figure 4.1E–F].

First, the kinetic images were processed through built-in image processing software, MetaAnalysis. By overlaying the acquired image stacks with nucleus staining, the software transformed the local fluorescence-intensity-changes-overtime into action potential traces for individual cells. Each cell was also given a specific tag containing information including plate/well/cell IDs and relative position in the well. The data were then transferred to the cloud-based trace analyzer. The algorithm of trace analyzer was written in R and uses the Prama package for initial peak and pit detection. The algorithm uses a combination of statistical heuristics, an input threshold value, and control well activity statistics to remove random noise, categorize well activity, and retrieve physiology metrics

and statistics in both bulk (well-based) and single-cell (cell-based) format. Well activity is categorized into one of four types, Inactive; the cells did not produce enough of a response to be considered for further analysis, Type 1; regular activity, Type 2; extended action potential duration, or Type 3; abnormally escalated peak counts. The algorithm produces a PDF of all cell activity with highlighted peaks as well as useful summary statistics such as action potential duration at 90%, 75%, 50%, 25%, 10% of repolarization (APD_{90}, APD_{75}, APD_{50}, APD_{25}, APD_{10}), peak-to-peak interval, number of ectopic peaks, peak rise/decay time, frequency, and more [Figure 4.2]. In conclusion, automated batch trace analysis software and algorithm enabled efficient data processing of the single-cell functional assessment of cardiomyocytes.

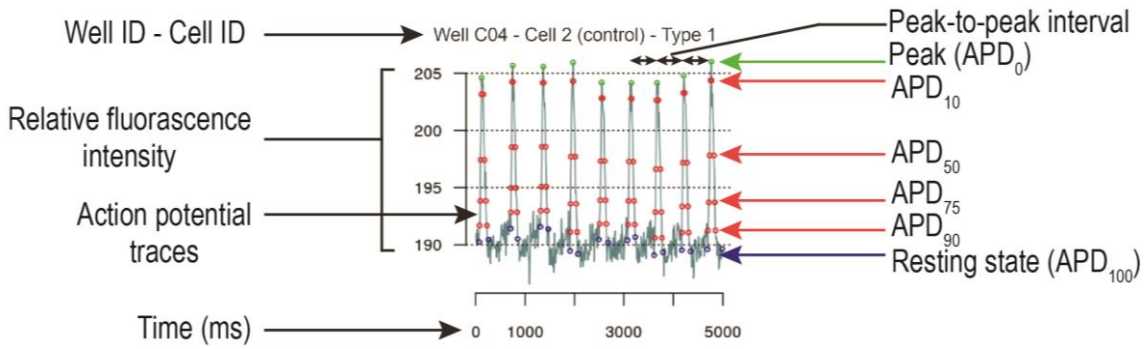

Figure 4.2 Physiology metrics of single-cell action potential trace analysis.

4.2.3 Single-cell Action Potential Assessment

To validate the single-cell functional assessment platform, we asked how does the action potential readouts between CM subtypes correlate to the results from patch-clamp physiology or mono-layer culture whole-well analysis. We firsts sparsely plated VCM and ACM respectively. After 2 days, cells were incubated with voltage sensing probe, imaged, and action potential traces were analyzed with single-cell analysis algorithm. The median

APD_{75} of the cells were calculated and binned into groups of 10 ms. Data was then presented through population distribution diagram with APD_{75} as x-axis and percentage frequency from the entire sampled population as the y-axis. The most noticeable feature of action potential morphology of a VCM is the elongated plateau of phase 2 that leads to longer APD. On the contrary, ACM presents shorter phase 2, with a more triangular-like shape of the action potential that has much shorter APD. The result showed that APD_{75} of ACM population clustered between 100 – 130 ms, with a median value of 115.6 ms, where the APD_{75} of VCM population clustered between 150 – 200 ms, with a median value of 181.5 ms [Figure 4.3A–C]. In this data, 147 ACMs and 73 VCMs were recorded and analyzed. Collectively, the action potential durations and morphologies match the data recorded via patch-clamp physiology and mono-layer culture whole-well analysis, suggested that the single-cell action potential assessment platform provide relatively accurate physiology results and an additional layer of in-depth cell-autonomous activity information, without sacrificing the throughput. To emphasize the advantages of the

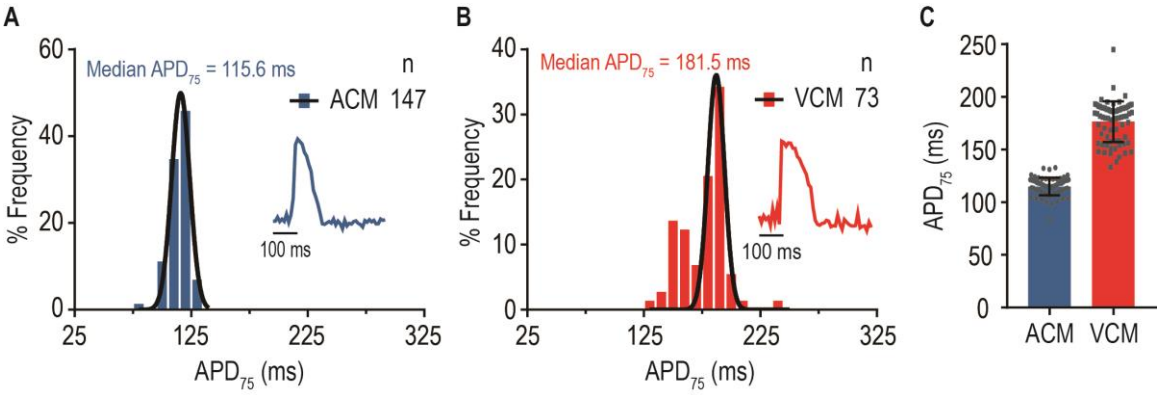

Figure 4.3 Single-cell action potential analysis on ACM and VCM. (A) ACM population distribution diagram of APD75 indicated general population of ACMs had APD_{75} between 100 – 130 ms, with triangular-shape like representitive traces. (B) VCM population distribution diagram showed the general APD_{75} ranged between 150 – 200 ms, with plateau-like shape during phase 2 of action potential. (C) Avearage APD_{75} of ACM and VCM. Compares to average result, poulation distribution diagram of single-cell APD_{75} analysis provides higher resolution of data.

platform, we co-cultured VCM and ACM in two distinct formats, mono-layer electrically coupled format, and sparsely plated single-cell-like format [Figure 4.4A–B]. The action potential was them analyzed through whole-well fluorescent readout and single-cell segregation readout respectively [Figure 4.4C–D]. As predicted, the whole-well analysis of action potential morphology of mix-cultured CM has action potential durations in between pure VCM population and ACM population. The result suggested that the subtype-specific action potential phenotype might be masked by an opposing effect on another in an electrical syncytium of multiple cell types. In the single-cell analysis, the system was able to detect two separate populations representing ACM and VCM in the mix-culture format. In summary, the result indicates the high sensitivity of the platform and highlight the ability to retrieve more accurate data from mix-population culture.

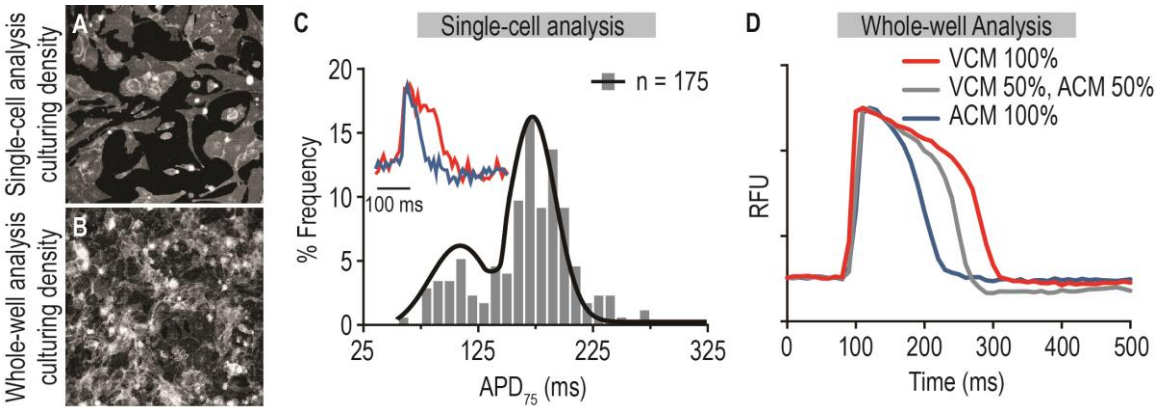

Figure 4.4 CM subtype co-culture experiments demonstrated the higher sensitivity of single-cell analysis. (A–B) ACM and VCM were co-cultured under desired density for single-cell and whole-well analysis. (C) Single-cell analysis was able to identify two distinctive populations with different action potential duration representing the subtpyes. (D) The whole-well action potential analysis of the mix population was situated in between the pure population of ACM and VCM with an intermediate action potential duration.

4.2.4 Atrial-like and Ventricular-like Cardiomyocyte Presented Differential Responses to Small Compounds

The potassium channel Kv1.5 is more abundant in human atrial than in ventricular cardiomyocytes, which contributes to the functional difference between the two chambers [83, 84]. Kv1.5 is encoded by the gene KCNA5, and responsible for the I_{Kur}, which is the basis for balancing the membrane potential at phase 2 and initiating the repolarization at phase 3 in the human atria.

To evaluate the subtype-specificity responses and exam the sensitivity of the platform, we acutely treated VCM and ACM with compounds that exclusively effect specific CM subtype. 4-aminopyridine (4-AP), a small organic compound, is a K^+ channel blocker that has high selectivity on the KCNA family. To assess the effect of 4-AP on CM subtypes, the cells were acutely treated with the compound before image acquisition. Population distribution diagram of APD_{75} and representative action potential traces were then generated. In accordance with expectation, APD_{75} of ACMs were generally prolonged due to the blockade of Kv1.5 by 4-AP, and no increase of APD_{75} observed on VCM [Figure 4.5A–B]. The data implicate the inhibition of Kv1.5, via 4-AP, induced prolongation of the action potential duration only in the ACM-specific manner.

Cytoplasmic Ca^{2+} concentration is critical throughout the CICR process. VCM, which generate stronger contraction force, relies on abundantly expressed L-type voltage-gated calcium channels [81]. The strong inward calcium current I_{CaL} produced the elongated plateau phase in VCM action potential traces, whereas in ACM, L-type voltage-gated calcium channels are mildly expressed. To assess subtype-specific response on differentially expressed L-type voltage-gated calcium channels, we acutely treated both

CM subtypes with nifedipine, an inhibitor of the influx of Ca^{2+} current by stabilizing the L-type voltage-gated calcium channels in their inactive conformation. As expected, VCM action potential is markedly shortened with the treatment of nifedipine, and the shortening effect of action potential duration is not significant in ACM [Figure 4.5C–D]. Based on these results, the single-cell action potential assessment platform provides a high-throughput physiological readout useful for action potential-related disease modeling and pharmacological target discoveries in a subtype-specific CM manner.

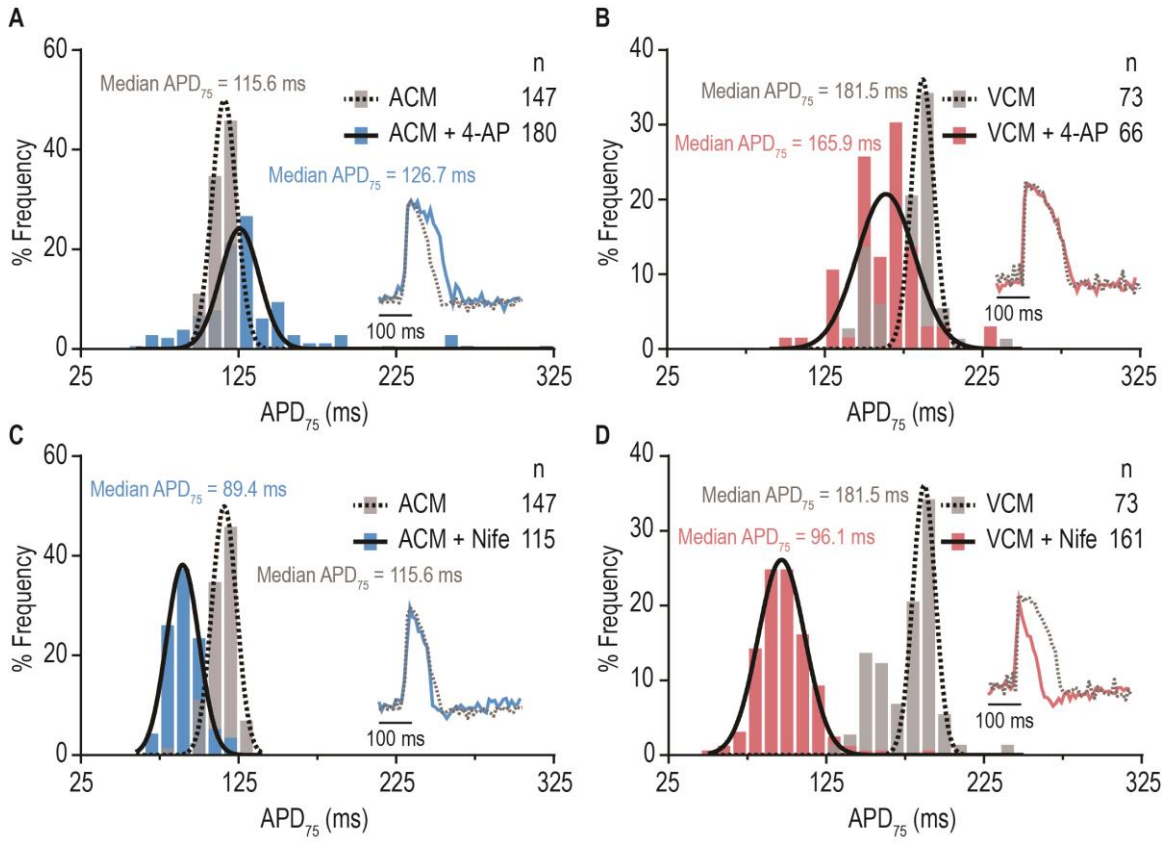

Figure 4.5 ACM and VCM responded differentially with the treatment of compounds, 4-AP and nifedipine that have subtype-specific effects. (A) Population distribution of APD_{75} of ACM treated with/without 4-AP. APD75 of ACM were prolonged after 4-AP treatment. (B) Population distribution of APD_{75} of VCM treated with/without 4-AP. No significant change of APD_{75} after 4-AP treatment. (C) Population distribution of APD_{75} of ACM treated with/without Nifedipine. APD75 of ACM were slightly shortened after nifedipine treatment. (D) Population distribution of APD_{75} of VCM treated with/without nifedipine. APD75 were dramatically shortened after nifedipine treatment.

4.3 Discussion

4.3.1 Advantages of the Platform

The modeling of arrhythmia in-a-dish and the identification of atrial-specific antiarrhythmic are the significant hurdles for the advancement of current pharmacological treatment of AF [85]. This fully automated system integrated with a liquid handler, high-throughput microscopy, and trace analysis software, formulates a simple yet powerful workflow for phenotypical screens and cardiac disease modeling. Compatible screening libraries including small compounds, microRNAs, siRNAs, lentiviruses, and CRISPRa (CRISPR activation) enables complex cross-library screens, counter screens, or sensitize screens. Several compelling advantages of the platform that would substantially advance the field including subtype-specific CM as a more physiologically relevant biological system; greater throughput comparing to currently available systems; stronger statistical power generated via single-cell analysis; less cellular materials required; analysis based on population provides insight in modeling local arrhythmia-like behaviors.

To further investigate the atrial-specificity of AF and the disease-causing mechanism, as well as developing antiarrhythmic treatments that unambiguously targets only the atria, the modeling and screening system require the specific atrial target space. Thus, applying ACM in the assay provides a more physiological relevant biological system.

From kinetic imaging to data retrieval, the streamlined workflow can process a fully loaded 384-well plate within less than 6 hours, with more than 27 million data points analyzed. The technique significantly increased the throughput as well as the statistic power of data analysis. Compare to the typical whole-well analysis, which generates one

“n” per well, and patch-clamp electrophysiology, with much lower throughput and time-consuming, single-cell analysis generates more than 70 “n” per field of view, and could easily expand the “n” via increasing additional imaging sites during the recording. Furthermore, the massive sample size unbiasedly represents the spectrum of the observed phenotypes across the entire population. Rather than only taking the mean value of the entire well, which frequently skewed the conclusion or overlooked substantial phenotype due to the heterogeneity within the culture.

Sparsely cellular culture condition substantially reduces the usage of cardiomyocytes per experiment up to 5 times compared to the mono-layer culture condition. Reducing the number of cells required per experiment also markedly reduce the time and expenses for cell production, which on the other hand increase the throughput of screening.

Lastly, single-cell analysis produces an additional layer of information specifically on cellular autonomous activities, which are crucial in modeling arrhythmia. The initiation of arrhythmia often appeared from local clusters such as the re-entry circuit which then propagates the ectopic electric stimulants to the neighboring cells and leads to arrhythmia [27]. On the contrary, the mono-layer culture condition is more appropriate for the studying of conduction functions due to the electrical syncytium of the cells. In summary, the high-throughput single-cell functional assessment platform provides subtype-specific target space, display stronger statistical power without sacrificing the throughput, reduce cardiomyocyte usage, and generate a higher resolution of data particularly applicable to arrhythmia modeling.

4.3.2 Limitations of the Platform

Limitations and critical areas for further improvement include the usage of fetus-like cardiomyocytes which may not fully recapitulate the phenotype of a human adult cardiomyocyte. According to the RNA-seq result and recently published report, hPSC-derived cardiomyocytes carry gene expression signatures similar to prenatal cardiomyocytes [86]. Further advanced CM maturation process may be required, and cross-referencing the result with the *in vivo* model is also necessary. Although the optical recording is an efficient approach that visualized the alternation of membrane potential and calcium handling, it is an indirect readout that cannot provide information of the activation or inactivation of the ion channels. Thus, requires whole-cell patch-clamp method as a mean of validation.

Also, due to the limitation of current microscopy system, we are unable to perform electrical stimulation on cardiomyocytes mimicking the aberrant electrical signal that triggers the fibrillation of the atria or increasing beat rate through pacing which sensitized the excitation-contraction coupling mechanism. However, other than the ectopic electrical signal, there are alternative triggers that may cause AF, including hormonal stimulations, ion channel agonists/antagonists, disrupting cellular calcium handling mechanisms, and abnormal electrical conduction. Finally, sparsely plated cardiomyocytes have poorly organized the sarcomeric structure and generate contraction tension from different angles, whereas the in vivo cardiomyocytes are tightly aligned with uniform contraction direction. A possible solution is plating cells on directional microgrooves plate, which restrict the orientation of sarcomeres[87, 88].

4.3.3 Application of High-throughput Single-cell Resolution Functional Assessment Platform

The tightly consolidated three factors made atrial arrhythmia in-a-dish modeling possible: (1) atrial-specific differentiation protocol that generates functional ACMs efficiently, (2) sparsely plated cell culture format that enables the occurrence of local arrhythmia-like behavior, and (3) single-cell action potential trace analysis provides in-depth phenotypical readouts for each recorded cell. The system provides unique features for evaluating arrhythmogenic gene candidates and discovering potential antiarrhythmic targets that complement conventional arrhythmia research approaches, such as patch-clamp electrophysiology, whole animals, or ex vivo heart preparations.

In addition, induced pluripotent stem cell technology and CRISPR gene-editing tool allow unbiased functional screens to be performed on normal and patient-specific mutations, accelerating our ability to identify novel cardiac rhythm-associated genes and elucidating the mechanisms of action on the electrical remodeling of the cardiac action potential. Moreover, functional genomic screening of proteins or genes using siRNAs or miRNAs that could partially or entirely phenocopy the arrhythmia enables sensitized screen for novel therapeutic target identification and drug discovery.

Most antiarrhythmics currently prescribed are nonspecific, regarding ion channels and heart chambers. The non-specificity of the targets may lead to serious off-target effect that could exacerbate the arrhythmia condition. Also, the non-specificity on both CM subtypes could create additional ventricular electrophysiology abnormalities that induce ventricular fibrillation (VF) or cardiac arrest while attempting to revert the atrial symptoms [89]. Thus, by conducting the subtype-specific screens provide physiologically relevant

target space for novel antiarrhythmic discovery. In summary, the platform provides an efficient way for both arrhythmia in-a-dish modeling as well as high-throughput phenotypical screenings for the identification of novel disease-associated gene candidates and antiarrhythmic drug discovery.

4.4 Conclusion

To achieve high-throughput screening efficiency, the platform was established in 384-well plate format, and ACMs were replated with an automated liquid handler. Cells were incubated with the voltage-sensing probe and recorded via high-speed microscopy. Movies were then analyzed by single-cell image processing software, and physiology metrics were retrieved by trance analysis algorithm. Compare to conventional electrophysiology or whole-well action potential analysis, the system provides: (1) Fully automated and high-throughput efficiency. (2) Single-cell resolution of physiology assessment. (3) Large sampling ability.

These features could greatly benefit the modeling of arrhythmia-like activity, due to sparse and electrically-uncoupled plating density with the aid of single-cell resolution to target specifically against irregular beating cells. Automated high-throughput and functional assessment aspect could advance the discovery of novel arrhythmia-causing gene candidates and antiarrhythmics.

Chapter 5

Modeling Arrhythmia-like Activity with AF-associated Genes and Perturbagens

5.1 Background

AF contributes significantly to population morbidity and mortality and due to the poorly understood of its pathogenesis, presently available antiarrhythmic-based therapeutic approaches have major limitations including low efficacy and high off-target effect. Thus, there are unmet medical needs to deconvolute the pathogenesis pathways that lead to arrhythmia and further provide insights for novel antiarrhythmic development.

Normal atrial cardiomyocytes display regular action potential changes over time, beginning from negative intracellular membrane potential (phase 0) and rapidly depolarized to the positive state (phase 1). During repolarization state, counteracts between Ca^{2+} influx and K^{+} efflux generates a short plateau shape of the action potential (phase 2), and then quickly repolarized back to the resting potential, at which it remains until the next

initiation of action potential cycle. Structural and electrical remodeling of the atria acts as substrates of AF which make atrial cells susceptible to aberrant electrical pulses from the pulmonary artery or atrial septum or other triggers such as parasympathetic activation, adrenergic stimulation, and aging [90-92]. Utilizing hPSC-derived ACM and high-throughput phenotypical platform described in Chapter II and III, respectively, we are able to functionally evaluate genes previously associated with AF, as well as identify novel genes of cardiac rhythm in an atrial-specific manner.

5.2 Result

5.2.1 Quantitatively defined arrhythmia in-a-dish

AF substrates can be categorized into two major groups, structural and electrical remodeling. Structural remodeling refers to the fibrosis of the cardiac tissue due to myocardial injuries such as myocardial infarction or surgical wounds [93]. The remodeling is composed of complex tissue morphology and lengthy duration that could be difficult to reproduce in cellular-based assays. Electrical remodeling, on the other hand, is the improper function of the ion channels that control cardiac cellular activity, which results in the prolongation and shortening of action potential duration. Under the effects of ectopic electric signals or other triggers, abnormal depolarizations may occur during or after the action potential plateau. Delayed afterdepolarizations (DADs) occur due to elevated cytosolic Ca^{2+} concentrations from the membrane Ca^{2+} channels or SR, NCX then propagates excess inward movement of 3 positively charged Na^{+} ions by extruding 2 Ca^{2+}, and depolarize the resting membrane potential. With less negative resting membrane

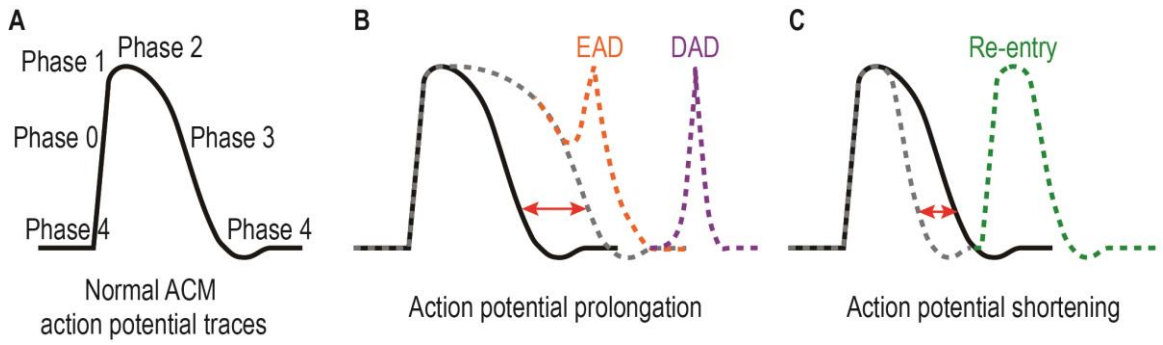

Figure 5.1 Electrical remodeling (the prolongation or shortening of action potential duration) could increase the susceptibility of AF. (A) Normal ACM action potential trace morphology. (B) Prolonged action potential trace could trigger pre-mature ectopic beats such as early after depolarization (EAD) if occurred during phase 2, or delayed after depolarization (DAD) in phase 4. (C) The shortening of action potential could induce rapid action potential cycle which than develop into a local re-entry loop.

potential, voltage-gated Na^+ channel becomes more susceptible to aberrant electric signals and induce ectopic beats [Figure 5.1A]. Early afterdepolarizations (EADs) occur with abnormal depolarization during phase 2 or phase 3. When the duration of action potential and effective refractory period (ERF) are significantly prolonged due to the impair of repolarization mechanisms, either excess inward currents (for example I_{CaL} or I_{Na}) and/or diminished outward currents (various potassium efflux currents), voltage-gated Ca^{2+} channel or voltage-gated Na^+ channel is reactivated in phase 2 or phase 3 causing abortive action potentials, respectively [Figure 5.1B]. The shortening of action potential duration would lead to the occurrence of re-entry loop. When there are two alternate conducting pathways, a premature beat might engage one pathway with shorter ERF, while successfully traveling through the other pathway. The propagating impulse could travel around the loop indefinitely, causing rapid and sustained beating behavior that may spread to the rest of the heart [Figure 5.1C]. In summary, the prolongation of action potential duration could lead to abnormal afterdepolarizations DADs and EADs, and the shortening of action potential duration could trigger the re-entry circuit.

Therefore, to quantitatively measure the arrhythmia-like behavior, we rely on two physiological parameters: action potential durations APD_{75} and the variation of peak-to-peak intervals within the peak train [Figure 5.2A]. To efficiently identify the conditions with abnormal APD_{75} from massive data sets generated from the single-cell high-throughput phenotypical platform, the medium APD_{75} from the peak train of each cell was calculated. Also, the ensemble phenotype from the formulation of the population regarding action potential duration was visualized via the APD_{75} population distribution diagram. The irregular peak-to-peak intervals could be quantified by the arrhythmia index (AI) derived from the following formula:

$$AI = \frac{StDev\ (peak - to - peak\ interval)}{Medium\ (peak - to - peak\ interval)} \times 100$$

AI describes the degree of irregular beating. Typical ACMs in control condition have AI less than 10, the higher the AI is, the more arrhythmia-like behavior the cell exhibits [Figure 5.2A–B]. According to different conditions, cells with varies AI values were plotted [Figure 5.2C]. Cells with AI under 20 presented relatively regular contracting activity, whereas cells with AI above 20 showed irregular peak-to-peak intervals with EADs/DADs in higher AI range [Figure 5.2D]. Thus, we consider cells with AI < 20 are in the "regular" category where no arrhythmia-like activities were observed; and cells with AI > 20 are in the "irregular" category where the arrhythmia-like activity occurred. Together, we could quantitatively and efficiently measure the degree of arrhythmia-like

behavior in single-cell resolution based on the prolongation or shortening of APD_{75} along with the AI value.

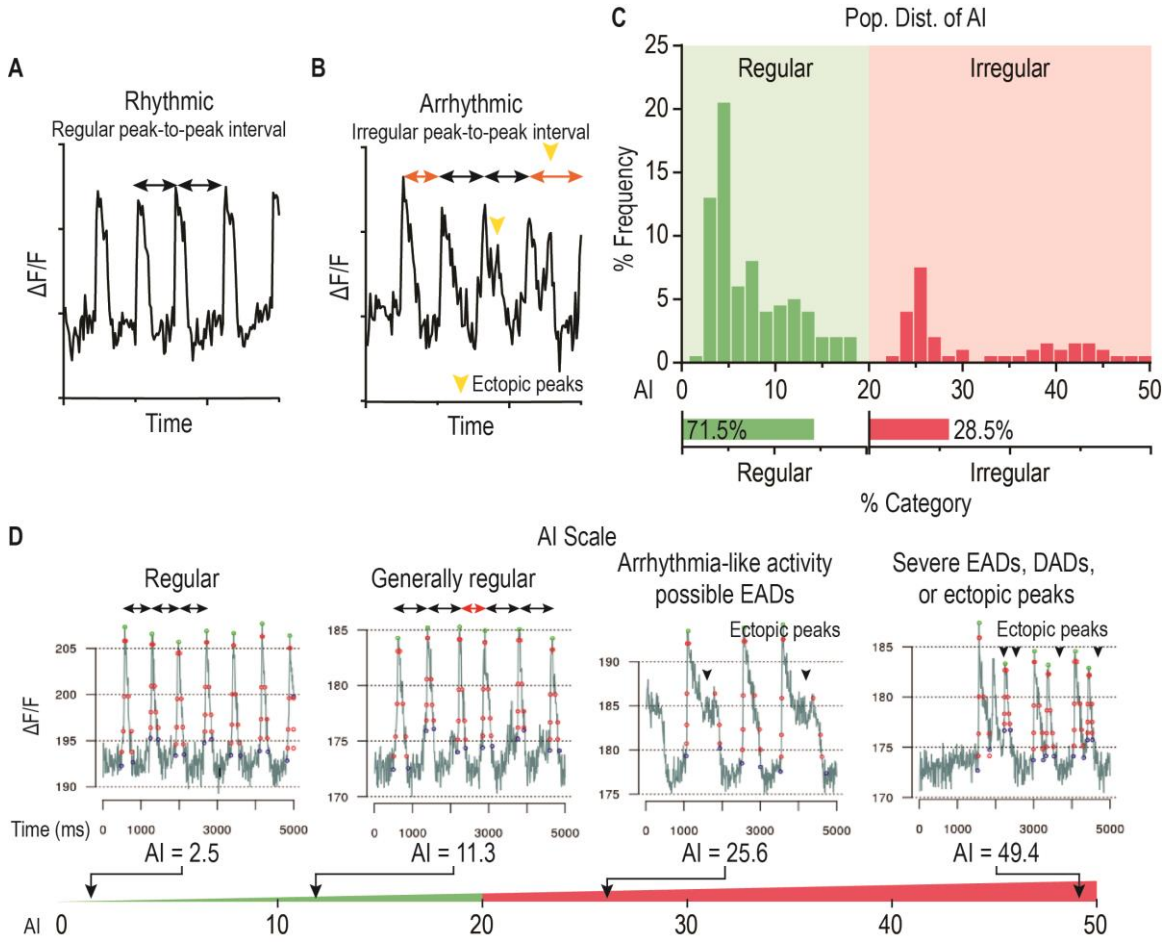

Figure 5.2 Quntify the degree of arrhythmia-like activity with arrhythmia index (AI). (A) Action potential trace of regular beating ACM. Peak-to-peak interval remains fairly constant. (B) Example of action potential trace of ACM with arrythmia-like behaviour. (C) Example of poulation distribution diagram of AI indicates there were subpopulations with distinct AI value. (D) Representitive acion potential traces of several AI values. Cells with AI < 20 were consider as regular beating CMs. Cells with AI > 20 were consider as irreguar (arrhythmic-like) beating cells.

5.2.2 Functional evaluation of known atrial fibrillation-associated genes

To further validate the system and examine data analysis pipeline, we functionally evaluated 20 genes previously associated with AF that were identified through rare variant studies and genome-wide association studies (GWAS) [94]. Rare variants are genetic

mutation identified within the cohorts of individuals with early onset (< 66 years) lone AF or familial AF which segregates as a Mendelian trait. Although several candidate genes have been validated in noncardiac-cellular models or animal models, it is still unclear whether variants in all of these genes are causative of AF in the patients. Furthermore, the studied cohort population and genes of interest were considerably small compares to the general AF population. On the other hand, GWAS studies on AF have identified 23 AF-associated single-nucleotide polymorphisms (SNPs) [95, 96]. The candidate genes are genetic variants that reached genome-wide significance in the meta-analysis. However, out of these 23 gene candidates, only one is identified as an exonic SNP (gene CAND2), and the rest of 22 SNPs are located in the intron or intergenic regions. Although genetic knockout animal models of some of the candidate genes have shown cardiac defects or arrhythmias, there is no direct evidence that the identified SNPs directly lead to AF [97].

We hypothesized that AF might be induced, not necessarily through genetic mutations, but through the dysregulation of the regulators of cardiac rhythm. Since rare variants and GWAS studies suggest an active link between candidate genes and AF, the overlap of the gene lists could act as positive controls for arrhythmia-like behavior induced by dysregulation of the candidate genes in our platform. The 20 overlapped gene candidates between rare variants and GWAS studies are listed below:

Table 5.1 List of previous known AF-associated genes identified through rare variant and GWAS.

Rare variant	GWAS locus	Gene abbreviation	Function category
X	X	HCN4	Ion channels
X		KCNA5	
X	X	KCND3	
X	X	KCNJ5	
X	X	KCNN3	
X	X	GATA4	Transcription factors
X	X	GATA5	
X	X	GATA6	
X	X	HAND2	
X	X	NKX2-5	
X	X	NKX2-6	
X	X	PITX2	
X	X	TBX5	
X	X	ZFHX3	
X	X	GJA1	Myocardial structural components
X	X	GJA5	
X	X	SYNE2	
X	X	PLN	
X		NPPA	Signaling
X	X	SH3PXD2A	

To test the hypothesis, we performed siRNA-mediated knock-down on all 20 AF-associated genes on day 25 ACMs. After 3 days, cells were incubated with the voltage-sensitive probe, imaged, and analyzed with single-cell trace analyzer [Figure 5.3A]. The compiled results from different batches of cells and experiments showed that out of all the gene candidates, 4 showed consistently prolonged APD_{75}, including GATA5, PITX2, KCNA5, and GATA6 [Figure 5.3B]. One showed shortening of the action potential duration, which is PLN. Among these gene candidates, GATA5 and 6 are the family members of the GATA-type zinc fingers, which involved in the regulation of cardiac development and adult heart [98]; PITX2 has an early role determining the asymmetry

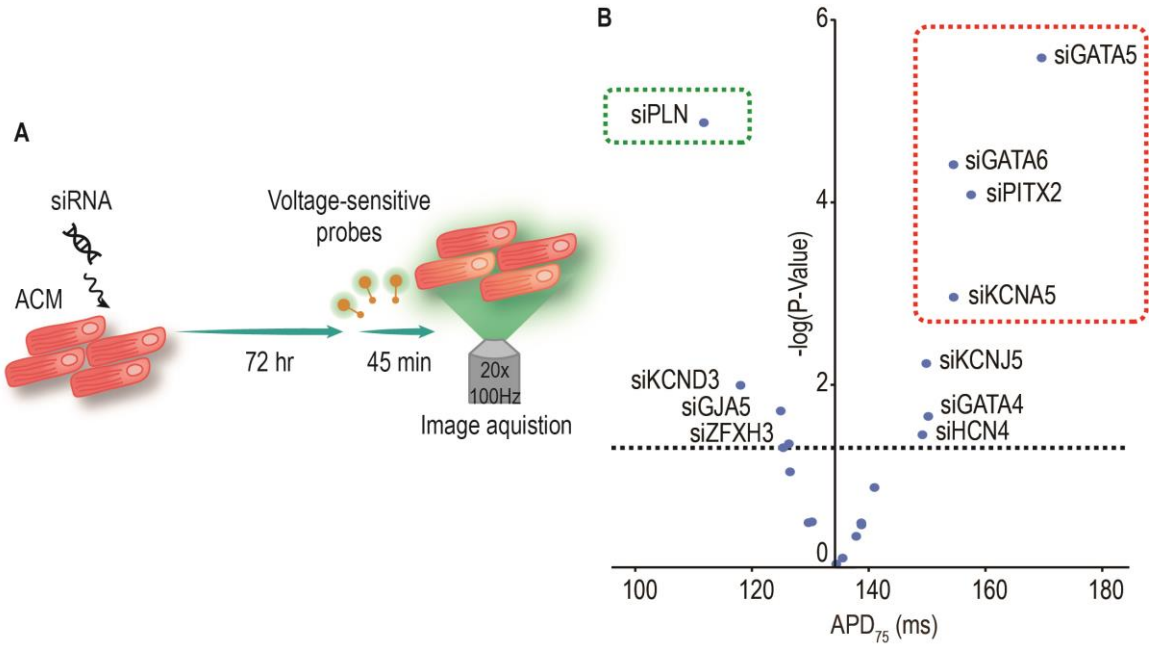

Figure 5.3 More than half of the previously known AF-associated genes induced electrical remodeling in the sytsem. (A) Schematic diagram showed the transfection of siRNA against 20 previously known AF-associated genes to ACM. (B) Out of 20 previously known AF-associated genes, 8 siRNA leads to the prolongation of action potential duration and 4 shortens the action potential duration.

during heart formation, and is one of the most significant AF-associated gene candidate reported from the GWAS study [99]; KCNA5 is an atrial-specific K^+ channel, and both gain and loss-of-function mutations in patients have been directly linked to AF [100]; PLN regulate the CICR cycle through the inhibition of Ca^{2+} uptake ability of SERCA2a on SR.

To elucidate the prolongation of action potential duration via siRNA-mediated knockdown against GATA5, KCNA5, PITX2, and PLN in the single-cell level, we analyzed and presented the data in APD_{75} population distribution plot and APD_{75}-peak count plot. Based on the result of APD_{75} population distribution plots of siGATA5, siKCNA5, and siPITX2, the knockdown of these genes prolonged the cellular population globally, where the entire population right-shifted towards greater APD_{75} [Figure 5.4A–C]. siGATA6 had minimal effect in prolonging action potential in ACM in the repeating experiments, thus was eliminated from the candidate list. In ACM transfected with siPLN,

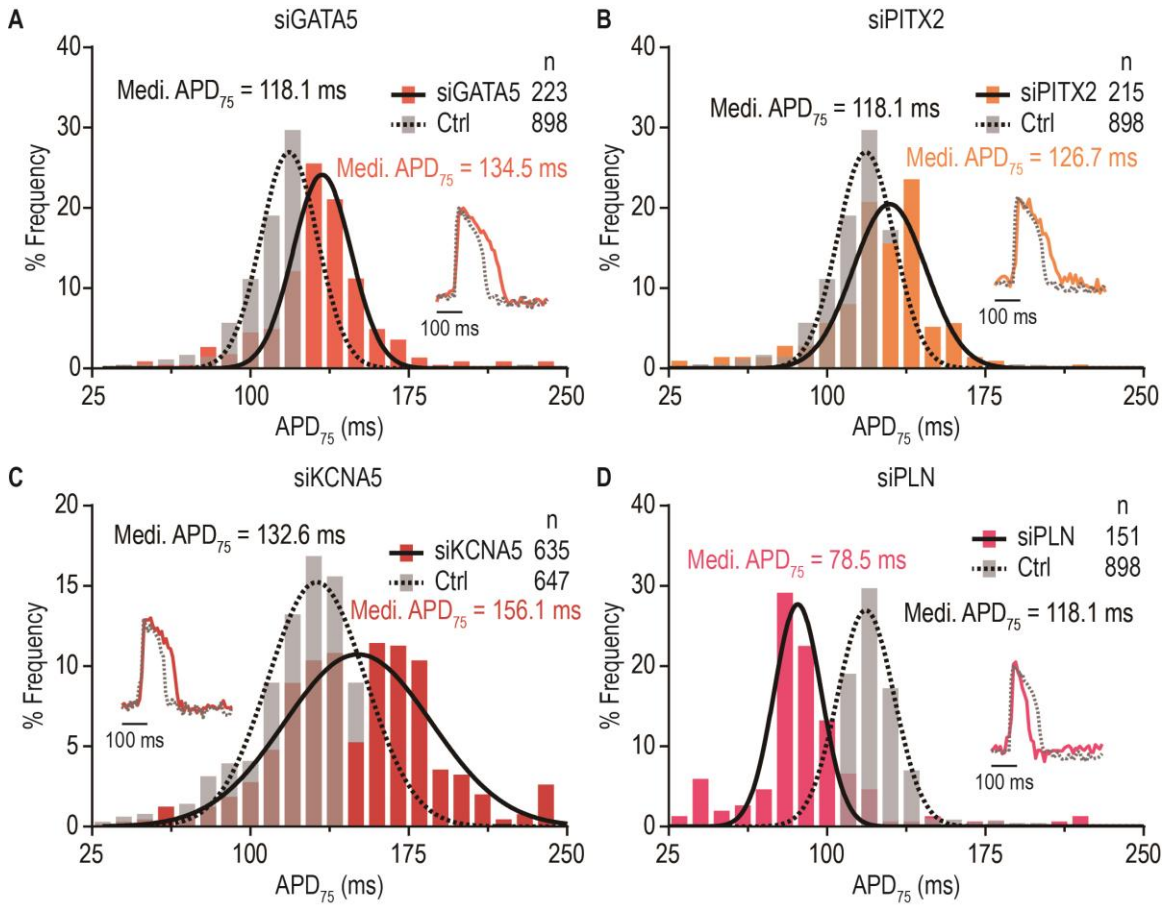

Figure 5.4 Transfecting siRNA against GATA5, PITX2, KCNA5, and PLN leads to electrical remodeling. (A–C) siGATA5, PITX2, KCNA5 prolongs the APD_{75} of ACM. (D) siPLN shortens the APD_{75} of ACM.

the entire population was left-shifted, indicating the knockdown of PLN shortens the action potential duration of the population [Figure 5.4D]. The number of peak counts and action potential duration are often correlated. Thus, to justify the phenotype of abnormal action potential duration is not the secondary result due to the increase or decrease of beat rate, we analyzed the alteration of action potential duration under fixed peak count. In all 3 siRNA-mediated knockdown conditions, APD_{75} are greater in the primary population under fixed peak counts (highlighted in the squares) [Figure 5.5A–C]. Whereas in siPLN

condition, the population shifts down-warded, suggests the main population has shorter action potential duration [Figure 5.5D].

In summary, siRNA-mediated knockdown of GATA5, KCNA5, PITX2 prolonged action potential duration under fixed peak counts, and siRNA against PLN shortened action potential duration. However, no arrhythmia-like activities were observed in all of the siRNA-mediated knockdown conditions [Figure 5.5E–H].

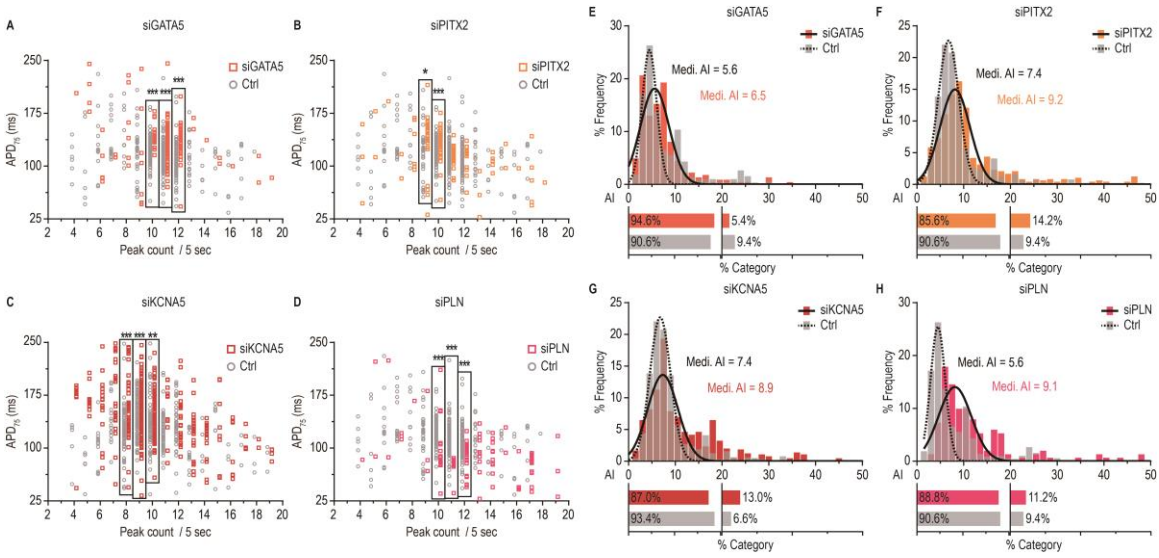

Figure 5.5 siRNA transfection does not induce arrhythmia-like activity. (A–D) Comapring siRNA transfected condition with control condition on APD_{75} under fixed peak count (fixed beat rate). General population (>60%) of siGATA5, siPITX2, siKCNA5 transfected ACMs had prolonged APD_{75}. siPLN tranfected group had shorter APD_{75}. (E–H) The poulation distribution diagram of AI of the siRNA against GATA5, PITX2, KCNA5, PLN did not induce high AI populations.

5.2.3 Induce arrhythmia in-a-dish with AF substrates and perturbagens

The onset and sustain of AF require a susceptible substrate and perturbagens, usually provided by stimulations such as adrenergic or cholinergic, or an ectopic beat. Here we examined 3 known AF-associated perturbagens alone and in combination with siRNA-mediated knockdowns as AF substrate to model and evaluate the occurrence of arrhythmia-like activities. Myocardial tissue fibrosis has close interactions between the onset and

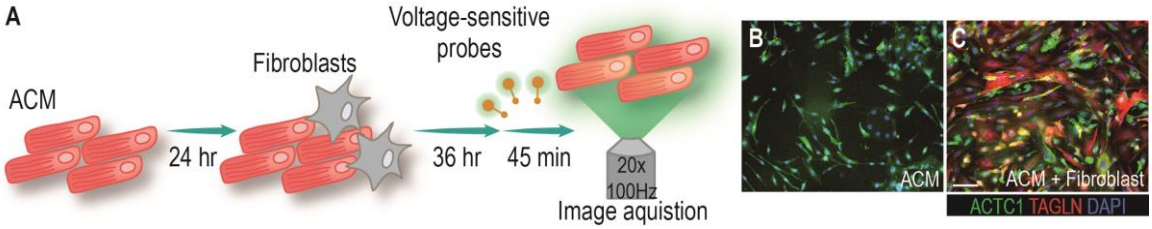

Figure 5.6 Co-culture fibroblasts with ACMs to mimic certain aspects of tissue fibrosis. (A) Schematic diagram of co-culturing fibroblasts with ACMs. (B) IF of pure ACMs (green) culture. (C) IF of ACMs (green) co-cultured with fibroblasts (red).

persistence of AF [101]. To mimic certain aspects of tissue fibrosis, which could lead to the impair of conduction, human neonatal foreskin fibroblasts (1,000 cells/well of a 384-well-plate) were added, 24 hours after the replate of ACMs (4,000 cells/well of a 384-well-plate) [Figure 5.6A–C]. Physiological metrics were analyzed with single-cell action potential analysis. From the APD_{75} population distribution diagram and fixed peak count diagram, co-culturing ACM with fibroblasts prolongs the action potential duration [Figure 5.7A, D]. However, it is not sufficient to induce arrhythmia-like activity [Figure 5.7G].

Next, to investigate the effect of adrenergic stimulation, isoproterenol and propranolol were acutely infused to the ACMs before the acquisition of the images. APD_{75} population distribution and fixed peak count analysis confirmed the shortening of action potential duration when treated with 1 μM of isoproterenol along with significantly increased beat rate [Figure 5.7B–E]. Action potential duration was dramatically prolonged and correlating with the decrease of the beat rate in the 81 μM propranolol condition [Figure 5.7C–F]. In conclusion, first, co-culturing fibroblast with ACM prolongs the action potential duration. Also, the beat rate increased, and action potential duration was shortened under the effect of isoproterenol, while ACM treated with propranolol exhibit decrease of beat rate and prolonged action potential duration. Lastly, although the pro-

arrhythmia effect of perturbagens is confirmed, no arrhythmia-like activity was detected in fibroblast co-culturing, nor the addition of isoproterenol and propranolol [Figure 5.7 H–I].

The key factors required for the inducing and maintaining of AF are substrates and abnormal stresses. Thus, we hypothesized that with the present of siRNA-mediated knockdown as the substrate, along with the conduction heterogeneity caused by co-culturing ACM with fibroblasts, and under adrenergic stresses, could further induce

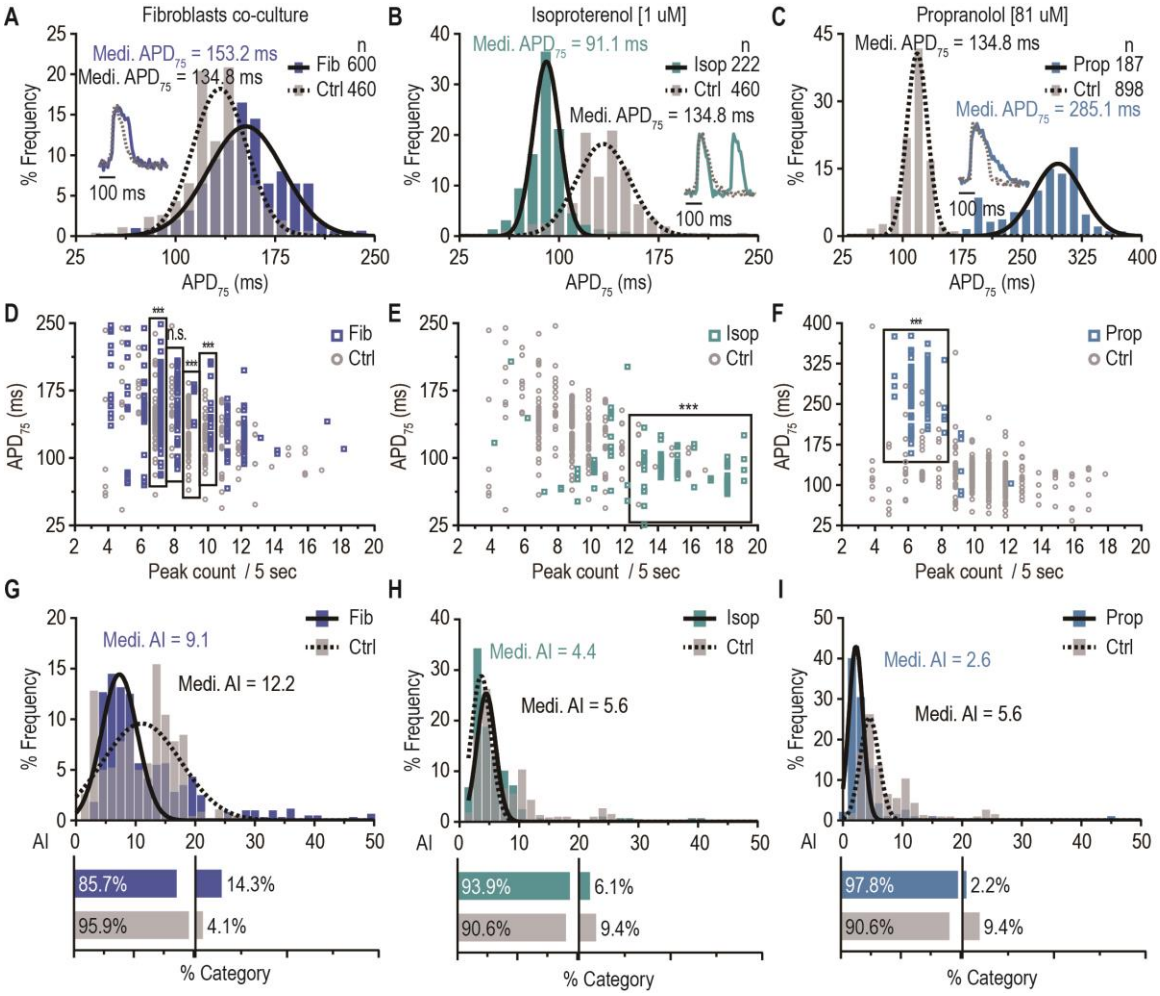

Figure 5.7 Perturbagens including fibroblasts co-culture, β-adrenergic agonist–isoproterenol, and antagonist–propranolol, caused electrical remodeling but not sufficient to trigger arrhythmia-like activity. (A–F) Population distribution diagram of APD_{75} and fixed beat rate diagram showed the prolongation of action potential duration caused by co-culturing fibroblasts with ACM. APD_{75} were significantly shortened with the treatment of isproterenol, and were prolonged with the treatment of propranolol. (G–I) The poulation distribution diagram of AI of the 3 perturbagens treatment did not trigger arrhythmia-like activity. Fib: fibroblasts co-culture; Isop: isoproterenol 1 μM; Prop: propranolol 81 μM.

arrhythmia-like activity in ACMs. To test the hypothesis, siRNA was transfected while the ACMs were replated into the 384-well-plate, and 24 hours later, fibroblasts were mixed in the culture. After 2 days, cells were incubated with voltage-sensitive probes, 1 uM of isoproterenol or 81 uM of propranolol were added acutely before the image acquisition [Figure 5.8A].

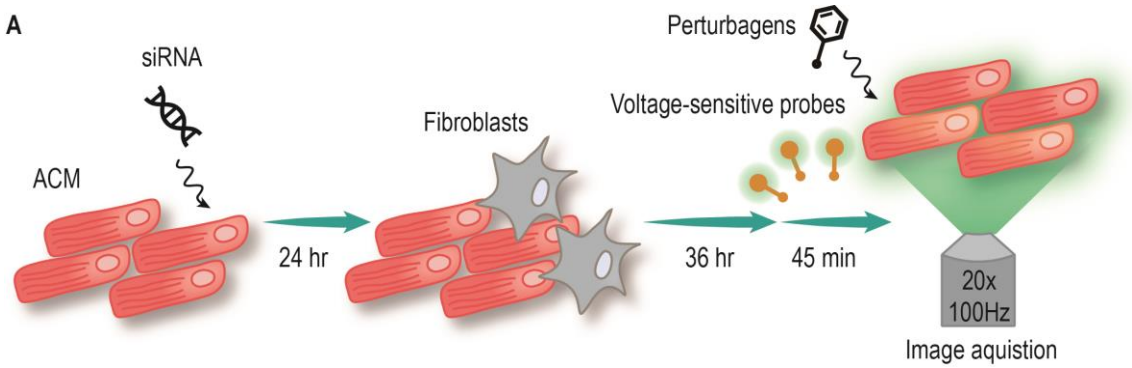

Figure 5.8 Schematic diagram of transfecting siRNA, co-culturing fibroblasts, and the treatment of small compound perturbagens.

Single-cell action potential data were analyzed in AI population distribution diagram. In the combinations of siRNA with one of the perturbagens, no arrhythmia-like activity was detected (data not shown). Moreover, AI was substantially escalated in the addition of fibroblasts along with propranolol in the siGATA5 transfected ACMs [Figure 5.9A]. Interestingly, AI value remained low in the siGATA5-fibroblast-isoproterenol condition, indicating arrhythmogenic activity is triggered only through specific combinations of substrate and perturbagens. Compare to the action potential traces of the control condition, siGATA5 along with fibroblasts co-culture and propranolol treatment induces irregular contracting behavior and ectopic peaks during the beginning of repolarization [Figure 5.9B–C]. Similarly, a subpopulation of cells with large AI was observed in the siPITX2-fibroblast-propranolol combination, while lower AI value in the siPITX2-fibroblast-isoproterenol condition [Figure 5.9D]. The resulting arrhythmia-like

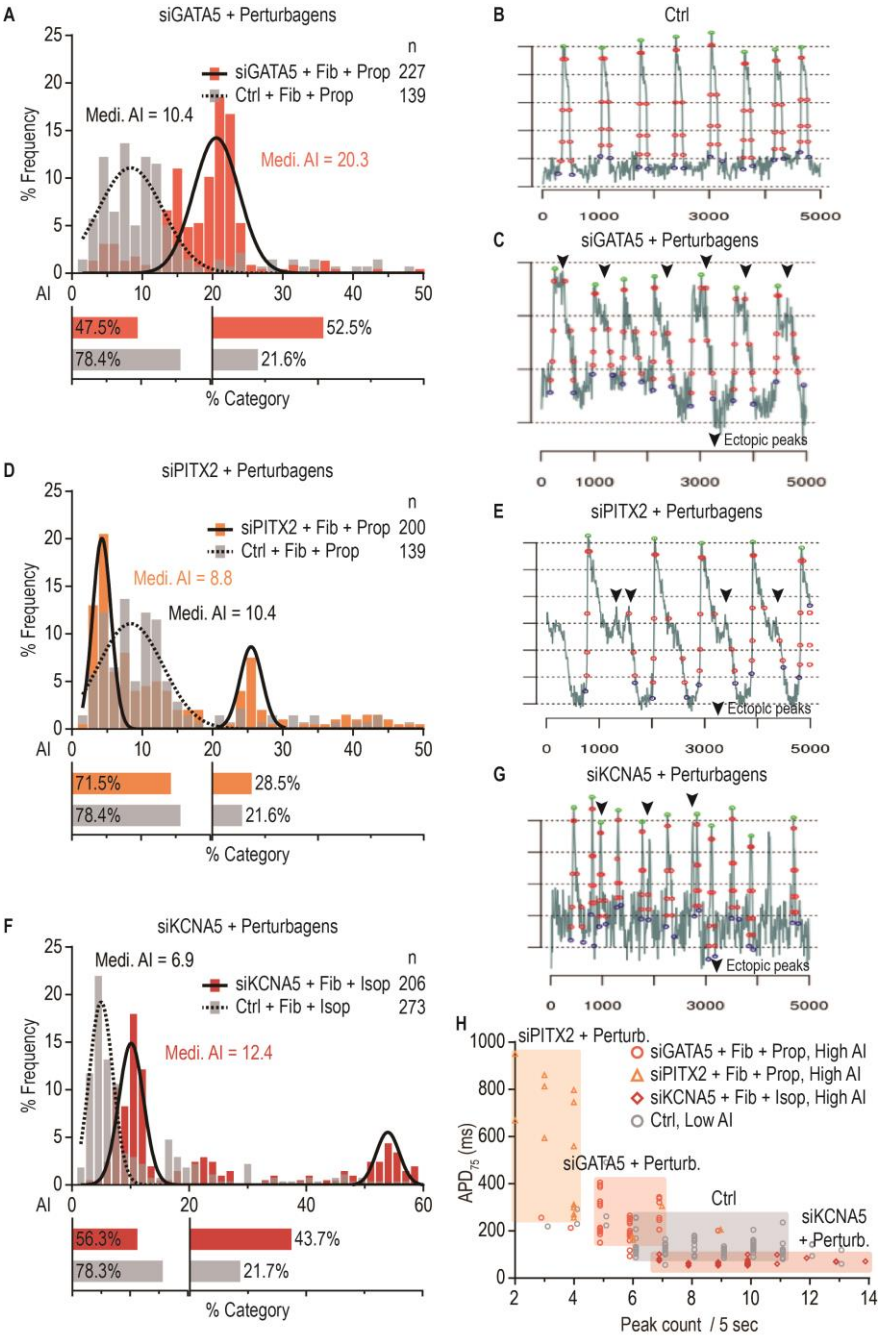

Figure 5.9 Specific combinations of AF-associated genes with perturbagens induced distinct arrhythmia-like activity. (A) Combination of siGATA5 with fibroblasts co-culture and propranolol induced high AI subpopulation. (B) Action potential trace of control ACM presented regular beating activity. (C) Action potential trace of siGATA5 with fibroblasts co-culture and propranolol showed premature ectopic peaks during the beginning of repolarization. (D) Combination of siPITX2 with fibroblasts co-culture and propranolol induced high AI subpopulation. (E) Action potential trace of siPITX2 with fibroblasts co-culture and propranolol showed extremely prolonged duration and EADs. (F) Combination of siKCNA5 with fibroblasts co-culture and isoproterenol induced high AI subpopulation. (G) Action potential trace of siKCNA5 with fibroblasts co-culture and isoproterenol had chaotic beating behavior with multiple double-peak events. (H) Cells with high AI from different combinations plotted on APD_{75} vs peak count diagram showed clusters of distinct AF-associated genes and perturbagens combinations. Fib: fibroblasts co-culture; Isop: isoproterenol 1 μM; Prop: propranolol 81 μM.

activity occurs due to series of dramatically extended action potential duration and profound EADs [Figure 5.9E]. siKCNA5-fibroblast-isoproterenol also generates a subpopulation with extreme high AI value, whereas siKCNA-fibroblasts-propranolol condition exhibit less AI value [Figure 5.9F]. Multiple double-peaks were observed in the action potential trace, where it also showed severe chaotic beating activity [Figure 5.9G]. Distinct types of arrhythmic behaviors were induced by different combinations of substrate and perturbagens [Figure 5.9H], which correlated with clinical findings indicating distinctive mechanisms that lead to various subtypes of AF. In summary, the arrhythmic behavior could be induced by specific combinations of substrate and perturbagens. Different sets of substrate-perturbagen combination also produced distinct forms of arrhythmia-like activities.

5.3 Discussion

5.3.1 Single-cell analysis is a novel method to identify cardiac rhythm regulators and potential antiarrhythmic therapeutic targets.

In the previous discussion, several advantages have been mentioned in functional assessment of cardiomyocytes. To fully utilize the platform for identifying cardiac rhythm regulators and potential antiarrhythmic therapeutic targets, the single-cell analysis provides in-depth information both in macroscopic, the deviation of entire cellular population behavior after the treatment, and microscopic views, where subpopulations segregated through conditions ex. fixed beat rate or local contracting clusters.

The single-cell analysis enables a general view of population distributions on all three major parameters that determine the arrhythmia-like activities of the examined ACM: beat rate, APD_{75}, and arrhythmia index (AI). Calculation of the mean values of these parameters directly across the cellular population with arrhythmia-like activity would generate unstable results with large standard deviation. These deviations were mainly contributed by subpopulations within the entire group. Heterogeneity within the culture is often observed, where subpopulations that have more severe phenotypes and others less, which reflects the heterogeneity of gene expressions mentioned in chapter 3 [85, 86]. By analyzing cellular arrhythmia-like behavior in single-cell level, the system could distinguish deviation and subpopulations from the bulk, which would be overlooked entirely via averaging the result of every cell, or applying classic whole-well analysis. Furthermore, the segregation of the subpopulation generates with single-cell analysis, produce meaningful results with statistical significance. Conversely, the averaging strategy generates inconclusive results with low statistical power and large standard deviation.

The beat rate of the cardiomyocyte and action potential duration are highly correlated, the higher beat rate is often paired with shorter action potential duration. Thus, distinguishing the prolongation or shortening of action potential duration should also consider the beat rate. Classic patch-clamp electrophysiology measures action potential duration difference through regulating and fixing the beat rate of the cell via electrostimulations. Similarly, the single-cell analysis could also cross-reference the parameters such as APD_{75} and AI by *in silico* fixing the beat rate. Simply categorize cells

with defined beat rate, the effect of the treatment which leads to the action potential duration difference could then be recognized.

Lastly, being able to segregate the analysis in single-cell level, made selectively filtering cellular responses in a mixed-culture condition possible. The mixed-culture condition, either unintentionally, such as heterogeneity during differentiation, or intentionally, for example, the co-culture of CM sub-types or CM with fibroblasts, causes difficulties in the whole-well analysis due to the asynchronous contracting event. Moreover, the arrhythmia-like activity also induces asynchronous contracting event in sub-clusters of cells. Segregation of cellular event into single-cell overcomes the problem which made detecting arrhythmia-like activity possible. In summary, the single-cell analysis provides macroscopic and microscopic aspects of evaluating functional results of cardiomyocytes that enable subpopulation analysis, *in silico* beat rate fixing for APD cross-reference, and segregating mix-population results.

5.3.2 siRNA-mediated knockdown of AF-associated genes induce abnormal action potential duration in ACM

Ectopic beats that induce arrhythmia and atrial fibrillation are caused by susceptible substrate and perturbagens. Single-cell action potential analysis results showed that the siRNA-mediated down-regulation of the 4 previously known AF-associated genes – GATA5, KCNA5, and PITX2 – as well as fibroblast co-culture significantly prolong the action potential duration of ACM. Conversely, the down-regulation of PLN abbreviates the action potential duration. The dysregulation or mutation of GATA5, KCNA5, PITX2, and

PLN, as well as the fibrosis of the cardiac tissue, have been shown to act as substrates of AF.

The family of GATA transcription factors regulates differentiation, growth, and survival of various cell types [102]. Within all 6 family members (GATA1-6), GATA4, 5, and 6 genes are explicitly expressed in mesoderm and endoderm-derived tissues [98, 103]. Functional overlapped with GATA4 and 6, GATA5 is a crucial transcription factor for proper cardiogenesis, particularly in the regulation of downstream GATA target gene expressions synergistically with NKX2-5 [104]. Evidence underscores several critical cardiac-specific genes with GATA binding elements such as sarcomeric genes, including myosin light chain-3 (MYL3), cardiac troponin C and I (TNNC1 and TNNI3). In addition, GATA family also regulates the expression of NCX, natriuretic peptide A and B (NPPA and NPPB), gap junction protein α 5 (GJA5), and Hand2 [105-110]. Lastly, multiple loss of function mutations of GATA5 have been identified in familial AF patients which points to the likely association of functionally impaired GATA5 with arrhythmia and AF [111, 112]. The role during and after cardiac development suggesting the potential association of miss-regulation or functionally compromised GATA5 with AF.

Previous studies have reported loss-of-function mutations in KCAN5 leads to decrease in I_{Kur} in lone AF patient [100, 113-115]. I_{Kur} is the major repolarizing current in human atrium and consistent with the result we have shown, the loss of I_{Kur} prolongs action potential duration as well as the effective refractory period (ERP) of the ACM, which increase the propensity for EADs [83, 116, 117]. Notably, the mutations of KCNA5 in lone AF patients is one of the few identified both in rare variant studies and GWAS analysis, indicating its vital link between AF.

PITX2, the paired-like homeodomain transcription factor, has a critical role during heart development (left-right asymmetry) and rhythm control [118, 119]. The adult-specific Pitx2 deletion in mice causes significant electrical remodeling of the heart and develop AF [120]. Also, the promoter region of PITX2 contains TBX5-dependent cis-regulatory elements (CREs), indicating TBX5, a transcription factor intensively involved in heart development, modulates PITX2 expression level. Moreover, studies have shown that PITX2 and TBX5 forms a TBX5-PITX2 incoherent feed-forward loop that regulates several atrial conduction genes and PITX2 along modulates the expression levels of several cardiac-specific genes such as HCN4, NPPA, and KCNQ1[120-122]. The dysregulation of PITX2 causes the onset of AF under triggers in mouse [122]. Markedly, PITX2 is the most significant and frequently reported AF-susceptibility locus in multiple GWAS studies [123-126]. Finally, 3 lost of function mutations have been identified in idiopathic AF patients, and all 3 mutations are located in homeodomain where amino acids are highly and even completely conserved among various species [127, 128]. Although the mechanisms of dysregulation or mutations of PITX2 lead to AF remains controversial, it is consistent that abnormality of PITX2 increases the susceptibility to AF [129].

PLN act as a regulator protein of Ca^{2+} cycling and mediator of the adrenergic effect through the inhibition or activation of SERCA2a. Under dephosphorylated normal state, PLN interacts and decreases the Ca^{2+} affinity of SERCA2a, which leads to the decrease of Ca^{2+} cycling and reduced cardiac output. Upon phosphorylation, the inhibition of SERCA2a is terminated, Ca^{2+} affinity is raised, and cardiac output is then increased. Concurred with our findings, siRNA-mediated downregulation of PLN greatly shortens the action potential duration of ACM. Although no PLN mutation identified in lone AF

patients, numerous mutations in PLN have been reported associated with cardiac rhythm abnormalities and tachycardia. Most of the patients with PLN mutation have long clinical histories of comorbid conditions including AF, ventricular tachycardia (VT), hypertrophic cardiomyopathy (HCM), dilated cardiomyopathy (DCM), heart failure (HF), and sudden cardiac death (SCD) [130, 131]. PLN heterozygote super-inhibition mutation in mouse exhibited high mortality at early stages (12 weeks postnatal), and Ca^{2+} uptake was dramatically inhibited [131, 132]. Whereas the hyperphosphorylation of PLN, which prevent the inhibition of SERCA2a, by excessive CaMKII activation induced AF in isolated human atrial myocytes [133, 134]. These data reveal the crucial role of PLN in Ca^{2+} cycling and rhythm control and correlates with our finds that the APD abbreviation of ACM is due to the siRNA-mediated down-regulation of PLN.

In summary, our functional genomics approach using siRNA-mediated knock-down results coincide with previous studies on the dysregulation of GATA5, KCAN5, PITX2, and PLN that leads to the predisposition of atrial arrhythmia. The conduction heterogeneity and abnormal action potential due to the co-culture of fibroblasts with ACM resonate with previously reported on structural remodeling induced AF.

5.3.3 AF-associated perturbagens induce abnormal action potential duration in ACM

Cardiac tissue fibrosis is a hallmark of pro-arrhythmogenic structural remodeling. As one of the most common features of AF, increased collagen deposition in lone-AF patients, as well as the positive correlation between extracellular matrix (ECM) volume with the persistence of AF [101, 135]. Atrial fibrosis results from a variety of cardiac insults

including but not limited to myocardial injuries due to infarction or surgeries, chronic heart failure, atrial dilation, or electrical abnormalities [136, 137]. Extensive research and experimental models have helped to elucidate the relationship between atrial fibrosis and AF [138, 139]. The conduction heterogeneity due to the structural remodeling leads to numerous local re-entry circuits that generate irregular rhythms or flutter activity [93, 140]. Thus, conduction abnormalities provide a basis for re-entry loop that shortens action potential duration or conduction delay that leads to the prolonging of action potential duration. Moreover, positive feedback model between electrical remodeling, structural remodeling, and AF is well established. Coincide with the ACM-fibroblasts co-culture result, a widely diffused population distribution was observed both in peak count and APD_{75}. The increase of AI, as well as greater numbers of local circuits in the culture, indicates the conduction abnormalities and pro-arrhythmic effect of co-culturing fibroblasts with ACM.

The isoproterenol challenge in AF patients and animal model with AF-associated substrates are arrhythmogenic [100, 141, 142]. Adrenergic stimulation has been shown to induce cytoplasmic Ca^{2+} load through various targets. The major targets of beta-adrenergic stimulation in the cardiomyocytes are the activation of L-type Ca^{2+} channels on the membrane; the activation of SR-located ryanodine receptors; phosphorylation of PLN which accelerates Ca^{2+} reuptake by the SR. These alternations induce faster CICR cycle thus increase stronger contraction and relaxation of the myofilament [143]. The cytoplasmic Ca^{2+} stress and the increase of beat rate act as perturbagens that induce arrhythmia-like behavior on ACM along with substances such as siGATA5 and siPITX2.

Propranolol is a non-selective beta-blocker with the affinity for both β 1 and 2 adrenergic receptors. It has been widely used as rhythm control treatment for AF since its discovered in the 1960s. With opposite mechanism of Isoproterenol, Propranolol reduces Ca^{2+} cycling, thus, decrease the beat rate and prolongs action potential duration. The antiarrhythmic property of Propranolol is by reducing the event of re-entry circuit and the decrease of heart rate that leads to AF or atrial flutter. However, under the state of prolonged action potential duration, applying Propranolol further exacerbate the delay of the Ca^{2+} cycle, which could act as a trigger of EADs and induce arrhythmia. Interestingly, in long QT syndrome 3 clinical studies, prescribing high concentration of Propranolol also resulted in a proarrhythmic effect [144].

In summary, the functional assessment result indicating these known AF-associated perturbagens cause abnormal action potential duration, which in the present of AF-substrate may further induce AF in patients or arrhythmia-like behavior *in vitro*.

5.3.4 Induce Arrhythmia-like activity with AF-substrate and perturbagens

The specific combination of arrhythmia substrate and the trigger could induce and sustain the arrhythmia behavior [142, 145, 146]. GATA5 down-regulation reduces the expression of contractile proteins, gap junction proteins, and several cardiac-specific proteins [109]. The addition of fibroblast in the culture further exacerbates the cell-cell coupling that leads to the heterogeneity of conduction. Under the Ca^{2+} handling stress induced by propranolol, action potential duration was abnormally extended, keeping the cell depolarized for more extended periods, thus, allowing the occurrence of EADs at phase 2 [Fig]. PITX2 have been known for regulating Ca^{2+} homeostasis [120]. The reduced

expression of PITX2 via siRNA knockdown impairs Ca^{2+} handling ability of the cardiomyocyte. With the co-culture of fibroblasts, the propagation of electrical signals was then fragmented. Under the effect of propranolol, cytoplasmic Ca^{2+} stress surged by the reduction of CICR cycling rate. Action potential duration as well as ERP was markedly prolonged, which leads to incomplete repolarizations and promotes premature beats [Fig]. Lastly, KCNA5 down-regulation decreases I_{Kur} and prolongs action potential. Disrupting normal excitation rhythm by the activation of adrenergic-stimulation increases the susceptibility to arrhythmia-like activity in ACMs. Irregular peak-to-peak interval and reoccurring ectopic peaks were detected in the action potential of the siKCNA5-fibroblast-isoproterenol condition. Consistent with our observations, the vulnerability to adrenergic stress observed due to compromised I_{Kur} have been described both in the murine model and AF patients with haploid KCNA5 loss-of-function mutation [100]. In conclusion, arrhythmic activities were observed in distinct combinations of electrical remodeling substrate and AF-associated perturbagens. Furthermore, differential molecular causes lead to diverse subtypes of arrhythmia-like phenotypes, reflecting the broad spectrum of AF mechanisms documented in the clinical data, and emphasizing the importance of targeting specific AF subtypes with particular anti-arrhythmic treatments.

5.4 Conclusion

To validate the platform, a list of siRNA against 20 previously known AF-associated genes identified both through rare variant and GWAS were transfected to ACM. 11 out of 20 siRNAs showed either prolong or shortening of the action potential duration,

however, none observed arrhythmia-like activity. Perturbagens that were commonly associated with AF, including the fibroblasts co-culture mimicking tissue fibrosis, isoproterenol and propranolol as β-adrenergic stimulation/inhibition, were then tested. Perturbagens also found inducing electrical remodeling, yet not arrhythmia-like activity.

Since AF is often triggered in the presence of both substrate (miss-regulation of AF-associated genes) and perturbagens, we than transfected the siRNA and applied perturbagens at the same time. Severe arrhythmia-like activities were detected in 3 different combinations: 1. siGATA5 with fibroblasts co-culture and propranolol; 2. siPITX2 with fibroblasts co-culture and propranolol; 3. siKCNA5 with fibroblasts co-culture and isoproterenol. Moreover, different combinations of substrate and perturbagens presented distinct arrhythmia phenotypes, indicating the complexity of the disease and the needs to identify and then target the specific regulatory pathway that leads to arrhythmia.

Chapter 6

Future work and Conclusion

6.1 Future Work

6.1.1 Recapitulate Arrhythmia-like Phenotype in Patient-specific Mutation ACMs

Phenotypical assessments mentioned above were done by utilizing siRNA-mediated knockdown of the expression of the genes. However, this loss-of-function experimental design does not fully recapitulate the disease mechanism of action. siRNA-mediated knockdown could mimic certain aspects of the misregulation of the genes that occurs in the general AF population, whereas in familial AF, arrhythmias are caused by the mutation of the genes. Thus, being able to generate patient-specific mutation ACMs are essential for validating the gene candidate and the system itself.

CRISPR-Cas9 gene editing technique is frequently used to generate specific point mutation lines. Single-strand guide RNA (sgRNA) was designed to induce a double strand break in the proximity of the desired point mutation base pair, and single-strand oligodeoxynucleotide (ssODN) acted as a repair template to facilitate homology-directed

repair (HDR) mechanism instead of activating non-homologous end joining (NHEJ) mechanism. sgRNA, ssODN, along with Cas9 protein were then transfected into hPSCs via electroporation, colonies were isolated and sequenced. Lines with heterozygous mutation, homozygous mutation, and isogenic controls were then expanded and differentiated into day 25 ACMs. We are currently functionally evaluating the loss-of-function mutation of KCAN5 p.E375X heterozygote ($KCNA5^{E375X/+}$) and homozygote ($KCNA5^{E375X/E375X}$) and the gain-of-function mutation of KCNA4 p.D322H heterozygote ($KCNA5^{D322H/+}$) and homozygote ($KCNA5^{D322H/D322H}$) [Figure 6.1A–B]. Meanwhile also generating various lines including lost-of function mutation GATA5 p.W200G, and loss-of-function mutation of PITX2c p.R122C.

siRNA-mediated knockdown functional screening platform provides tremendous throughput for primary and secondary (validation) assays. CRISPR-Cas patient-specific mutation technique could then further validate the resulting candidates and elucidate detailed disease mechanism of action.

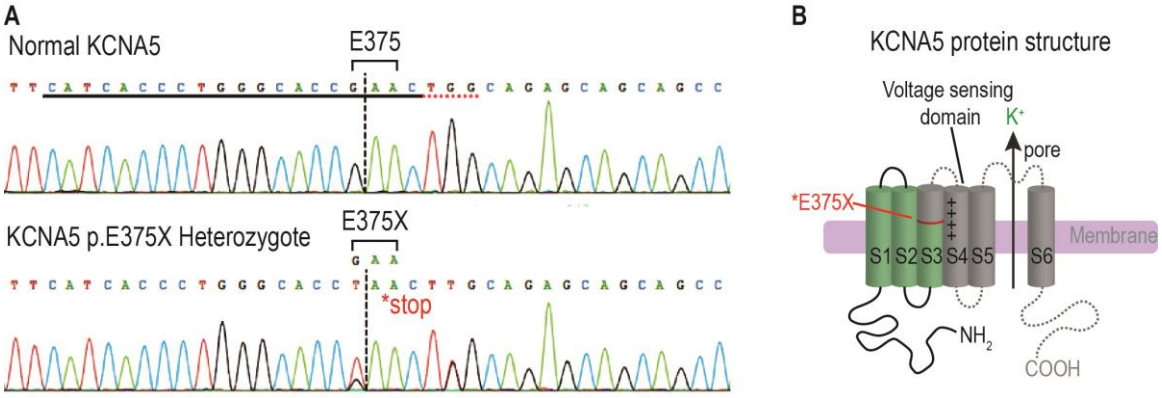

Figure 6.1 Generation of KCNA5 AF patient-specific lost-of-function mutation with CRISPR-Cas gene editing technique. (A) Sequence chromatogram of normal (wild type) KCNA5 vs. KCNA5 patient-specific lost-of-function mutation p.E375X heterozygote. (B) Schematic diagram of KCNA5 protein structure. E375X mutation truncates half of the structure including the voltage sensing domain and the pore domain.

6.1.2 Large-scale phenotypical screens across the genome

Maintaining the throughput and without sacrificing the readout resolution is the most considerabel advantages of the system. We currently are conducting a large-scale screen focusing on the "druggable" library and candidates that play essential roles in regulating CM physiology. The list of siRNA candidates (4239) includes G-protein receptors, kinases, phosphatases, transcription factors, epigenetic regulators, ubiquitins, and atrial differentially-expressed transcripts. All of the candidates were screened in both baseline condition and under β-adrenergic stress. Readouts were based on APD_{75} to evaluate the effect of electrical remodeling on prolonging or shortening the action potential duration, as well as through AI to assess the degree of arrhythmia-like activities [Figure 6.2A–B].

Throughout the large-scale phenotypical screens, we will identify novel cardiac rhythm regulators and potential arrhythmia-causing genes. Once the candidates are validated and confirmed, we are planning to conduct sensitized screen on small compounds

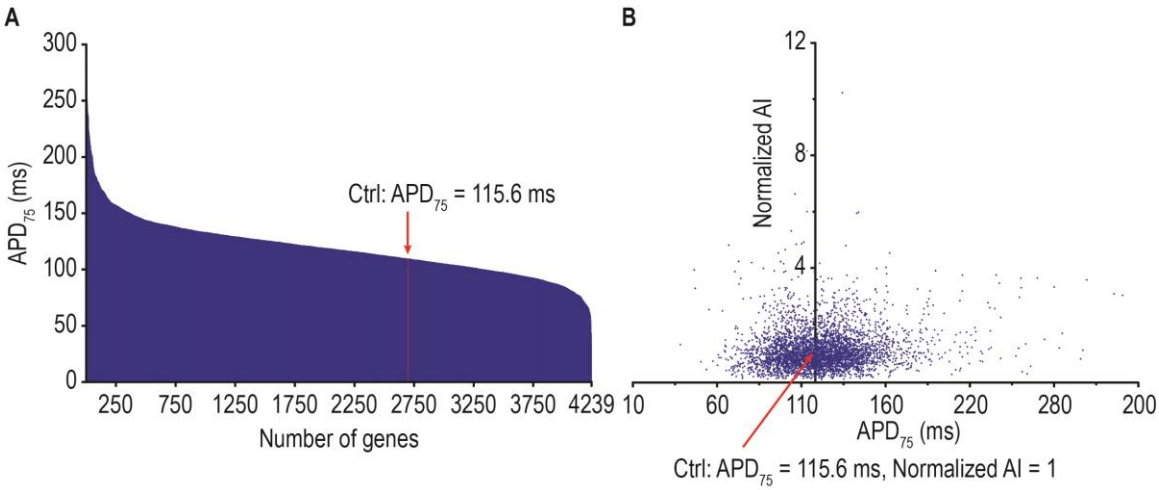

Figure 6.2 Large-scale phenotypical screens with the high-throughput single-cell functional screening platform. (A) Total 4239 candidates screened. The result plotted in the order of the length of APD_{75}. (B) The screening result plotted in APD_{75} vs.. normalized AI.

by transfecting siRNA against these candidate genes to explore potential anti-arrhythmic treatments.

6.1.3 Functional genomics as novel anti-arrhythmic treatments

According to the experimental result in 5.3.2, several siRNA against previously known AF-associated genes prolongs the action potential duration, including siGATA5. On the contrary, siPLN and other candidates shorten the action potential duration [Figure 6.3A–B]. Thus, by co-transfecting siGATA5 and siPLN, the resulting action potential duration was situated between the duration of the single transfection of siGATA5 and siPLN. The result indicates abnormal action potential duration can potentially be reverted to normal by inducing a "functionally antagonist" [Figure 6.3C]. Moreover, siRNAs and small compounds that inhibit target gene function may also be potential antiarrhythmics.

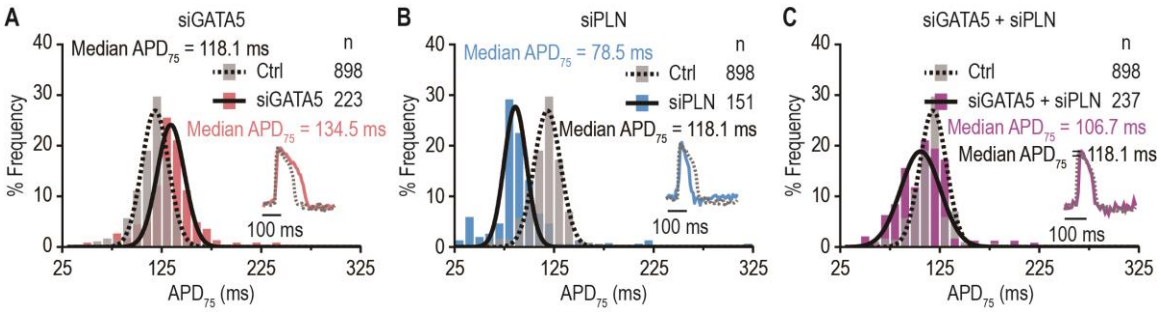

Figure 6.3 Applying functional genomics to identify novel anti-arrhythmics. (A) Transfection of siGATA5 prolongs the action potential duration of ACM. (B) Transfection of siPLN shortens the action potential duration. (C) Co-transfect both siGATA5 and siPLN revert the phenotype and normalized the action potential duration.

6.2 Conclusion

This thesis summarized an original system that utilizes hPSC-derived ACM on a high-throughput single-cell phenotypical screening platform to identify novel AF-associated genes.

Genome-wide microarray screen identified Id1 is required and sufficient to differentiate MCPs from hPSCs. Gene regulatory network of MCP reveals Id1's role in the early mesoderm specification stage. Id1 activates the expression of mesoderm genes KDR and MESP1, as well as suppressing endoderm genes such as FOXA2. Furthermore, *in vivo* studies revealed the overexpression of Id1 enlarges mesoderm formation and followed by larger cardiac tissue in Xenopus. Also, from the Id-quadruple knockout mouse embryo mutant, we confirmed Id gene family is required during mammalian early heart formation. Thus, we have established a highly efficient cardiogenic mesoderm differentiation protocol to generate large-scales of CM for the study of cardiac physiology, regeneration medicine, cell-based therapy, disease modeling, and drug discovery.

Atrial fibrillation is an arrhythmia occurs only in the atrium, to further study and model AF, ACM is required. Applying retinoic acid as a pro-atrial differentiation cue on day 5 CMP generates highly homogenous ACMs. ACM s were than molecularly validated through RNA-seq, and functionally validated with: 1. action potential; 2. calcium handling; 3. contractility; 4. atrial-specific compound 4-aminopyridine.

To efficiently screen through large-scale libraries to identify novel AF-associated genes, we established a fully automated high-throughput and single-cell functional screening platform. ACMs were replated into 384-well-plate and incubated with voltage-sensitive probe via a liquid handler. Cells were then recorded under high-speed microscopy and analyzed by image processing software. The analysis algorithm generated single cell action potential traces and retrieved physiological metrics. To evaluate the degree of arrhythmia-like activity, APD_{75} and AI value were plotted against cell population.

Lastly, siRNA of 20 previous know AF-associated genes were transfected individually to validate the system. According to the result, a few leads to the electrical remodeling (prolongation or shortening of APD) of ACM, yet not sufficient to induce arrhythmia-like activity. Furthermore, along with distinct combinations of perturbagens (fibroblasts co-culture, isoproterenol, propranolol), these siRNA induced distinct arrhythmia-like-activity. The result indicates the different mechanism of actions could lead to distinct arrhythmia phenotypes, and require specific anti-arrhythmic treatments. Thus, the prerequisite of developing phenotype-specific antiarrhythmics is to identify novel cardiac rhythm regulators and AF-causing genes. This original high-throughput functional screening platform enables single-cell resolution large-scale arrhythmia-like phenotypical screens to identify novel AF-causing candidates.

Bibliography

1. Saga, Y., S. Kitajima, and S. Miyagawa-Tomita, *Mesp1 expression is the earliest sign of cardiovascular development.* Trends Cardiovasc Med, 2000. **10**(8): p. 345-52.

2. Yoshida, T., P. Vivatbutsiri, G. Morriss-Kay, Y. Saga, and S. Iseki, *Cell lineage in mammalian craniofacial mesenchyme.* Mech Dev, 2008. **125**(9-10): p. 797-808.

3. Colas, A.R., W.L. McKeithan, T.J. Cunningham, P.J. Bushway, L.X. Garmire, G. Duester, S. Subramaniam, and M. Mercola, *Whole-genome microRNA screening identifies let-7 and mir-18 as regulators of germ layer formation during early embryogenesis.* Genes Dev, 2012. **26**(23): p. 2567-79.

4. Kee, B.L., *E and ID proteins branch out.* Nat Rev Immunol, 2009. **9**(3): p. 175-84.

5. Yang, J., X. Li, and N.W. Morrell, *Id proteins in the vasculature: from molecular biology to cardiopulmonary medicine.* Cardiovasc Res, 2014. **104**(3): p. 388-98.

6. Wang, L.H. and N.E. Baker, *E Proteins and ID Proteins: Helix-Loop-Helix Partners in Development and Disease.* Dev Cell, 2015. **35**(3): p. 269-80.

7. Fraidenraich, D., E. Stillwell, E. Romero, D. Wilkes, K. Manova, C.T. Basson, and R. Benezra, *Rescue of cardiac defects in id knockout embryos by injection of embryonic stem cells.* Science, 2004. **306**(5694): p. 247-52.

8. Tam, P.P., M. Kanai-Azuma, and Y. Kanai, *Early endoderm development in vertebrates: lineage differentiation and morphogenetic function.* Curr Opin Genet Dev, 2003. **13**(4): p. 393-400.

9. Whitman, M., *Nodal signaling in early vertebrate embryos: themes and variations.* Dev Cell, 2001. **1**(5): p. 605-17.

10. McLean, A.B., K.A. D'Amour, K.L. Jones, M. Krishnamoorthy, M.J. Kulik, D.M. Reynolds, A.M. Sheppard, H. Liu, Y. Xu, E.E. Baetge, and S. Dalton, *Activin a efficiently specifies definitive endoderm from human embryonic stem cells only when phosphatidylinositol 3-kinase signaling is suppressed.* Stem Cells, 2007. **25**(1): p. 29-38.

11. Sumi, T., N. Tsuneyoshi, N. Nakatsuji, and H. Suemori, *Defining early lineage specification of human embryonic stem cells by the orchestrated balance of canonical Wnt/beta-catenin, Activin/Nodal and BMP signaling.* Development, 2008. **135**(17): p. 2969-79.

12. Hollnagel, A., V. Oehlmann, J. Heymer, U. Ruther, and A. Nordheim, *Id genes are direct targets of bone morphogenetic protein induction in embryonic stem cells.* J Biol Chem, 1999. **274**(28): p. 19838-45.

13. Katagiri, T., M. Imada, T. Yanai, T. Suda, N. Takahashi, and R. Kamijo, *Identification of a BMP-responsive element in Id1, the gene for inhibition of myogenesis.* Genes Cells, 2002. **7**(9): p. 949-60.

14. Korchynskyi, O. and P. ten Dijke, *Identification and functional characterization of distinct critically important bone morphogenetic protein-specific response elements in the Id1 promoter.* J Biol Chem, 2002. **277**(7): p. 4883-91.

15. Lopez-Rovira, T., E. Chalaux, J. Massague, J.L. Rosa, and F. Ventura, *Direct binding of Smad1 and Smad4 to two distinct motifs mediates bone morphogenetic protein-specific transcriptional activation of Id1 gene.* J Biol Chem, 2002. **277**(5): p. 3176-85.

16. Jamora, C., R. DasGupta, P. Kocieniewski, and E. Fuchs, *Links between signal transduction, transcription and adhesion in epithelial bud development.* Nature, 2003. **422**(6929): p. 317-22.

17. Sasai, Y., B. Lu, S. Piccolo, and E.M. De Robertis, *Endoderm induction by the organizer-secreted factors chordin and noggin in Xenopus animal caps.* EMBO J, 1996. **15**(17): p. 4547-55.

18. Saga, Y., S. Miyagawa-Tomita, A. Takagi, S. Kitajima, J. Miyazaki, and T. Inoue, *MesP1 is expressed in the heart precursor cells and required for the formation of a single heart tube.* Development, 1999. **126**(15): p. 3437-47.

19. Bondue, A. and C. Blanpain, *Mesp1: a key regulator of cardiovascular lineage commitment.* Circ Res, 2010. **107**(12): p. 1414-27.

20. Bondue, A., S. Tannler, G. Chiapparo, S. Chabab, M. Ramialison, C. Paulissen, B. Beck, R. Harvey, and C. Blanpain, *Defining the earliest step of cardiovascular progenitor specification during embryonic stem cell differentiation.* J Cell Biol, 2011. **192**(5): p. 751-65.

21. Vincent, S.D. and M.E. Buckingham, *How to make a heart: the origin and regulation of cardiac progenitor cells.* Curr Top Dev Biol, 2010. **90**: p. 1-41.

22. Lescroart, F., S. Chabab, X. Lin, S. Rulands, C. Paulissen, A. Rodolosse, H. Auer, Y. Achouri, C. Dubois, A. Bondue, B.D. Simons, and C. Blanpain, *Early lineage restriction in temporally distinct populations of Mesp1 progenitors during mammalian heart development.* Nat Cell Biol, 2014. **16**(9): p. 829-40.

23. Ng, S.Y., C.K. Wong, and S.Y. Tsang, *Differential gene expressions in atrial and ventricular myocytes: insights into the road of applying embryonic stem cell-*

derived cardiomyocytes for future therapies. Am J Physiol Cell Physiol, 2010. **299**(6): p. C1234-49.

24. Giles, W.R. and Y. Imaizumi, *Comparison of potassium currents in rabbit atrial and ventricular cells.* J Physiol, 1988. **405**: p. 123-45.

25. Liu, X., H. Yagi, S. Saeed, A.S. Bais, G.C. Gabriel, Z. Chen, K.A. Peterson, Y. Li, M.C. Schwartz, W.T. Reynolds, M. Saydmohammed, B. Gibbs, Y. Wu, W. Devine, B. Chatterjee, N.T. Klena, D. Kostka, K.L. de Mesy Bentley, M.K. Ganapathiraju, P. Dexheimer, L. Leatherbury, O. Khalifa, A. Bhagat, M. Zahid, W. Pu, S. Watkins, P. Grossfeld, S.A. Murray, G.A. Porter, Jr., M. Tsang, L.J. Martin, D.W. Benson, B.J. Aronow, and C.W. Lo, *The complex genetics of hypoplastic left heart syndrome.* Nat Genet, 2017. **49**(7): p. 1152-1159.

26. Corrado, D., A. Zorzi, M. Cerrone, I. Rigato, M. Mongillo, B. Bauce, and M. Delmar, *Relationship Between Arrhythmogenic Right Ventricular Cardiomyopathy and Brugada Syndrome: New Insights From Molecular Biology and Clinical Implications.* Circ Arrhythm Electrophysiol, 2016. **9**(4): p. e003631.

27. Wakili, R., N. Voigt, S. Kaab, D. Dobrev, and S. Nattel, *Recent advances in the molecular pathophysiology of atrial fibrillation.* J Clin Invest, 2011. **121**(8): p. 2955-68.

28. Burridge, P.W., E. Matsa, P. Shukla, Z.C. Lin, J.M. Churko, A.D. Ebert, F. Lan, S. Diecke, B. Huber, N.M. Mordwinkin, J.R. Plews, O.J. Abilez, B. Cui, J.D. Gold, and J.C. Wu, *Chemically defined generation of human cardiomyocytes.* Nat Methods, 2014. **11**(8): p. 855-60.

29. Kattman, S.J., A.D. Witty, M. Gagliardi, N.C. Dubois, M. Niapour, A. Hotta, J. Ellis, and G. Keller, *Stage-specific optimization of activin/nodal and BMP signaling promotes cardiac differentiation of mouse and human pluripotent stem cell lines.* Cell Stem Cell, 2011. **8**(2): p. 228-40.

30. Laflamme, M.A., K.Y. Chen, A.V. Naumova, V. Muskheli, J.A. Fugate, S.K. Dupras, H. Reinecke, C. Xu, M. Hassanipour, S. Police, C. O'Sullivan, L. Collins, Y. Chen, E. Minami, E.A. Gill, S. Ueno, C. Yuan, J. Gold, and C.E. Murry, *Cardiomyocytes derived from human embryonic stem cells in pro-survival factors enhance function of infarcted rat hearts.* Nat Biotechnol, 2007. **25**(9): p. 1015-24.

31. Lian, X., C. Hsiao, G. Wilson, K. Zhu, L.B. Hazeltine, S.M. Azarin, K.K. Raval, J. Zhang, T.J. Kamp, and S.P. Palecek, *Robust cardiomyocyte differentiation from human pluripotent stem cells via temporal modulation of canonical Wnt signaling.* Proc Natl Acad Sci U S A, 2012. **109**(27): p. E1848-57.

32. Willems, E., J. Cabral-Teixeira, D. Schade, W. Cai, P. Reeves, P.J. Bushway, M. Lanier, C. Walsh, T. Kirchhausen, J.C. Izpisua Belmonte, J. Cashman, and M.

Mercola, *Small molecule-mediated TGF-beta type II receptor degradation promotes cardiomyogenesis in embryonic stem cells.* Cell Stem Cell, 2012. **11**(2): p. 242-52.

33. Yang, L., M.H. Soonpaa, E.D. Adler, T.K. Roepke, S.J. Kattman, M. Kennedy, E. Henckaerts, K. Bonham, G.W. Abbott, R.M. Linden, L.J. Field, and G.M. Keller, *Human cardiovascular progenitor cells develop from a KDR+ embryonic-stem-cell-derived population.* Nature, 2008. **453**(7194): p. 524-8.

34. Palpant, N.J., L. Pabon, C.E. Friedman, M. Roberts, B. Hadland, R.J. Zaunbrecher, I. Bernstein, Y. Zheng, and C.E. Murry, *Generating high-purity cardiac and endothelial derivatives from patterned mesoderm using human pluripotent stem cells.* Nat Protoc, 2017. **12**(1): p. 15-31.

35. Cai, C.L., X. Liang, Y. Shi, P.H. Chu, S.L. Pfaff, J. Chen, and S. Evans, *Isl1 identifies a cardiac progenitor population that proliferates prior to differentiation and contributes a majority of cells to the heart.* Dev Cell, 2003. **5**(6): p. 877-89.

36. Meilhac, S.M., M. Esner, R.G. Kelly, J.F. Nicolas, and M.E. Buckingham, *The clonal origin of myocardial cells in different regions of the embryonic mouse heart.* Dev Cell, 2004. **6**(5): p. 685-98.

37. de Pater, E., L. Clijsters, S.R. Marques, Y.F. Lin, Z.V. Garavito-Aguilar, D. Yelon, and J. Bakkers, *Distinct phases of cardiomyocyte differentiation regulate growth of the zebrafish heart.* Development, 2009. **136**(10): p. 1633-41.

38. Gessert, S. and M. Kuhl, *Comparative gene expression analysis and fate mapping studies suggest an early segregation of cardiogenic lineages in Xenopus laevis.* Dev Biol, 2009. **334**(2): p. 395-408.

39. Niederreither, K., J. Vermot, N. Messaddeq, B. Schuhbaur, P. Chambon, and P. Dolle, *Embryonic retinoic acid synthesis is essential for heart morphogenesis in the mouse.* Development, 2001. **128**(7): p. 1019-31.

40. Hochgreb, T., V.L. Linhares, D.C. Menezes, A.C. Sampaio, C.Y. Yan, W.V. Cardoso, N. Rosenthal, and J. Xavier-Neto, *A caudorostral wave of RALDH2 conveys anteroposterior information to the cardiac field.* Development, 2003. **130**(22): p. 5363-74.

41. Zhang, Z., J. Wang, X. Dai, Y. Ding, and Y. Li, *Prevention of retinoic acid-induced early craniofacial abnormalities by vitamin B12 in mice.* Cleft Palate Craniofac J, 2011. **48**(4): p. 355-62.

42. Devalla, H.D., V. Schwach, J.W. Ford, J.T. Milnes, S. El-Haou, C. Jackson, K. Gkatzis, D.A. Elliott, S.M. Chuva de Sousa Lopes, C.L. Mummery, A.O. Verkerk, and R. Passier, *Atrial-like cardiomyocytes from human pluripotent stem cells are a*

robust preclinical model for assessing atrial-selective pharmacology. EMBO Mol Med, 2015. **7**(4): p. 394-410.

43. Wu, S.P., C.M. Cheng, R.B. Lanz, T. Wang, J.L. Respress, S. Ather, W. Chen, S.J. Tsai, X.H. Wehrens, M.J. Tsai, and S.Y. Tsai, *Atrial identity is determined by a COUP-TFII regulatory network.* Dev Cell, 2013. **25**(4): p. 417-26.

44. Pereira, F.A., Y. Qiu, G. Zhou, M.J. Tsai, and S.Y. Tsai, *The orphan nuclear receptor COUP-TFII is required for angiogenesis and heart development.* Genes Dev, 1999. **13**(8): p. 1037-49.

45. Pradhan, A., X.I. Zeng, P. Sidhwani, S.R. Marques, V. George, K.L. Targoff, N.C. Chi, and D. Yelon, *FGF signaling enforces cardiac chamber identity in the developing ventricle.* Development, 2017. **144**(7): p. 1328-1338.

46. Grego-Bessa, J., L. Luna-Zurita, G. del Monte, V. Bolos, P. Melgar, A. Arandilla, A.N. Garratt, H. Zang, Y.S. Mukouyama, H. Chen, W. Shou, E. Ballestar, M. Esteller, A. Rojas, J.M. Perez-Pomares, and J.L. de la Pompa, *Notch signaling is essential for ventricular chamber development.* Dev Cell, 2007. **12**(3): p. 415-29.

47. Houweling, A.C., M.M. van Borren, A.F. Moorman, and V.M. Christoffels, *Expression and regulation of the atrial natriuretic factor encoding gene Nppa during development and disease.* Cardiovasc Res, 2005. **67**(4): p. 583-93.

48. Bers, D.M., *Cardiac excitation-contraction coupling.* Nature, 2002. **415**(6868): p. 198-205.

49. Amin, A.S., H.L. Tan, and A.A. Wilde, *Cardiac ion channels in health and disease.* Heart Rhythm, 2010. **7**(1): p. 117-26.

50. Grant, A.O., *Cardiac ion channels.* Circ Arrhythm Electrophysiol, 2009. **2**(2): p. 185-94.

51. Abriel, H. and E.V. Zaklyazminskaya, *Cardiac channelopathies: genetic and molecular mechanisms.* Gene, 2013. **517**(1): p. 1-11.

52. Bootman, M.D., I. Smyrnias, R. Thul, S. Coombes, and H.L. Roderick, *Atrial cardiomyocyte calcium signalling.* Biochim Biophys Acta, 2011. **1813**(5): p. 922-34.

53. Piroddi, N., A. Belus, B. Scellini, C. Tesi, G. Giunti, E. Cerbai, A. Mugelli, and C. Poggesi, *Tension generation and relaxation in single myofibrils from human atrial and ventricular myocardium.* Pflugers Arch, 2007. **454**(1): p. 63-73.

54. McKeithan, W.L., A. Savchenko, M.S. Yu, F. Cerignoli, A.A.N. Bruyneel, J.H. Price, A.R. Colas, E.W. Miller, J.R. Cashman, and M. Mercola, *An Automated*

Platform for Assessment of Congenital and Drug-Induced Arrhythmia with hiPSC-Derived Cardiomyocytes. Front Physiol, 2017. **8**: p. 766.

55. Miller, E.W., *Small molecule fluorescent voltage indicators for studying membrane potential.* Curr Opin Chem Biol, 2016. **33**: p. 74-80.

56. Nerbonne, J.M. and R.S. Kass, *Molecular physiology of cardiac repolarization.* Physiol Rev, 2005. **85**(4): p. 1205-53.

57. Schram, G., P. Melnyk, M. Pourrier, Z. Wang, and S. Nattel, *Kir2.4 and Kir2.1 K(+) channel subunits co-assemble: a potential new contributor to inward rectifier current heterogeneity.* J Physiol, 2002. **544**(Pt 2): p. 337-49.

58. Cheng, H. and S.Q. Wang, *Calcium signaling between sarcolemmal calcium channels and ryanodine receptors in heart cells.* Front Biosci, 2002. **7**: p. d1867-78.

59. Chi, N.C., R.M. Shaw, B. Jungblut, J. Huisken, T. Ferrer, R. Arnaout, I. Scott, D. Beis, T. Xiao, H. Baier, L.Y. Jan, M. Tristani-Firouzi, and D.Y. Stainier, *Genetic and physiologic dissection of the vertebrate cardiac conduction system.* PLoS Biol, 2008. **6**(5): p. e109.

60. Shimozono, S., T. Iimura, T. Kitaguchi, S. Higashijima, and A. Miyawaki, *Visualization of an endogenous retinoic acid gradient across embryonic development.* Nature, 2013. **496**(7445): p. 363-6.

61. Kumar, S. and G. Duester, *Retinoic acid controls body axis extension by directly repressing Fgf8 transcription.* Development, 2014. **141**(15): p. 2972-7.

62. Harvey, R.P., *Patterning the vertebrate heart.* Nat Rev Genet, 2002. **3**(7): p. 544-56.

63. Studer, M., H. Popperl, H. Marshall, A. Kuroiwa, and R. Krumlauf, *Role of a conserved retinoic acid response element in rhombomere restriction of Hoxb-1.* Science, 1994. **265**(5179): p. 1728-32.

64. Makita, T., G. Hernandez-Hoyos, T.H. Chen, H. Wu, E.V. Rothenberg, and H.M. Sucov, *A developmental transition in definitive erythropoiesis: erythropoietin expression is sequentially regulated by retinoic acid receptors and HNF4.* Genes Dev, 2001. **15**(7): p. 889-901.

65. Kumar, S. and G. Duester, *Retinoic acid signaling in perioptic mesenchyme represses Wnt signaling via induction of Pitx2 and Dkk2.* Dev Biol, 2010. **340**(1): p. 67-74.

66. Molotkova, N., A. Molotkov, and G. Duester, *Role of retinoic acid during forebrain development begins late when Raldh3 generates retinoic acid in the ventral subventricular zone.* Dev Biol, 2007. **303**(2): p. 601-10.

67. Sandell, L.L., B.W. Sanderson, G. Moiseyev, T. Johnson, A. Mushegian, K. Young, J.P. Rey, J.X. Ma, K. Staehling-Hampton, and P.A. Trainor, *RDH10 is essential for synthesis of embryonic retinoic acid and is required for limb, craniofacial, and organ development.* Genes Dev, 2007. **21**(9): p. 1113-24.

68. Kastner, P., N. Messaddeq, M. Mark, O. Wendling, J.M. Grondona, S. Ward, N. Ghyselinck, and P. Chambon, *Vitamin A deficiency and mutations of RXRalpha, RXRbeta and RARalpha lead to early differentiation of embryonic ventricular cardiomyocytes.* Development, 1997. **124**(23): p. 4749-58.

69. Kostetskii, I., Y. Jiang, E. Kostetskaia, S. Yuan, T. Evans, and M. Zile, *Retinoid signaling required for normal heart development regulates GATA-4 in a pathway distinct from cardiomyocyte differentiation.* Dev Biol, 1999. **206**(2): p. 206-18.

70. Xavier-Neto, J., C.M. Neville, M.D. Shapiro, L. Houghton, G.F. Wang, W. Nikovits, Jr., F.E. Stockdale, and N. Rosenthal, *A retinoic acid-inducible transgenic marker of sino-atrial development in the mouse heart.* Development, 1999. **126**(12): p. 2677-87.

71. Bruneau, B.G., M. Logan, N. Davis, T. Levi, C.J. Tabin, J.G. Seidman, and C.E. Seidman, *Chamber-specific cardiac expression of Tbx5 and heart defects in Holt-Oram syndrome.* Dev Biol, 1999. **211**(1): p. 100-8.

72. Pei, F., J. Jiang, S. Bai, H. Cao, L. Tian, Y. Zhao, C. Yang, H. Dong, and Y. Ma, *Chemical-defined and albumin-free generation of human atrial and ventricular myocytes from human pluripotent stem cells.* Stem Cell Res, 2017. **19**: p. 94-103.

73. Diez del Corral, R., I. Olivera-Martinez, A. Goriely, E. Gale, M. Maden, and K. Storey, *Opposing FGF and retinoid pathways control ventral neural pattern, neuronal differentiation, and segmentation during body axis extension.* Neuron, 2003. **40**(1): p. 65-79.

74. Sirbu, I.O., X. Zhao, and G. Duester, *Retinoic acid controls heart anteroposterior patterning by down-regulating Isl1 through the Fgf8 pathway.* Dev Dyn, 2008. **237**(6): p. 1627-35.

75. D'Amato, G., G. Luxan, and J.L. de la Pompa, *Notch signalling in ventricular chamber development and cardiomyopathy.* FEBS J, 2016. **283**(23): p. 4223-4237.

76. High, F.A. and J.A. Epstein, *The multifaceted role of Notch in cardiac development and disease.* Nat Rev Genet, 2008. **9**(1): p. 49-61.

77. Luxan, G., G. D'Amato, D. MacGrogan, and J.L. de la Pompa, *Endocardial Notch Signaling in Cardiac Development and Disease.* Circ Res, 2016. **118**(1): p. e1-e18.

78. Bruneau, B.G., G. Nemer, J.P. Schmitt, F. Charron, L. Robitaille, S. Caron, D.A. Conner, M. Gessler, M. Nemer, C.E. Seidman, and J.G. Seidman, *A murine model of Holt-Oram syndrome defines roles of the T-box transcription factor Tbx5 in cardiogenesis and disease.* Cell, 2001. **106**(6): p. 709-21.

79. Bloch, K.D., J.G. Seidman, J.D. Naftilan, J.T. Fallon, and C.E. Seidman, *Neonatal atria and ventricles secrete atrial natriuretic factor via tissue-specific secretory pathways.* Cell, 1986. **47**(5): p. 695-702.

80. Bou-Abboud, E., H. Li, and J.M. Nerbonne, *Molecular diversity of the repolarizing voltage-gated K+ currents in mouse atrial cells.* J Physiol, 2000. **529 Pt 2**: p. 345-58.

81. Bootman, M.D., D.R. Higazi, S. Coombes, and H.L. Roderick, *Calcium signalling during excitation-contraction coupling in mammalian atrial myocytes.* J Cell Sci, 2006. **119**(Pt 19): p. 3915-25.

82. Walden, A.P., K.M. Dibb, and A.W. Trafford, *Differences in intracellular calcium homeostasis between atrial and ventricular myocytes.* J Mol Cell Cardiol, 2009. **46**(4): p. 463-73.

83. Wang, Z., B. Fermini, and S. Nattel, *Sustained depolarization-induced outward current in human atrial myocytes. Evidence for a novel delayed rectifier K+ current similar to Kv1.5 cloned channel currents.* Circ Res, 1993. **73**(6): p. 1061-76.

84. Krapivinsky, G., E.A. Gordon, K. Wickman, B. Velimirovic, L. Krapivinsky, and D.E. Clapham, *The G-protein-gated atrial K+ channel IKACh is a heteromultimer of two inwardly rectifying K(+)-channel proteins.* Nature, 1995. **374**(6518): p. 135-41.

85. Piccini, J.P. and L. Fauchier, *Rhythm control in atrial fibrillation.* Lancet, 2016. **388**(10046): p. 829-40.

86. DeLaughter, D.M., A.G. Bick, H. Wakimoto, D. McKean, J.M. Gorham, I.S. Kathiriya, J.T. Hinson, J. Homsy, J. Gray, W. Pu, B.G. Bruneau, J.G. Seidman, and C.E. Seidman, *Single-Cell Resolution of Temporal Gene Expression during Heart Development.* Dev Cell, 2016. **39**(4): p. 480-490.

87. Morez, C., M. Noseda, M.A. Paiva, E. Belian, M.D. Schneider, and M.M. Stevens, *Enhanced efficiency of genetic programming toward cardiomyocyte creation through topographical cues.* Biomaterials, 2015. **70**: p. 94-104.

88. Mackenzie, L., H.L. Roderick, M.J. Berridge, S.J. Conway, and M.D. Bootman, *The spatial pattern of atrial cardiomyocyte calcium signalling modulates contraction.* J Cell Sci, 2004. **117**(Pt 26): p. 6327-37.

89. Dobrev, D., *Cardiomyocyte Ca2+ overload in atrial tachycardia: is blockade of L-type Ca2+ channels a promising approach to prevent electrical remodeling and arrhythmogenesis?* Naunyn Schmiedebergs Arch Pharmacol, 2007. **376**(4): p. 227-30.

90. Nattel, S., *Therapeutic implications of atrial fibrillation mechanisms: can mechanistic insights be used to improve AF management?* Cardiovasc Res, 2002. **54**(2): p. 347-60.

91. Nattel, S., B. Burstein, and D. Dobrev, *Atrial remodeling and atrial fibrillation: mechanisms and implications.* Circ Arrhythm Electrophysiol, 2008. **1**(1): p. 62-73.

92. Dobrev, D., *Electrical remodeling in atrial fibrillation.* Herz, 2006. **31**(2): p. 108-12; quiz 142-3.

93. Burstein, B. and S. Nattel, *Atrial fibrosis: mechanisms and clinical relevance in atrial fibrillation.* J Am Coll Cardiol, 2008. **51**(8): p. 802-9.

94. Fatkin, D., C.F. Santiago, I.G. Huttner, S.A. Lubitz, and P.T. Ellinor, *Genetics of Atrial Fibrillation: State of the Art in 2017.* Heart Lung Circ, 2017. **26**(9): p. 894-901.

95. Christophersen, I.E., M. Rienstra, C. Roselli, X. Yin, B. Geelhoed, J. Barnard, H. Lin, D.E. Arking, A.V. Smith, C.M. Albert, M. Chaffin, N.R. Tucker, M. Li, D. Klarin, N.A. Bihlmeyer, S.K. Low, P.E. Weeke, M. Muller-Nurasyid, J.G. Smith, J.A. Brody, M.N. Niemeijer, M. Dorr, S. Trompet, J. Huffman, S. Gustafsson, C. Schurmann, M.E. Kleber, L.P. Lyytikainen, I. Seppala, R. Malik, A. Horimoto, M. Perez, J. Sinisalo, S. Aeschbacher, S. Theriault, J. Yao, F. Radmanesh, S. Weiss, A. Teumer, S.H. Choi, L.C. Weng, S. Clauss, R. Deo, D.J. Rader, S.H. Shah, A. Sun, J.C. Hopewell, S. Debette, G. Chauhan, Q. Yang, B.B. Worrall, G. Pare, Y. Kamatani, Y.P. Hagemeijer, N. Verweij, J.E. Siland, M. Kubo, J.D. Smith, D.R. Van Wagoner, J.C. Bis, S. Perz, B.M. Psaty, P.M. Ridker, J.W. Magnani, T.B. Harris, L.J. Launer, M.B. Shoemaker, S. Padmanabhan, J. Haessler, T.M. Bartz, M. Waldenberger, P. Lichtner, M. Arendt, J.E. Krieger, M. Kahonen, L. Risch, A.J. Mansur, A. Peters, B.H. Smith, L. Lind, S.A. Scott, Y. Lu, E.B. Bottinger, J. Hernesniemi, C.M. Lindgren, J.A. Wong, J. Huang, M. Eskola, A.P. Morris, I. Ford, A.P. Reiner, G. Delgado, L.Y. Chen, Y.I. Chen, R.K. Sandhu, M. Li, E. Boerwinkle, L. Eisele, L. Lannfelt, N. Rost, C.D. Anderson, K.D. Taylor, A. Campbell, P.K. Magnusson, D. Porteous, L.J. Hocking, E. Vlachopoulou, N.L. Pedersen, K. Nikus, M. Orho-Melander, A. Hamsten, J. Heeringa, J.C. Denny, J. Kriebel, D. Darbar, C. Newton-Cheh, C. Shaffer, P.W. Macfarlane, S. Heilmann-Heimbach, P. Almgren, P.L. Huang, N. Sotoodehnia, E.Z. Soliman, A.G.

Uitterlinden, A. Hofman, O.H. Franco, U. Volker, K.H. Jockel, M.F. Sinner, H.J. Lin, X. Guo, M.C.o.t. ISGC, C.C. Neurology Working Group of the, M. Dichgans, E. Ingelsson, C. Kooperberg, O. Melander, R.J.F. Loos, J. Laurikka, D. Conen, J. Rosand, P. van der Harst, M.L. Lokki, S. Kathiresan, A. Pereira, J.W. Jukema, C. Hayward, J.I. Rotter, W. Marz, T. Lehtimaki, B.H. Stricker, M.K. Chung, S.B. Felix, V. Gudnason, A. Alonso, D.M. Roden, S. Kaab, D.I. Chasman, S.R. Heckbert, E.J. Benjamin, T. Tanaka, K.L. Lunetta, S.A. Lubitz, P.T. Ellinor and A.F. Consortium, *Large-scale analyses of common and rare variants identify 12 new loci associated with atrial fibrillation.* Nat Genet, 2017. **49**(6): p. 946-952.

96. Christophersen, I.E. and P.T. Ellinor, *Genetics of atrial fibrillation: from families to genomes.* J Hum Genet, 2016. **61**(1): p. 61-70.

97. Mommersteeg, M.T., N.A. Brown, O.W. Prall, C. de Gier-de Vries, R.P. Harvey, A.F. Moorman, and V.M. Christoffels, *Pitx2c and Nkx2-5 are required for the formation and identity of the pulmonary myocardium.* Circ Res, 2007. **101**(9): p. 902-9.

98. Pikkarainen, S., H. Tokola, R. Kerkela, and H. Ruskoaho, *GATA transcription factors in the developing and adult heart.* Cardiovasc Res, 2004. **63**(2): p. 196-207.

99. Lubitz, S.A., K.L. Lunetta, H. Lin, D.E. Arking, S. Trompet, G. Li, B.P. Krijthe, D.I. Chasman, J. Barnard, M.E. Kleber, M. Dorr, K. Ozaki, A.V. Smith, M. Muller-Nurasyid, S. Walter, S.K. Agarwal, J.C. Bis, J.A. Brody, L.Y. Chen, B.M. Everett, I. Ford, O.H. Franco, T.B. Harris, A. Hofman, S. Kaab, S. Mahida, S. Kathiresan, M. Kubo, L.J. Launer, P.W. MacFarlane, J.W. Magnani, B. McKnight, D.D. McManus, A. Peters, B.M. Psaty, L.M. Rose, J.I. Rotter, G. Silbernagel, J.D. Smith, N. Sotoodehnia, D.J. Stott, K.D. Taylor, A. Tomaschitz, T. Tsunoda, A.G. Uitterlinden, D.R. Van Wagoner, U. Volker, H. Volzke, J.M. Murabito, M.F. Sinner, V. Gudnason, S.B. Felix, W. Marz, M. Chung, C.M. Albert, B.H. Stricker, T. Tanaka, S.R. Heckbert, J.W. Jukema, A. Alonso, E.J. Benjamin, and P.T. Ellinor, *Novel genetic markers associate with atrial fibrillation risk in Europeans and Japanese.* J Am Coll Cardiol, 2014. **63**(12): p. 1200-1210.

100. Olson, T.M., A.E. Alekseev, X.K. Liu, S. Park, L.V. Zingman, M. Bienengraeber, S. Sattiraju, J.D. Ballew, A. Jahangir, and A. Terzic, *Kv1.5 channelopathy due to KCNA5 loss-of-function mutation causes human atrial fibrillation.* Hum Mol Genet, 2006. **15**(14): p. 2185-91.

101. Xu, J., G. Cui, F. Esmailian, M. Plunkett, D. Marelli, A. Ardehali, J. Odim, H. Laks, and L. Sen, *Atrial extracellular matrix remodeling and the maintenance of atrial fibrillation.* Circulation, 2004. **109**(3): p. 363-8.

102. Patient, R.K. and J.D. McGhee, *The GATA family (vertebrates and invertebrates).* Curr Opin Genet Dev, 2002. **12**(4): p. 416-22.

103. Charron, F. and M. Nemer, *GATA transcription factors and cardiac development.* Semin Cell Dev Biol, 1999. **10**(1): p. 85-91.

104. Searcy, R.D., E.B. Vincent, C.M. Liberatore, and K.E. Yutzey, *A GATA-dependent nkx-2.5 regulatory element activates early cardiac gene expression in transgenic mice.* Development, 1998. **125**(22): p. 4461-70.

105. Ip, H.S., D.B. Wilson, M. Heikinheimo, Z. Tang, C.N. Ting, M.C. Simon, J.M. Leiden, and M.S. Parmacek, *The GATA-4 transcription factor transactivates the cardiac muscle-specific troponin C promoter-enhancer in nonmuscle cells.* Mol Cell Biol, 1994. **14**(11): p. 7517-26.

106. Murphy, A.M., W.R. Thompson, L.F. Peng, and L. Jones, 2nd, *Regulation of the rat cardiac troponin I gene by the transcription factor GATA-4.* Biochem J, 1997. **322 (Pt 2)**: p. 393-401.

107. McGrew, M.J., N. Bogdanova, K. Hasegawa, S.H. Hughes, R.N. Kitsis, and N. Rosenthal, *Distinct gene expression patterns in skeletal and cardiac muscle are dependent on common regulatory sequences in the MLC1/3 locus.* Mol Cell Biol, 1996. **16**(8): p. 4524-34.

108. Koban, M.U., S.A. Brugh, D.R. Riordon, K.A. Dellow, H.T. Yang, D. Tweedie, and K.R. Boheler, *A distant upstream region of the rat multipartite Na(+)-Ca(2+) exchanger NCX1 gene promoter is sufficient to confer cardiac-specific expression.* Mech Dev, 2001. **109**(2): p. 267-79.

109. Zhang, Y., N. Rath, S. Hannenhalli, Z. Wang, T. Cappola, S. Kimura, E. Atochina-Vasserman, M.M. Lu, M.F. Beers, and E.E. Morrisey, *GATA and Nkx factors synergistically regulate tissue-specific gene expression and development in vivo.* Development, 2007. **134**(1): p. 189-98.

110. McFadden, D.G., J. Charite, J.A. Richardson, D. Srivastava, A.B. Firulli, and E.N. Olson, *A GATA-dependent right ventricular enhancer controls dHAND transcription in the developing heart.* Development, 2000. **127**(24): p. 5331-41.

111. Yang, Y.Q., J. Wang, X.H. Wang, Q. Wang, H.W. Tan, M. Zhang, F.F. Shen, J.Q. Jiang, W.Y. Fang, and X. Liu, *Mutational spectrum of the GATA5 gene associated with familial atrial fibrillation.* Int J Cardiol, 2012. **157**(2): p. 305-7.

112. Wang, X.H., C.X. Huang, Q. Wang, R.G. Li, Y.J. Xu, X. Liu, W.Y. Fang, and Y.Q. Yang, *A novel GATA5 loss-of-function mutation underlies lone atrial fibrillation.* Int J Mol Med, 2013. **31**(1): p. 43-50.

113. Yang, Y., J. Li, X. Lin, Y. Yang, K. Hong, L. Wang, J. Liu, L. Li, D. Yan, D. Liang, J. Xiao, H. Jin, J. Wu, Y. Zhang, and Y.H. Chen, *Novel KCNA5 loss-of-function mutations responsible for atrial fibrillation.* J Hum Genet, 2009. **54**(5): p. 277-83.

114. Yang, T., P. Yang, D.M. Roden, and D. Darbar, *Novel KCNA5 mutation implicates tyrosine kinase signaling in human atrial fibrillation.* Heart Rhythm, 2010. **7**(9): p. 1246-52.

115. Christophersen, I.E., M.S. Olesen, B. Liang, M.N. Andersen, A.P. Larsen, J.B. Nielsen, S. Haunso, S.P. Olesen, A. Tveit, J.H. Svendsen, and N. Schmitt, *Genetic variation in KCNA5: impact on the atrial-specific potassium current IKur in patients with lone atrial fibrillation.* Eur Heart J, 2013. **34**(20): p. 1517-25.

116. Wang, Z., B. Fermini, and S. Nattel, *Delayed rectifier outward current and repolarization in human atrial myocytes.* Circ Res, 1993. **73**(2): p. 276-85.

117. Wettwer, E., O. Hala, T. Christ, J.F. Heubach, D. Dobrev, M. Knaut, A. Varro, and U. Ravens, *Role of IKur in controlling action potential shape and contractility in the human atrium: influence of chronic atrial fibrillation.* Circulation, 2004. **110**(16): p. 2299-306.

118. Ryan, A.K., B. Blumberg, C. Rodriguez-Esteban, S. Yonei-Tamura, K. Tamura, T. Tsukui, J. de la Pena, W. Sabbagh, J. Greenwald, S. Choe, D.P. Norris, E.J. Robertson, R.M. Evans, M.G. Rosenfeld, and J.C. Izpisua Belmonte, *Pitx2 determines left-right asymmetry of internal organs in vertebrates.* Nature, 1998. **394**(6693): p. 545-51.

119. Franco, D. and M. Campione, *The role of Pitx2 during cardiac development. Linking left-right signaling and congenital heart diseases.* Trends Cardiovasc Med, 2003. **13**(4): p. 157-63.

120. Tao, Y., M. Zhang, L. Li, Y. Bai, Y. Zhou, A.M. Moon, H.J. Kaminski, and J.F. Martin, *Pitx2, an atrial fibrillation predisposition gene, directly regulates ion transport and intercalated disc genes.* Circ Cardiovasc Genet, 2014. **7**(1): p. 23-32.

121. Nadadur, R.D., M.T. Broman, B. Boukens, S.R. Mazurek, X. Yang, M. van den Boogaard, J. Bekeny, M. Gadek, T. Ward, M. Zhang, Y. Qiao, J.F. Martin, C.E. Seidman, J. Seidman, V. Christoffels, I.R. Efimov, E.M. McNally, C.R. Weber, and I.P. Moskowitz, *Pitx2 modulates a Tbx5-dependent gene regulatory network to maintain atrial rhythm.* Sci Transl Med, 2016. **8**(354): p. 354ra115.

122. Wang, J., E. Klysik, S. Sood, R.L. Johnson, X.H. Wehrens, and J.F. Martin, *Pitx2 prevents susceptibility to atrial arrhythmias by inhibiting left-sided pacemaker specification.* Proc Natl Acad Sci U S A, 2010. **107**(21): p. 9753-8.

123. Tucker, N.R. and P.T. Ellinor, *Emerging directions in the genetics of atrial fibrillation.* Circ Res, 2014. **114**(9): p. 1469-82.

124. Gudbjartsson, D.F., D.O. Arnar, A. Helgadottir, S. Gretarsdottir, H. Holm, A. Sigurdsson, A. Jonasdottir, A. Baker, G. Thorleifsson, K. Kristjansson, A. Palsson,

T. Blondal, P. Sulem, V.M. Backman, G.A. Hardarson, E. Palsdottir, A. Helgason, R. Sigurjonsdottir, J.T. Sverrisson, K. Kostulas, M.C. Ng, L. Baum, W.Y. So, K.S. Wong, J.C. Chan, K.L. Furie, S.M. Greenberg, M. Sale, P. Kelly, C.A. MacRae, E.E. Smith, J. Rosand, J. Hillert, R.C. Ma, P.T. Ellinor, G. Thorgeirsson, J.R. Gulcher, A. Kong, U. Thorsteinsdottir, and K. Stefansson, *Variants conferring risk of atrial fibrillation on chromosome 4q25.* Nature, 2007. **448**(7151): p. 353-7.

125. Lubitz, S.A., B.A. Yi, and P.T. Ellinor, *Genetics of atrial fibrillation.* Heart Fail Clin, 2010. **6**(2): p. 239-47.

126. Kaab, S., D. Darbar, C. van Noord, J. Dupuis, A. Pfeufer, C. Newton-Cheh, R. Schnabel, S. Makino, M.F. Sinner, P.J. Kannankeril, B.M. Beckmann, S. Choudry, B.S. Donahue, J. Heeringa, S. Perz, K.L. Lunetta, M.G. Larson, D. Levy, C.A. MacRae, J.N. Ruskin, A. Wacker, A. Schomig, H.E. Wichmann, G. Steinbeck, T. Meitinger, A.G. Uitterlinden, J.C. Witteman, D.M. Roden, E.J. Benjamin, and P.T. Ellinor, *Large scale replication and meta-analysis of variants on chromosome 4q25 associated with atrial fibrillation.* Eur Heart J, 2009. **30**(7): p. 813-9.

127. Qiu, X.B., Y.J. Xu, R.G. Li, L. Xu, X. Liu, W.Y. Fang, Y.Q. Yang, and X.K. Qu, *PITX2C loss-of-function mutations responsible for idiopathic atrial fibrillation.* Clinics (Sao Paulo), 2014. **69**(1): p. 15-22.

128. Zhou, Y.M., P.X. Zheng, Y.Q. Yang, Z.M. Ge, and W.Q. Kang, *A novel PITX2c lossoffunction mutation underlies lone atrial fibrillation.* Int J Mol Med, 2013. **32**(4): p. 827-34.

129. Li, N., D. Dobrev, and X.H. Wehrens, *PITX2: a master regulator of cardiac channelopathy in atrial fibrillation?* Cardiovasc Res, 2016. **109**(3): p. 345-7.

130. Liu, G.S., A. Morales, E. Vafiadaki, C.K. Lam, W.F. Cai, K. Haghighi, G. Adly, R.E. Hershberger, and E.G. Kranias, *A novel human R25C-phospholamban mutation is associated with super-inhibition of calcium cycling and ventricular arrhythmia.* Cardiovasc Res, 2015. **107**(1): p. 164-74.

131. Haghighi, K., F. Kolokathis, A.O. Gramolini, J.R. Waggoner, L. Pater, R.A. Lynch, G.C. Fan, D. Tsiapras, R.R. Parekh, G.W. Dorn, 2nd, D.H. MacLennan, D.T. Kremastinos, and E.G. Kranias, *A mutation in the human phospholamban gene, deleting arginine 14, results in lethal, hereditary cardiomyopathy.* Proc Natl Acad Sci U S A, 2006. **103**(5): p. 1388-93.

132. Medin, M., M. Hermida-Prieto, L. Monserrat, R. Laredo, J.C. Rodriguez-Rey, X. Fernandez, and A. Castro-Beiras, *Mutational screening of phospholamban gene in hypertrophic and idiopathic dilated cardiomyopathy and functional study of the PLN -42 C>G mutation.* Eur J Heart Fail, 2007. **9**(1): p. 37-43.

133. Lenski, M., G. Schleider, M. Kohlhaas, L. Adrian, O. Adam, Q. Tian, L. Kaestner, P. Lipp, M. Lehrke, C. Maack, M. Bohm, and U. Laufs, *Arrhythmia causes lipid accumulation and reduced glucose uptake.* Basic Res Cardiol, 2015. **110**(4): p. 40.

134. Tessier, S., P. Karczewski, E.G. Krause, Y. Pansard, C. Acar, M. Lang-Lazdunski, J.J. Mercadier, and S.N. Hatem, *Regulation of the transient outward K(+) current by Ca(2+)/calmodulin-dependent protein kinases II in human atrial myocytes.* Circ Res, 1999. **85**(9): p. 810-9.

135. Frustaci, A., C. Chimenti, F. Bellocci, E. Morgante, M.A. Russo, and A. Maseri, *Histological substrate of atrial biopsies in patients with lone atrial fibrillation.* Circulation, 1997. **96**(4): p. 1180-4.

136. Ponten, A., E.B. Folestad, K. Pietras, and U. Eriksson, *Platelet-derived growth factor D induces cardiac fibrosis and proliferation of vascular smooth muscle cells in heart-specific transgenic mice.* Circ Res, 2005. **97**(10): p. 1036-45.

137. Schotten, U., H.R. Neuberger, and M.A. Allessie, *The role of atrial dilatation in the domestication of atrial fibrillation.* Prog Biophys Mol Biol, 2003. **82**(1-3): p. 151-62.

138. Everett, T.H.t. and J.E. Olgin, *Atrial fibrosis and the mechanisms of atrial fibrillation.* Heart Rhythm, 2007. **4**(3 Suppl): p. S24-7.

139. Lin, C.S., L.P. Lai, J.L. Lin, Y.L. Sun, C.W. Hsu, C.L. Chen, S.J. Mao, and S.K. Huang, *Increased expression of extracellular matrix proteins in rapid atrial pacing-induced atrial fibrillation.* Heart Rhythm, 2007. **4**(7): p. 938-49.

140. Allessie, M., J. Ausma, and U. Schotten, *Electrical, contractile and structural remodeling during atrial fibrillation.* Cardiovasc Res, 2002. **54**(2): p. 230-46.

141. Sumitomo, N., H. Sakurada, K. Taniguchi, M. Matsumura, O. Abe, M. Miyashita, H. Kanamaru, K. Karasawa, M. Ayusawa, S. Fukamizu, I. Nagaoka, M. Horie, K. Harada, and M. Hiraoka, *Association of atrial arrhythmia and sinus node dysfunction in patients with catecholaminergic polymorphic ventricular tachycardia.* Circ J, 2007. **71**(10): p. 1606-9.

142. Sharifov, O.F., V.V. Fedorov, G.G. Beloshapko, A.V. Glukhov, A.V. Yushmanova, and L.V. Rosenshtraukh, *Roles of adrenergic and cholinergic stimulation in spontaneous atrial fibrillation in dogs.* J Am Coll Cardiol, 2004. **43**(3): p. 483-90.

143. Bers, D.M., *Calcium cycling and signaling in cardiac myocytes.* Annu Rev Physiol, 2008. **70**: p. 23-49.

144. Thomas, G., M.J. Killeen, A.A. Grace, and C.L. Huang, *Pharmacological separation of early afterdepolarizations from arrhythmogenic substrate in*

DeltaKPQ Scn5a murine hearts modelling human long QT 3 syndrome. Acta Physiol (Oxf), 2008. **192**(4): p. 505-17.

145. Dzeshka, M.S., G.Y. Lip, V. Snezhitskiy, and E. Shantsila, *Cardiac Fibrosis in Patients With Atrial Fibrillation: Mechanisms and Clinical Implications.* J Am Coll Cardiol, 2015. **66**(8): p. 943-59.

146. Dobrev, D. and S. Nattel, *New antiarrhythmic drugs for treatment of atrial fibrillation.* Lancet, 2010. **375**(9721): p. 1212-23.